36th CRC Real World Emissions Workshop

Session Summaries

March 8–11, 2026 · San Diego, CA

Prepared by Dr. Zisimos Toumasatos UCR CE-CERT

1. Air Quality and Impact of Regional Emissions: Real-World Impacts of Policy

MULTI-DAY EMISSIONS TESTING FROM COMMERCIAL HARBOR CRAFT TIER 4 -TIER 2

Kent Johnson, Elizabeth DeFrance, Andrew Burnette, Tom Durbin, George Karavalakis, Elizabeth Melgoza, Andrew Damiano

Scope of the Study

The study aimed to quantify and characterize in-use off-cycle emissions from commercial harbor craft, specifically tugboats and ferries, across Tier 2 to Tier 4 engines. Off-cycle emissions refer to pollutants generated under real-world operating conditions that are not captured in regulatory certification test cycles.

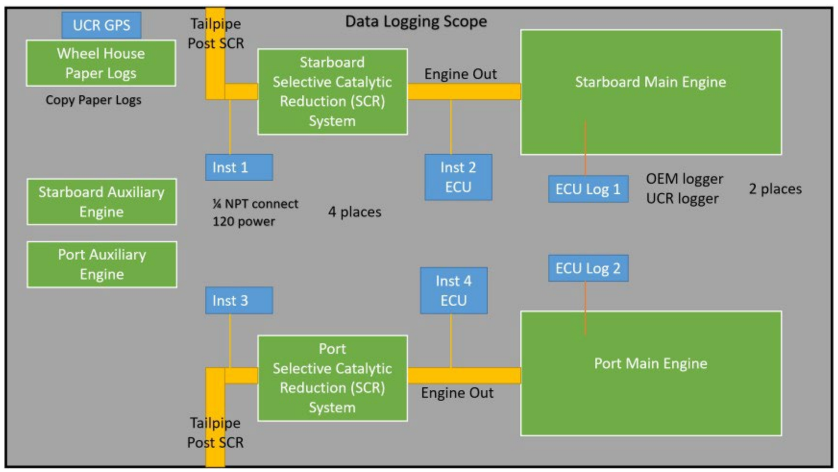

Figure 1 Measurement layout of the marine testing methodology

To achieve this, multi-day field testing was conducted using portable emissions measurement systems (PEMS), including Horiba PG350, 3DATX systems, and OEM ECU-based sensors. The experimental design focused on capturing emissions across different vessel types and operational tiers under realistic duty cycles.

Emissions were analyzed across distinct operational modes, including standby, low-speed transit, high-speed transit, and ship-assist activities. The study also examined variability in emissions resulting from changes in loads, speeds, and engine activity patterns, providing a more comprehensive understanding of real-world vessel emissions behavior.

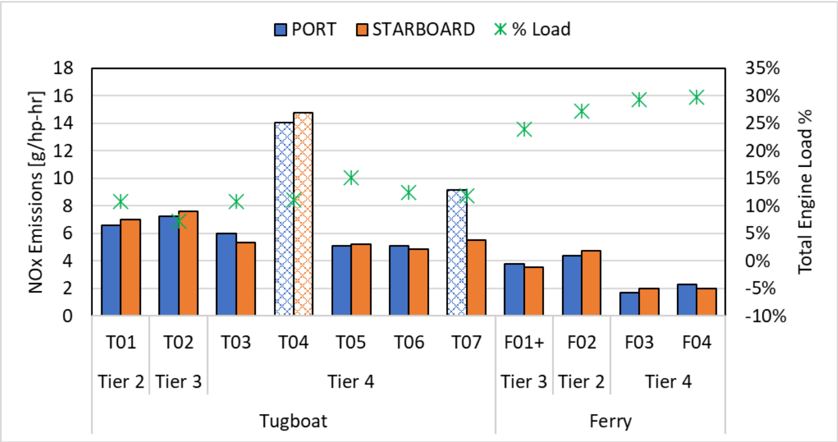

Figure 2 NOx emission rates per marine application and emission regulation type

Results

Tier 4 engines showed the lowest NOx emissions for both tugboats and ferries compared to Tier 2 and Tier 3 engines.

Tier 4 tugboats exhibited higher NOx emissions than both Tier 2 and Tier 3, while ferries showed emissions higher than Tier 3 but generally lower than Tier 2.

Tier 4 engines produced higher emissions than earlier tiers, likely due to highly variable load and transient conditions.

For ferries, Tier 4 engines produced higher emissions than previous tiers, while tugboats showed comparable or slightly reduced emissions.

Tugboats spent the largest proportion of time in ship assist operations (47%), while ferries operated mostly in high-speed transit (42%), influencing overall emissions profiles.

Off-Cycle Emissions vs Certification Limits:

- Daily average off-cycle NOx emissions ranged from 3.5–7.6 g/hp-hr for tugboats and 1.7–4.7 g/hp-hr for ferries.
- These values frequently exceeded the Tier 4 certification limit (1.3 g/hp-hr), particularly under low-speed and variable-load conditions.

Conclusions

While Tier 4 engines significantly reduce emissions under steady high-speed conditions, they can produce higher emissions under real-world, off-cycle operating conditions, especially during low-speed and transient operations. This highlights a gap between certification performance and actual in-use emissions.

Mitigating air pollution from fuel changes with a vehicle replacementprogram

Jeremy Martin, Ph.D., Georgia Klein

Scope of the Study

This study evaluates the air quality impacts of increased fuel flexibility in California's gasoline market and explores how those impacts can be mitigated through vehicle replacement programs. Specifically, it investigates the potential environmental consequences of allowing the use of non-California gasoline formulations (e.g., U.S. conventional or reformulated gasoline) during supply shortages, which could improve fuel availability but may increase emissions.

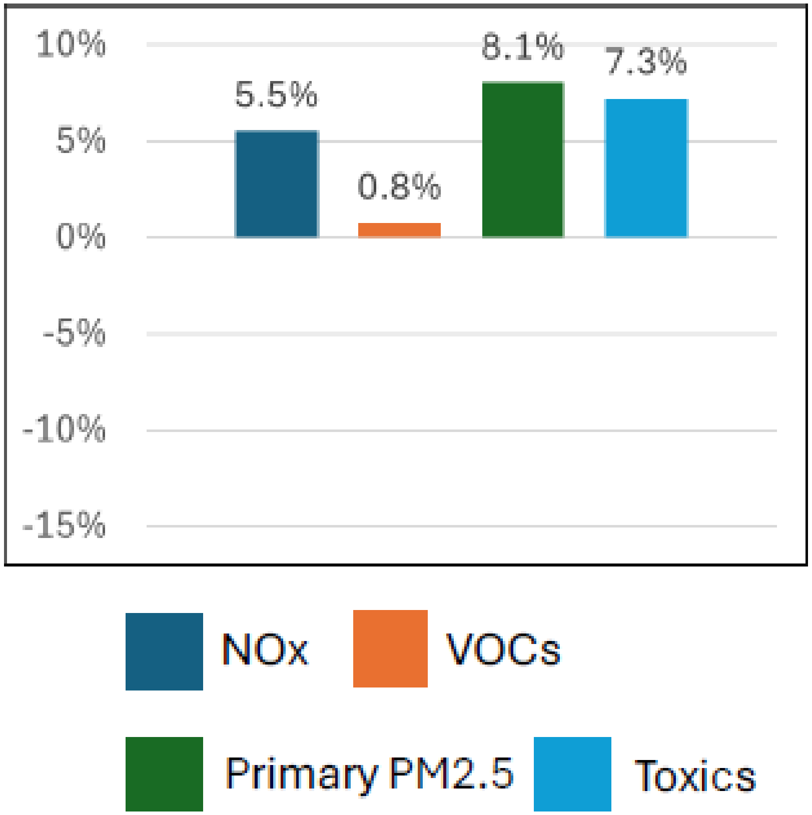

Figure 3 relative change in emissions rate for 2030 if 100% of CA-RFG is replaced with US-Avg gasoline

The analysis uses the EPA MOVES5 (2024) model in combination with CARB's EMFAC fleet data to simulate emissions from gasoline-powered passenger vehicles. The study focuses on six key pollutants: nitrogen oxides (NOx), volatile organic compounds (VOCs), fine particulate matter

(PM2.5), and a toxics index including benzene, formaldehyde, 1,3-butadiene, and acetaldehyde.

Additionally, the study examines the role of older vehicles (pre-2004), which contribute disproportionately to emissions, and evaluates policy scenarios combining fuel flexibility with programs that incentivize replacing older vehicles with electric vehicles (EVs) or cleaner alternatives. A proposed mitigation mechanism includes a fee-based system on non-compliant fuels to fund vehicle replacement initiatives.

Results

Replacing California's cleaner gasoline (CA-RFG) with average U.S. gasoline increases emissions across key pollutants, although the difference is smaller than in the past due to improvements in fuel quality nationwide.

Older vehicles contribute a disproportionately large share of total emissions, particularly for NOx, VOCs, PM2.5, and toxic pollutants. Their impact is also linked to environmental justice concerns, as they are more common in lower-income communities.

Replacing 500,000 pre-2004 vehicles with 90% EVs leads to substantial reductions in all major pollutants, significantly outweighing the emissions increases caused by fuel substitution.

A proposed $0.25 per gallon mitigation fee on non-California gasoline could:

- Generate approximately $3 billion (assuming full market substitution).
- Fund replacement of over 500,000 older vehicles within two years.
- Offset the additional emissions caused by using less stringent fuel formulations.

Even if only 10% of gasoline supply is replaced with non-California fuel, the resulting revenues could support approximately 50,000 vehicle replacements, partially mitigating emissions increases.

Analysis of historical price differences suggests that greater fuel flexibility could have reduced gasoline costs by $5.4 billion over five years, while still funding significant emissions reduction programs.

Conclusions

The study concludes that retiring older vehicles is more effective for reducing air pollution than maintaining marginally stricter fuel specifications. A combined policy approach—introducing fuel flexibility while funding accelerated vehicle replacement—can both stabilize fuel markets and improve air quality, with additional equity benefits for disadvantaged communities.

DIFFUSION TUBES: LOW-TECH BUT USEFUL

Karl Ropkins, Christopher Rushton, James Tate,

Said Muni, Andy Smith, Anthony Walker and Tony Clark

Scope of the Study

This study evaluates the effectiveness of nitrogen dioxide (NO_2) diffusion tubes as a low-cost air quality monitoring tool and demonstrates their application in assessing policy impacts, specifically within the Bradford Clean Air Zone (CAZ) in the UK.

Diffusion tubes are widely used due to their simplicity, low cost, and ability to provide long-term average measurements (typically over 4-week periods), although they have limitations in accuracy, temporal resolution, and require manual handling and post-processing.

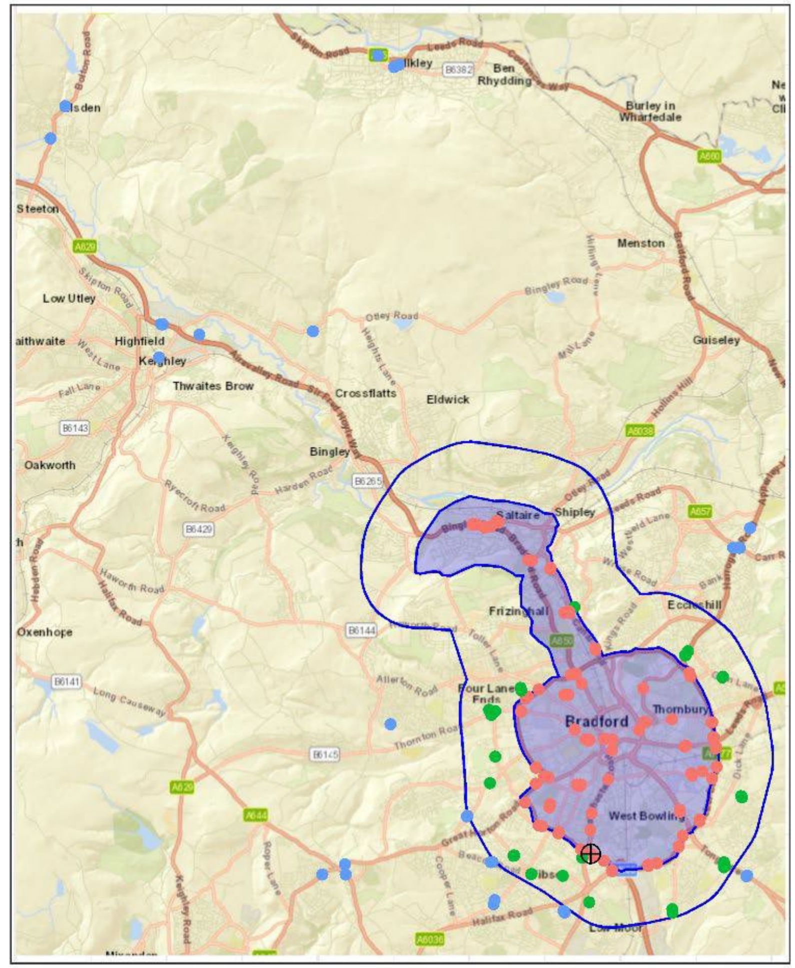

Figure 4 Area of interest

The research utilizes a large dataset comprising over 10,000 samples from 148 monitoring sites collected between 2020 and 2025, with a focus on 2022–2024. Analytical methods include:

- Difference-in-Differences (DiD) modeling to estimate the causal impact of the CAZ intervention
- Breakpoint/segment analysis to identify changes in pollution trends over time
- Cluster analysis to examine spatial and temporal variability in NO_2 patterns
- Development of regional models to separate background trends from policy-driven impacts

The study aims to distinguish between broader regional improvements in air quality and direct effects attributable to the CAZ policy intervention.

Results

The findings demonstrate both the strengths of diffusion tube data and the nuanced impacts of the CAZ:

NO_2 concentrations showed a consistent decline of approximately 1.5 µg/m³ per year across the region, indicating significant background improvements unrelated to the CAZ.

Prior to CAZ implementation, NO_2 levels were already decreasing. After implementation, the rate of decrease slowed slightly, and overall levels were about 0.65 µg/m³ higher than expected, suggesting broader regional factors influencing trends.

When compared to areas outside the CAZ, NO_2 concentrations within the CAZ were approximately 0.45 µg/m³ lower, indicating a modest but measurable positive impact of the policy.

The impact of the CAZ was highly heterogeneous:

- Improvements up to –1.9 µg/m³ were observed within central CAZ areas
- In some surrounding areas, increases up to +1.3 µg/m³ were detected, likely due to displacement of higher-emitting vehicles

Breakpoint analysis identified more pronounced improvements at certain sites, particularly emerging during 2023–2024, suggesting delayed policy effects.

Despite their limitations (±12–25% uncertainty and lower precision than continuous monitors), diffusion tubes proved effective for large-scale, long-term policy evaluation, especially when combined with robust statistical methods.

Conclusions

Air quality improvements in Bradford are driven by both regional background trends and localized CAZ effects, with the latter showing modest but spatially variable benefits. Diffusion tubes, while low-tech, remain a valuable and practical tool for large-scale environmental monitoring and policy assessment when appropriately analyzed.

Mexico City intra- and inter-regional comparison of real-world emissions

An evaluation of inspection and maintenance programs

Michelle Meyer

Scope of the Study

This study evaluates real-world emissions from gasoline light-duty vehicles in Mexico City (CDMX) and compares them both within the region and with another major city (Bogotá). The objective is to assess the effectiveness of inspection and maintenance (I&M) programs and to understand the implications of proposed regulatory changes, particularly regarding NOx emission limits.

Figure 5 View of the measurement layout during the remote sensing measurements

The analysis is based on remote sensing measurements collected between February and April 2022, comprising approximately 74,500 vehicle observations, with about 70% from Mexico City and 30% from the surrounding State of Mexico. The study also incorporates comparative data from Bogotá, with approximately 146,000 measurements collected in 2023.

Key contextual factors include differences in fuel quality, emission standards, inspection frequency, and vehicle fleets. Mexico City operates a relatively strict I&M program with periodic inspections and driving restrictions (e.g., *Hoy No Circula*), while Bogotá has less stringent inspection requirements and historically higher sulfur fuel levels.

The study aims to (1) evaluate how well current I&M policies control emissions, (2) assess proposed regulatory changes, and (3) identify regional discrepancies in emissions performance.

Results

The results highlight significant insights into the effectiveness of I&M programs and regional emission differences:

Real-world data show that NOx emissions in Mexico City have been steadily declining, despite no major changes in emission standards. This suggests that I&M programs, combined with vehicle restrictions and related policies, are effectively reducing emissions and promoting cleaner vehicles.

Compliance with NOx Limits: The majority of gasoline vehicles emit well below the proposed NOx limit, with:

- 94% of “00” certified vehicles and 78% of “0” certified vehicles emitting below 250 ppm This indicates that current standards are widely achievable and that relaxing limits may not be necessary.

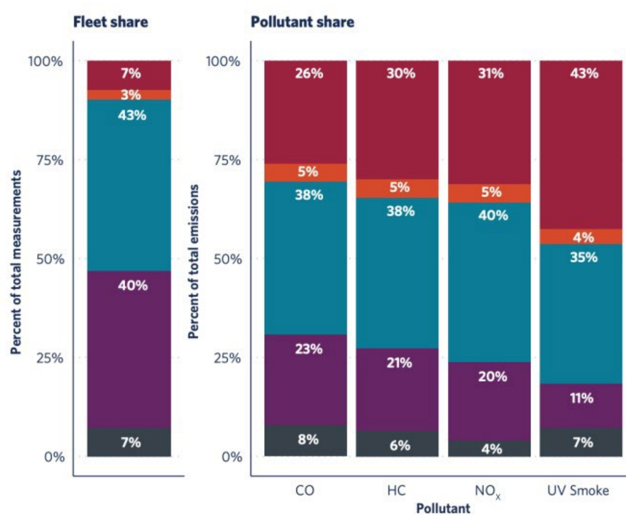

Figure 6 A small share of the fleet (~7% of older vehicles registered in the State of Mexico) contributes disproportionately to emissions, accounting for 26–43% of total emissions

Disproportionate Impact of Older Vehicles: A small share of the fleet (~7% of older vehicles registered in the State of Mexico) contributes disproportionately to emissions, accounting for 26–43% of total emissions, highlighting inconsistencies in regional enforcement and fleet quality.

Regional Inequality in I&M Programs: Differences in inspection rigor between Mexico City and the State of Mexico lead to higher emissions from vehicles registered outside the city, suggesting non-uniform implementation of I&M procedures.

Mexico City vs Bogotá Comparison**:** Newer vehicles in Mexico City show substantially lower NOx emissions than those in Bogotá. In some cases, specific vehicle models in Bogotá exhibited up to 9 times higher NOx emissions

Influence of External Factors: Higher emissions in Bogotá are attributed to factors such as:

- Historically higher sulfur fuel content (leading to emission control deterioration)
- Less stringent emission standards and inspection programs
- Absence of NOx testing in periodic inspections

Conclusions: The study demonstrates that robust I&M programs, supported by real-world emissions monitoring, play a critical role in reducing vehicle emissions, even without stricter standards. Consistent enforcement, improved fuel quality, and harmonization of policies across regions are essential to achieving further air quality improvements.

IMPLEMENTATION OF THE NEW EU AMBIENT AIR QUALITY DIRECTIVE FOR ULTRAFINE PARTICLE MONITORING IN SACRAMENTO

Alberto Ayala, Janice Lam-Snyder, Levi Ford, and Danny Kam

Sacramento Metro AQMD

Manfred Linke, Petra Kotnik, Johannes Murg

Scope of the Study

This study examines the implementation of ultrafine particle (UFP) monitoring in Sacramento in alignment with the European Union's Ambient Air Quality Directive (AAQD 2024/2881). The directive recognizes that traditional particulate matter metrics (e.g., $PM_{2.5}$ and PM_{10} mass concentrations) are insufficient to fully characterize air quality and requires the inclusion of UFP monitoring based on particle number and size.

Figure 7 Measurement setup

The primary objective is to integrate advanced ultrafine particle monitoring technology into Sacramento's regulatory air quality network and evaluate spatial and temporal patterns of UFP concentrations. Monitoring was conducted at three representative sites: a near-roadway location, a neighborhood-scale site, and a rural site, enabling comparison across different exposure environments.

The study also aims to compare UFP levels in Sacramento with those in European cities (e.g., Graz and Vienna) and to assess relationships between UFP concentrations and traditional metrics such as $PM_{2.5}$ and black carbon. Data were collected using specialized particle counters, with a focus on real-world environmental conditions and traffic influences.

Results

The findings provide important insights into UFP monitoring and behavior:

Successful Implementation: Ultrafine particle monitoring was successfully integrated into Sacramento's existing air quality monitoring network, demonstrating feasibility for regulatory applications.

Spatial and Temporal Variability: UFP concentrations showed clear spatial differences across monitoring sites and temporal variability, including:

- Diurnal patterns linked to traffic activity
- Seasonal variations, with higher concentrations during peak summer temperatures
- Strong influence from nearby roadway emissions

Weak Correlation with PM Mass Metrics: UFP concentrations exhibited weak to moderate correlation with $PM_{2.5}$ and black carbon, indicating that PM mass is not a reliable predictor of UFP pollution.

Traffic and Roadway Influence: Near-roadway monitoring confirmed that traffic emissions are a major source of UFP exposure, particularly in high-traffic corridors.

International Comparison: The study enabled direct comparison between U.S. and European cities, supporting the need for harmonized monitoring approaches and highlighting similarities in UFP behavior across regions.

Policy and Monitoring Implications: Results reinforce the EU's position that particle number-based monitoring is necessary, as reliance on PM mass alone overlooks significant aspects of air quality and exposure.

Conclusions

Ultrafine particle pollution represents an important but under-monitored component of air quality. The study demonstrates that integrating UFP monitoring into regulatory networks is feasible and necessary, and that traditional PM metrics alone are insufficient to capture the full impact of particulate pollution.

Section 2. Emissions Inventories and Modeling

Quantifying Emission Benefits for Future Tier Off-Road Engines

Julie Schiffman, Cory Parmer — California Air Resources Board (Off-Road Emission Inventory)

Scope of the Study

This analysis evaluates the emission profiles of off-road diesel mobile engines and quantifies the benefits of new engine standards, requiring a comprehensive understanding of how engines actually operate in the field. A previous 2016 CARB study had simulated PEMS testing on 27 pieces of construction equipment and showed higher NOx at low loads, but it lacked real-world operations data and contained no Tier 4 Final data — the technology that now represents the largest equipment population. To close that gap, the new methodology combines real-world activity data with controlled emissions testing. Activity data came from 156 individual tests collected between 2016 and 2023 using Hydraulic, Electrical, and Mechanical (HEM) data loggers, with each unit monitored for several months to a year. Emissions data came from 50 PEMS tests (2011 and 2019) of 4–8 hours each, designed to capture a wide variety of engine load points. Together these identify the time spent and average NOx emissions for idle and each load bin, providing the empirical basis for revised emission factors.

Results

The work produced three central findings. Finding #1 established how off-road diesel engines spend their time: averaged across 206 tests, roughly one-third of activity is spent idling and another third operating at low loads, so about 60% of total activity occurs at idle plus low loads — the green and blue bars dominate the activity distribution for both engines under 175 hp (32% idle) and 175+ hp engines (34% idle). Finding #2 examined how engines emit at different loads, showing that engines emit dramatically higher NOx per unit of work at low loads than at high loads, and that they emit above the NOx engine standard during low-load operation. These two findings feed directly into California's off-road mobile diesel inventories: because engines spend most of their time at idle and low loads where they emit above the standard, overall inventory emissions increase relative to certification-cycle assumptions, prompting updates to both the 2025 In-Use Off-Road Inventory and the 2025 Forestry Inventory. Finding #3 concluded that future emission standards should be calculated differently — with explicit idling emission limits and low-load emission limits (for operation under 30% load) rather than a single standard addressed only through a certification cycle. Looking forward to Tier 5, the projected NOx reductions from Tier 4 Final to Tier 5 Final are substantial: 92.0% for 75–175 hp engines and 80.6% for 175–750 hp engines, with a Low Load Cycle applied to the 75–750 hp range.

Key Conclusion

Real-world data demonstrate that idle and low-load operation dominate off-road diesel activity and drive disproportionately high NOx emissions that exceed the engine standard. This justifies a fundamental shift toward multiple, load-binned emission standards — separate limits for idle, low loads, and higher loads — in the Tier 5 rulemaking, replacing the single certification-cycle approach. A worked example for a 137 hp engine showed Tier 5 Final could cut hourly NOx from 21.8 g to about 1.75 g, roughly a 92% reduction, illustrating the magnitude of benefit available from controlling the operating regimes that real-world activity data reveal to be most important.

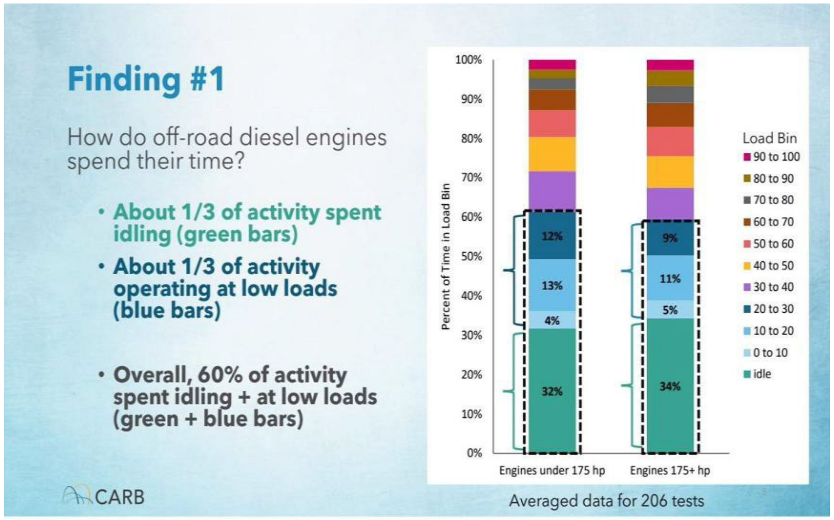

Figure 8 Finding #1 — off-road diesel engines spend about one-third of their time idling and one-third at low loads (≈60% combined), for both engine size classes (averaged over 206 tests).

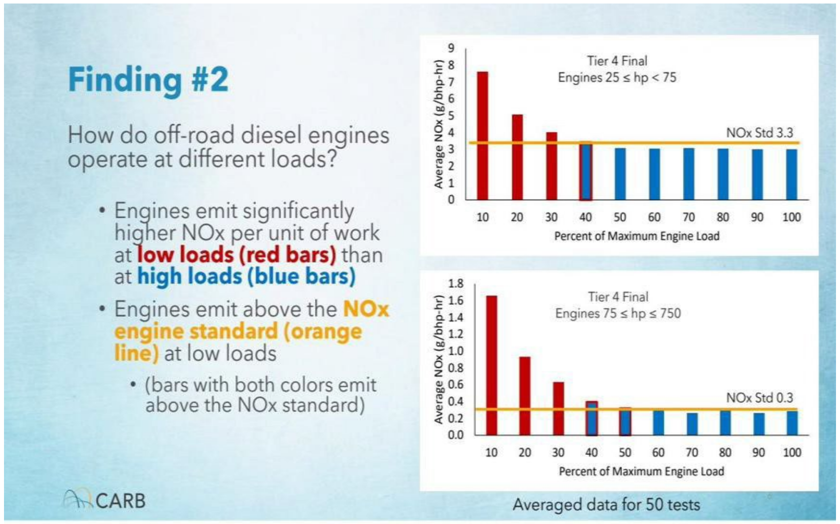

Figure 9 Finding #2 — NOx per unit of work is far higher at low loads (red) than high loads (blue), exceeding the Tier 4 Final NOx standard at low loads.

Characterization and Modeling of Port Vehicle Fleet Carbon and Criteria Pollutant Emissions

Daisy Thomas, Ph.D., Matthew Berry, Andrew Burnette — 3DATX

Scope of the Study

Modern sea ports rely on a wide range of cargo-handling vehicles operating under non-standard duty cycles that differ markedly from on-road driving — frequent idling, low-speed maneuvering, repeated short trips, stop-start behavior, and high load variability that depends on cargo weight and handling activity. As a result, real-world emissions and fuel consumption can differ substantially from certification or laboratory values, and these vehicles contribute local air pollutants (NOx, PM, PN, CO, HC) and CO_2 in areas close to workers and nearby communities, making ports both an air-quality and occupational-exposure concern. Guided by the premise that "you can't manage what you can't measure," the project set out to characterize the real-world emissions and fuel consumption of selected port vehicles and develop representative models linking vehicle activity, engine operation, and environmental impact. Measurements used the parSYNC FLEX iPEMS, which captures gases (CO, CO_2, HC, O_2, NO, NO_2) via NDIR and electrochemical cells, particulates (PN and PM) via scattering/ionization/opacity sensors, an ambient weather station and GPS, and an ECU reader providing fuel rate, speed, load, torque, and coolant temperature, alongside extensive telematics.

Results

Understanding vehicle behavior in port-specific duty cycles enabled more accurate port and regional inventories, identification of high-emission operating modes and activities, and evaluation of fuel-saving strategies. The analysis broke emissions down by operating mode (idle, low, medium, and high load) and identified specific high-emitting behaviors per asset. For example, asset RS-154 exhibited SCR cooling during idling, producing higher NOx during idle and for a short period after the engine was reloaded; its NOx began increasing after only a few hundred seconds of idling, leading to a recommendation to limit that asset's idle time. RS-154 also showed relatively high idle NOx per gallon of fuel consumed. The fuel and CO_2 intensity of idling was modeled, indicating that reducing idling by one hour per day would save approximately 4.8 litres of fuel and 6.8 kg CO_2 for FL-223, 1.84 litres and 2.6 kg for FL-165, 9.6 litres and 11.2 kg for RS-190, and 11.2 litres and 14 kg for RS-154. Model coefficients combined with onboard telematics enable real-time emissions estimation during operation, while an emissions baseline built on current operations and fleet characteristics allows future improvements to be quantified.

Key Conclusion

High-emitting activities were identified for individual vehicles, and practical methods to reduce overall port emissions of CO2 and criteria pollutants were suggested, including idle-time limits. Critically, the study demonstrates that a single measurement framework can support both regulatory-grade pollutant quantification and greenhouse-gas accounting, because the same operational states and asset-specific behaviors drive both pollutant and CO2 emissions. Real-world emissions data and carbon accounting are therefore not parallel efforts but different perspectives on the same vehicle behavior, letting ports address compliance, air-quality management, fuel efficiency, and carbon reduction through one unified data approach. Periodic measurement campaigns are recommended to capture fleet changes, and quantified reductions could support carbon-tax savings or carbon-credit opportunities. The pilot program won first place in Environmental Practices (Large Port) at the American Association of Port Authorities Lighthouse Awards.

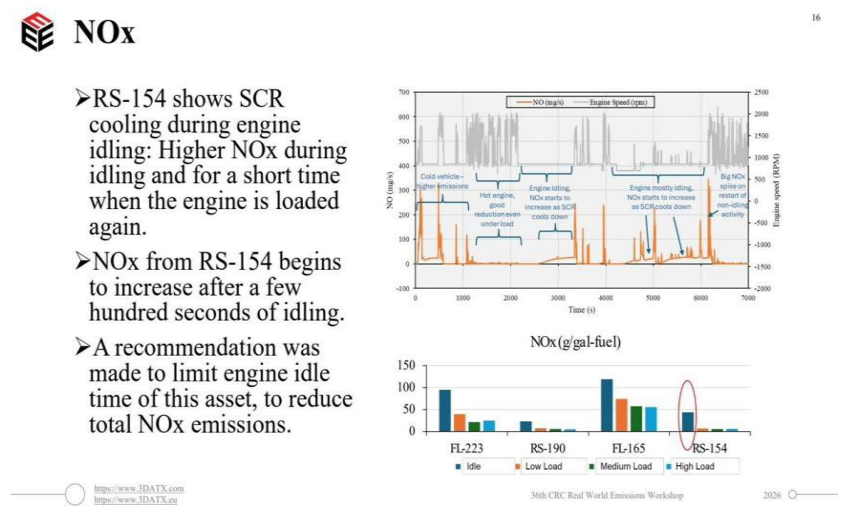

Figure 10 Asset RS-154 shows SCR cooling during idling — NOx rises during idle and briefly after reloading; idle NOx per gallon of fuel is comparatively high (circled).

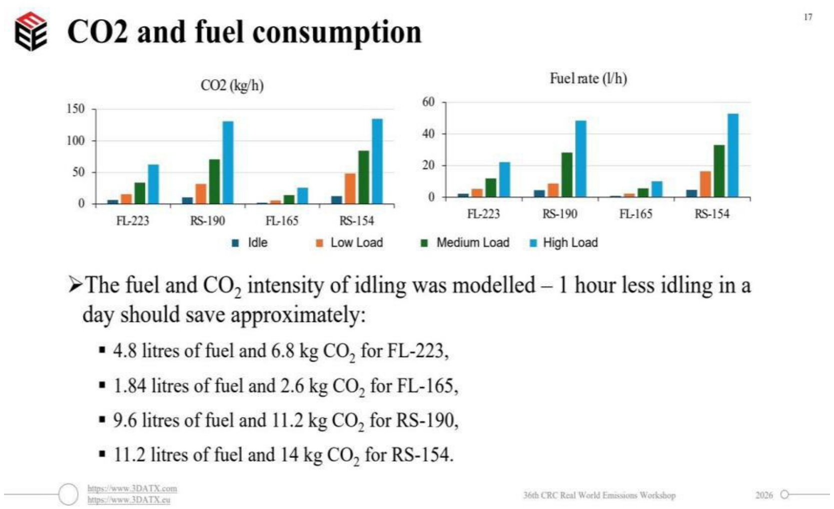

Figure 11 Modeled fuel and CO2 intensity of idling by asset; cutting one hour of daily idling saves roughly 1.8–11.2 litres of fuel and 2.6–14 kg CO2 depending on the vehicle.

Quantifying Heavy-Duty Extended Idling Activity

Rodolfo Souza — Texas A&M Transportation Institute

Scope of the Study

Heavy-duty extended idling — long-haul trucks (GVWR > 33,000 lbs) idling for over an hour during the FMCSA-mandated 10-hour rest periods to maintain cabin climate — is a significant on-road emissions source. Idling consumes roughly 0.8–1.0 gallons per hour at 900–1,200 RPM and accounts for about 1,800 hours per truck per year nationally, while engines at idle operate at only about 11% thermal efficiency with increased wear and soot. Hotelling inputs have an "extremely high" effect (over 50%) on truck NOx and PM. The problem is that MOVES depends on national defaults and averages that can miss local idling patterns and conditions, yet accurate idling activity is needed for inventories, conformity, and State Implementation Plans. The opportunity is to use high-resolution activity data (GPS, electronic logging devices, surveys) to build representative, location-specific idling profiles. The objective was to create a Texas-wide method to identify truck parking locations and quantify extended idling, drawing on EROAD telematics data for 2024, truck-parking locations from web sources and EROAD clusters, and vehicle-miles-traveled data to characterize activity.

Results

The EROAD data captured location events roughly every 250 meters along with turning, ignition, harsh-braking, and moving/stopped events tied to engine attributes, carrier and trip metadata. From the 2024 dataset of 4,898 vehicles and 16.9 million events, the analysis identified 196,427 stops of at least 3,600 seconds, 104,568 idling events, and 18,400 idling events occurring in facilities (both designated truck-parking facilities and non-designated sites such as warehouses after business hours). The distribution of idling duration was approximately lognormal for most hours, but the 12–15 and 16–19 hour-bins showed a bimodality with one peak around 2.5 hours and a second around 10 hours, a pattern also reflected in the statewide distribution. Temporally, event peaks occurred between 7 and 9 AM, with longer durations outside business hours. A statistical framework computed the frequency of stops, the probability of extended idling given a stop, and the expected number and duration of idling events as functions of VMT and stop characteristics. Spatially, idling concentrated along major freight corridors and metropolitan hubs — Harris, Dallas, Tarrant, Bexar, and El Paso counties — with additional clusters in the Permian Basin (oil and gas) and South Texas border counties (cross-border freight). Twenty-eight counties showed zero idling while 55 exceeded 2,500 hours per day; the top TxDOT districts were Houston (42,598 hours/day), Odessa (42,489), San Antonio (32,941), Dallas (32,543), and El Paso (25,978).

Key Conclusion

A telematics-based framework was developed to estimate county-level extended idling using 33.7 million EROAD records across all 254 Texas counties. Multi-source geospatial integration enabled classification of both designated and non-designated parking locations, revealing significant idling at unofficial sites such as industrial warehouses and commercial lots. Preliminary results showed idling concentrating in major metros and freight corridors with consistent idling rates (0.43–0.49) across the top counties. Next steps include combining multiple data providers to expand fleet coverage, refining hotelling-site classification, and evaluating idle-reduction technologies — all aimed at replacing national MOVES defaults with representative, location-specific idling activity for more accurate inventories and conformity analyses.

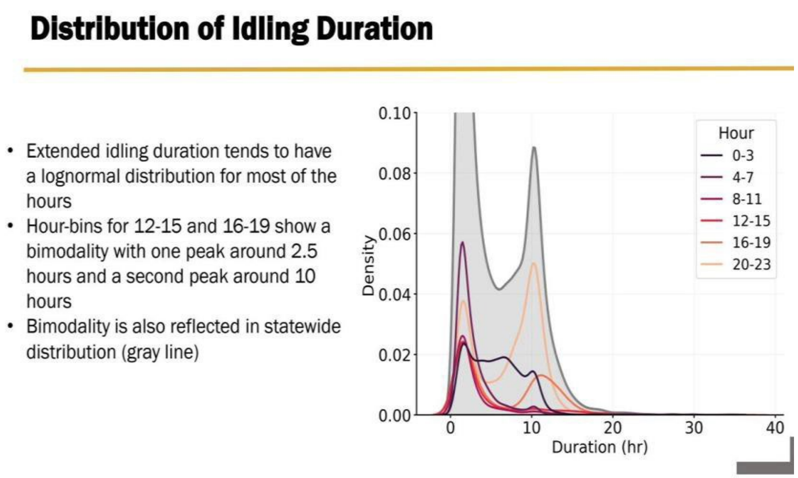

Figure 12 Distribution of extended-idling duration is approximately lognormal, with a bimodal pattern (peaks near 2.5 and 10 hours) in certain hour-bins.

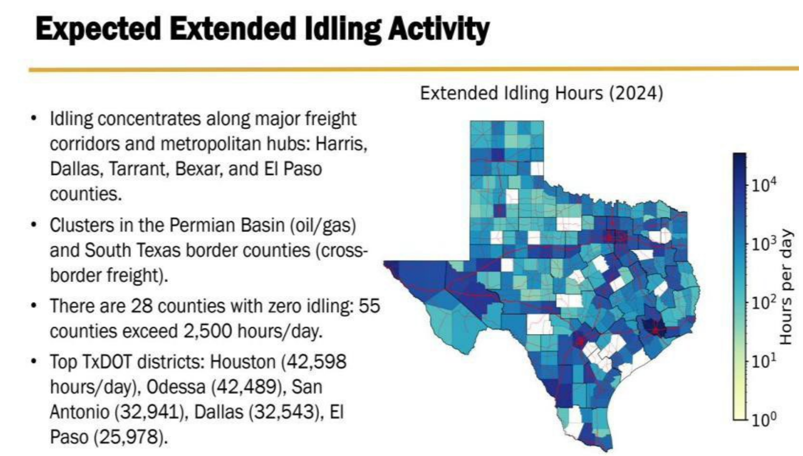

Figure 13 Expected 2024 extended-idling hours concentrate along major Texas freight corridors and metro hubs (Harris, Dallas, Tarrant, Bexar, El Paso) plus the Permian Basin and border counties.

Integrating Vehicle Surveillance and High-Speed Testing into California's On-Road Emissions Model

Sanika Ravindra Nishandar, Waqas Quadri, Lucas Algrim, Steven Magbuhat, Jinhyok Heo, Satya Sardar, Jeff Long, David Quiros — California Air Resources Board

Scope of the Study

CARB's light-duty Vehicle Surveillance Program (VSP) began in the 1970s to collect emissions data representing the in-use fleet and to update the EMFAC model, focusing on gasoline vehicles and both exhaust and evaporative emissions. The current LDVSP21 effort procures test vehicles by querying California DMV registration records across all state counties, offering volunteer participants an incentive and a rental vehicle. The program's objectives are to update Base Emission Rates, start emission factors across varying soak times, and Speed Correction Factors; to update correction factors for temperature, relative humidity, and air-conditioning use; to collect organic-gas and PM speciation data for photochemical models and CARB's speciation database; and to gather nitrous oxide and ammonia data for the GHG inventory. Data collection includes baseline tests (Smog Check, FTP, Unified Cycle, US06), start-emissions tests, four arterial and seven freeway driving cycles, evaporative tests, and on-road PEMS measurements. A parallel high-speed driving effort addresses the fact that real freeway speeds exceed the ranges historically tested.

Results

High-speed driving data were drawn from two large sources: the National Emissions Inventory Streetlight dataset (a nationwide set of 13 billion trips recorded by 20 million devices, based on one year of 2020 data with a top speed bin of 75 mph) and a UC Davis datalogging study of 200+ internal-combustion vehicles logged for a year from 2015–2020 with no top-speed limit. Vehicle selection for testing covered passenger cars, SUVs, and trucks up to 10,000 lbs GVWR, model years 2015–2023, with three new high-speed dynamometer cycles — Freeway Cycle 8 (average 83 mph), Freeway Cycle 9 (93 mph), and Freeway Cycle 10 (103 mph) — added on top of the existing FC1–FC7 reference cycles. Base Emission Rates were reconstructed from Regime Fractions (the percentage of vehicles in low, normal, moderate, and high emission regimes by mileage bin, from the In-Use Verification Program) and Regime Emission Rates (the mean emission rate of vehicles in each regime, from VSP). Technology-group updates spanned LEV I through LEV III, with LEV III sub-categories sharing base regressions with LEV II equivalents or scaled by a ratio-of-standards derived from certification limits. Speed Correction Factors were generated by normalizing emissions to Unified Cycle Bag 2, binning averaged emission rates in 5-mph increments, and fitting curves; example HC, CO, and NOx correction-factor curves were produced across the full speed range.

Key Conclusion

Vehicle Surveillance Program data combined with high-speed driving testing significantly enhance CARB's ability to reflect real-world California driving conditions. The effort updated the VMT distribution, Base Emission Rates, and Speed Correction Factors to improve the accuracy of emissions modeling, and these enhancements strengthen CARB's capacity to support air-quality planning and regulatory development with more robust emissions estimates. The high-speed correction factors are particularly relevant given that a growing share of the EMFAC2025 vehicle population is subject to them, ensuring the model captures the elevated emissions associated with sustained freeway speeds that earlier test cycles did not represent.

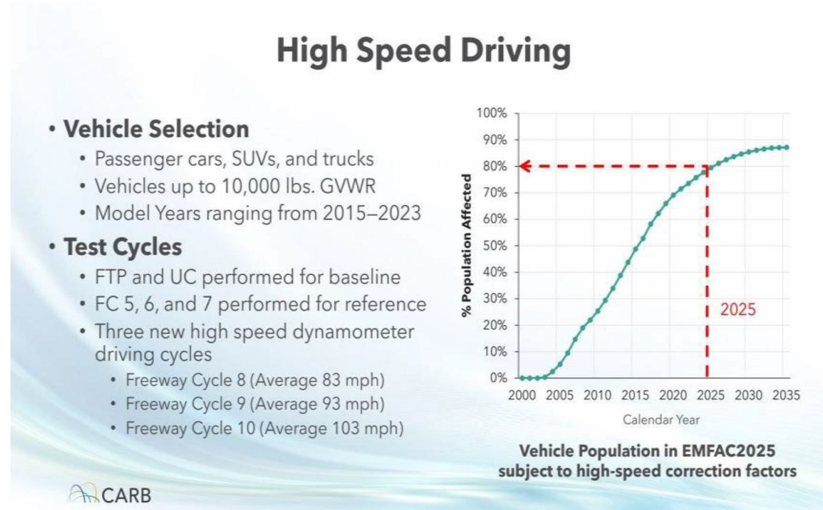

Figure 14 High-speed driving program: passenger cars, SUVs, and light trucks (MY 2015–2023) tested on three new dynamometer cycles averaging 83, 93, and 103 mph, addressing a growing share of the EMFAC2025 population.

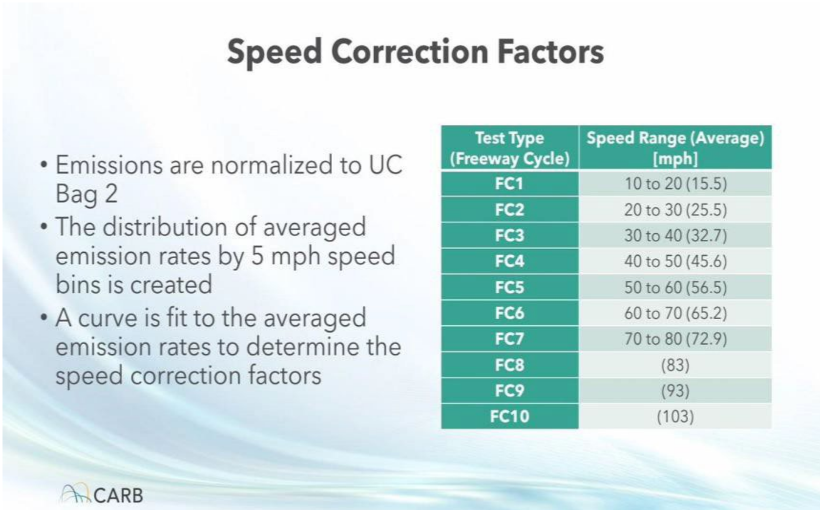

Figure 15 Speed Correction Factors are built by normalizing emissions to Unified Cycle Bag 2 and fitting curves across 5-mph speed bins, spanning freeway cycles from 15.5 to 103 mph average.

Comprehensive Update of Aircraft Emissions Inventory for South Coast AQMD

Rui Zhang, Zorik Pirveysian, Eric Praske, Marc Carreras Sospedra, Cui Ge, Sang-Mi Lee — South Coast AQMD and Integra Environmental Consulting

Scope of the Study

Aviation accounts for a significant portion of emissions in the South Coast Air Basin and is projected to increase, even as ground support equipment and on-airport ground transportation are accounted for under other source categories. With the basin needing further reductions to attain the 70 ppb ozone standard, the study updated emissions inventories for a total of 41 airports — 7 commercial, 31 general aviation, and 3 military — for the 2023 base year and 2032, 2036, and 2041 milestone years. The FAA's Aviation Environmental Design Tool (AEDT version 3g) was used for commercial and general-aviation airports, while military airports provided official activity data and emissions estimates. The update applied the Landing and Take-off (LTO) cycle for commercial and GA airports and the Flight Operation (FO) cycle for military airports, with all available aircraft types considered (excluding helicopters at commercial and GA airports). Input data were refined extensively: total operations and fleet mix from major airports and FAA databases, detailed airframe/engine models and purchased FlightAware 2023 data, representative mixing-layer heights from WRF meteorological modeling rather than the AEDT 3,000-ft default, and aircraft-specific stage lengths.

Results

The update incorporated airport-specific taxi times (for example, LAX taxi-out rising from the AEDT default of 14.55 minutes to 17.37 minutes in 2023 and a projected 23.56 minutes in 2041), runway-utilization patterns, and auxiliary power unit (APU) times that exceed AEDT defaults. For the 2023 base year, South Coast aircraft emissions were estimated at 19.34 tons/day of NOx and 0.65 tons/day of PM2.5, alongside VOC, CO, and SOx. Commercial airports accounted for the majority of emissions — 88% of NOx and approximately 42% of PM2.5 — with LAX alone contributing 62% of NOx. APUs contributed about 7% of total NOx and roughly 54% of total PM2.5 at commercial airports, prompting CARB to consider a regulatory concept to reduce APU emissions under its Statewide Clean Aviation Initiative. A notable finding was that certain newer-generation engines improve fuel efficiency but increase NOx, especially during take-off mode — for example, replacing a Boeing 737-800 with a 737-MAX8 can raise LTO NOx even as fuel use falls. Consequently, NOx emissions at commercial airports are projected to grow faster than total aircraft operations. Gate operations and taxiing together contribute about 23% of NOx and 73–80% of PM2.5 at commercial airports.

Key Conclusion

South Coast AQMD developed an updated, comprehensive aircraft emissions inventory for 2023, 2032, 2036, and 2041 using AEDT v3g with updated activity, fleet mix, airport-specific parameters, and improvements for general aviation, military aircraft, and APU emissions. By 2041, aircraft emissions are projected to increase 77% for NOx and 38% for PM2.5, driven partly by fleet-mix changes in which newer engines trade fuel efficiency for higher take-off NOx. The substantial refinement of taxi times, mixing-layer heights, stage lengths, and APU estimates markedly improves the inventory's real-world representativeness and supports regulatory planning, including emerging concepts to control APU emissions.

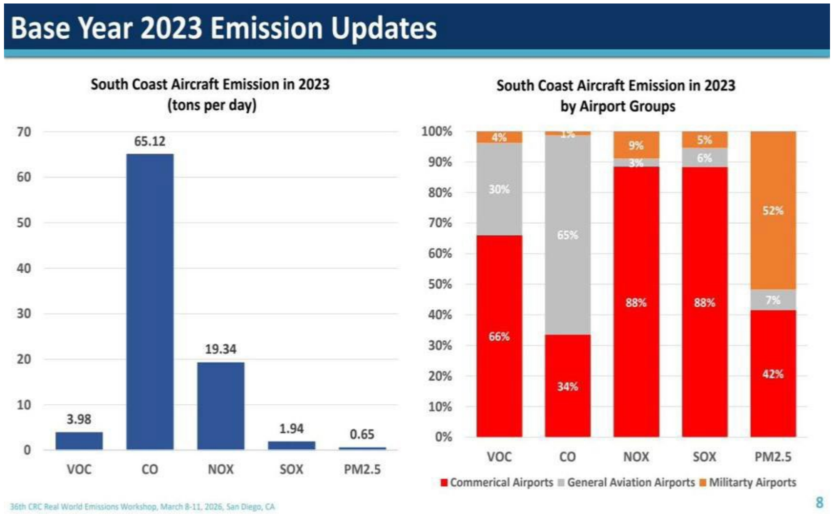

Figure 16 2023 South Coast aircraft emissions by pollutant and airport group; commercial airports dominate (88% of NOx, ~42% of PM2.5), with NOx at 19.34 tons/day and PM2.5 at 0.65 tons/day.

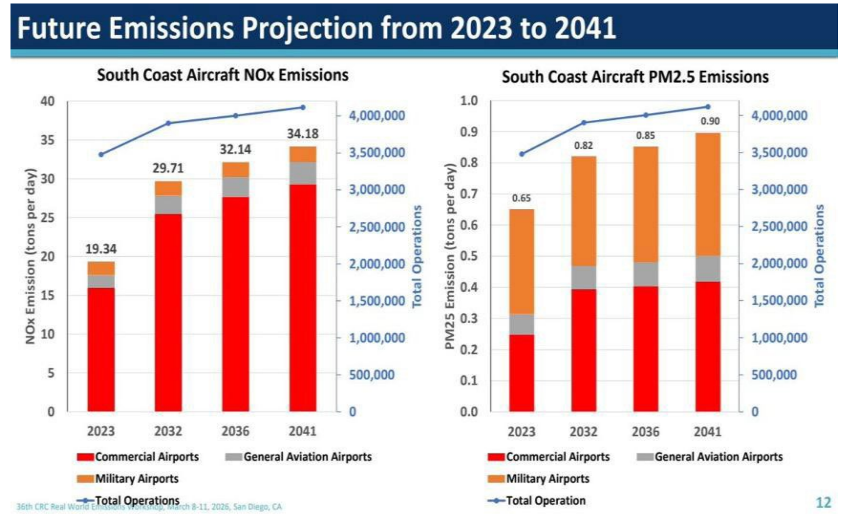

Figure 17 Future projection 2023–2041: NOx rises faster than total operations (to ~34 tons/day) because newer engines increase take-off NOx even as fuel efficiency improves; PM2.5 also climbs.

Section 3. Inspection, Maintenance, and Compliance Programs

Overview — Clean Truck Check Referee Program (CARBTest)

Thomas Durbin, Kent Johnson, Georgios Karavalakis, Ryan Vazquez (UC Riverside); Athanasios Alexandrou (CSU Fresno); Andrew Burnette (Measure Mission)

Scope of the Study

Heavy-duty diesel vehicles represented 52% of on-road NOx and 54% of on-road PM in 2020, and CARB field testing found that approximately 11–17% of HDDVs had a malfunction indicator light on, suggesting a maintenance or repair need. Senate Bill 210 (Leyva, 2019) directed CARB to develop a comprehensive heavy-duty inspection and maintenance program, now implemented as Clean Truck Check. Within that program, the CARBTest Referee Program provides independent evaluations of heavy-duty vehicles and services for vehicles with inspection incompatibilities or compliance issues, acting as a critical backstop to ensure compliance testing can be completed in rare situations where a vehicle cannot complete the normal test or is flagged by CARB for further inspection. The program offers free testing assistance for complicated inspection cases, conducting visual inspections, smoke-opacity tests for pre-2013 vehicles and OBD scans for 2013+ vehicles, verifying engine changes, alternative-fuel-system retrofits, and motorhome conversions, providing a part-locator service and support center, and approving compliance extensions.

Results

The Clean Truck Check program is expected to be one of the most impactful CARB programs approved in decades. Projected emissions reductions include 8.6 tons per day of NOx and 0.09 tpd of PM in the San Joaquin Valley in 2024, and statewide reductions of 81.3 tpd NOx and 0.7 tpd PM by 2037. The associated health benefits include roughly 7,500 avoided premature deaths and 6,000 avoided hospitalizations statewide, with monetized benefits of $75.8 billion over 2023–2050; the program would reduce NOx from heavy-duty vehicles over 14,000 lbs by 50% in 2031, rising to 56% by 2037 versus baseline. Organizationally, UC Riverside is the prime contractor with CSU Fresno subcontracting for the San Joaquin Valley, operating across three regions (Southern California, San Joaquin Valley, Northern California) through 10 referee sites staffed by trained field inspectors. Phase 1 test sites at UCR and CSU Fresno began operating in 2023; Phase 2 added eight further locations at community colleges and other facilities in 2024–2025 (Rio Hondo, Santa Ana, Palomar, Miramar, Bakersfield, Las Positas, Sacramento Depot Park, and Alameda), supplemented by virtual inspections. From March 2025 through February 2026, the program completed 681 total referee inspections spanning state-directed actions, tampering cases, refusals, CTC referrals, motorhome-conversion and engine-change verifications, alternative-fuel-system retrofits, and test-incompatibility cases.

Key Conclusion

CARBTest provides a critical compliance backstop and free testing assistance for the most complicated heavy-duty inspection cases, integrated with CARB's Clean Truck Check Vehicle Inspection System (CTC-VIS) portal and the CARBTest.org scheduling dashboard. As the Clean Truck Check program continues to be fully implemented, the referee program's monthly inspection volumes have grown sharply (from 18 in March 2025 to over 100 per month by early 2026). Next steps include ramping up inspections, expanding inspection capacity, and enhancing integration with the CTC-VIS website to support the program's substantial projected NOx and PM reductions and associated public-health benefits.

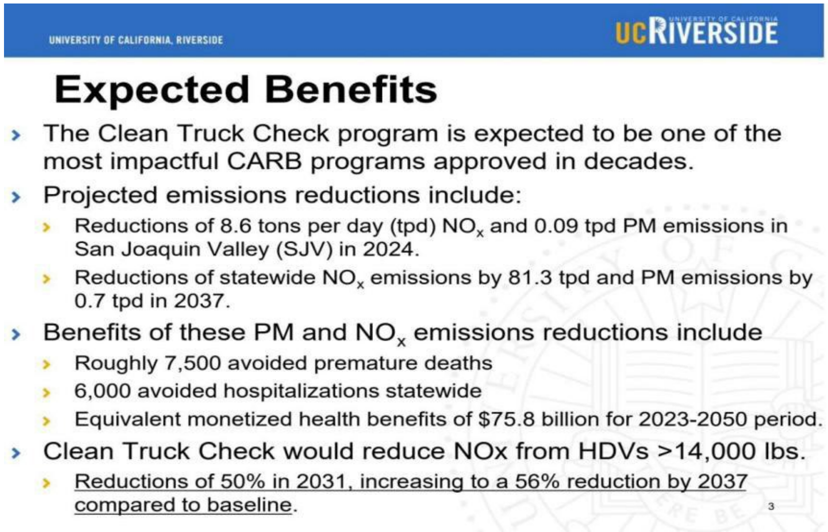

Figure 18 Projected Clean Truck Check benefits: 81.3 tpd NOx and 0.7 tpd PM reductions statewide by 2037, ~7,500 avoided premature deaths, and $75.8 billion in monetized health benefits.

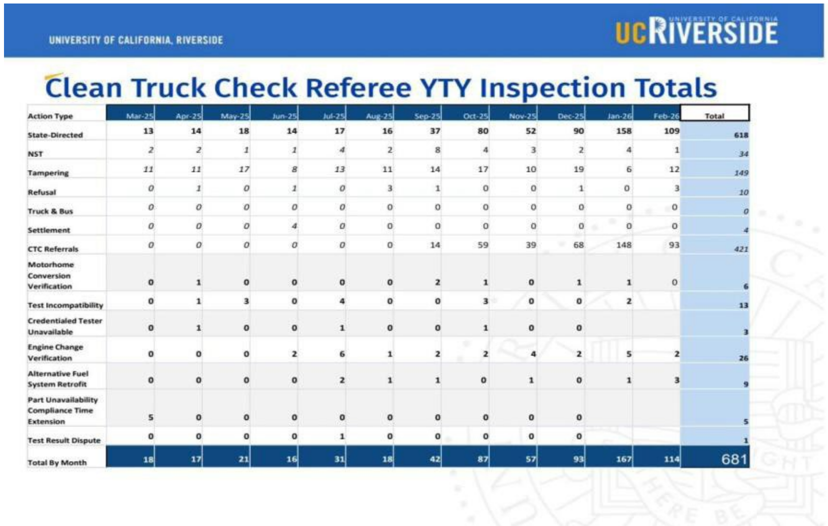

UNIVERSITY OF CALIFORNIA, RIVERSIDE

UCRIVERSIDE

Clean Truck Check Referee YTY Inspection Totals

Action Type	Mar-25	Apr-25	May-25	Jun-25	Jul-25	Aug-25	Sep-25	Oct-25	Nov-25	Dec-25	Jan-26	Feb-26	Total
State-Directed	13	14	18	14	17	16	37	80	52	90	158	109	618
NST	2	2	1	1	4	2	8	4	3	2	4	1	34
Tampering	11	11	17	8	13	11	14	17	10	19	6	12	149
Refusal	0	1	0	1	0	3	1	0	0	1	0	3	10
Truck & Bus	0	0	0	0	0	0	0	0	0	0	0	0	0
Settlement	0	0	0	4	0	0	0	0	0	0	0	0	4
CTC Referrals	0	0	0	0	0	0	14	59	39	68	148	93	421
Motorhome Conversion Verification	0	1	0	0	0	0	2	1	0	1	1	0	6
Test Incompatibility	0	1	3	0	4	0	0	3	0	0	2		13
Credentialed Tester Unavailable	0	1	0	0	1	0	0	1	0	0			3
Engine Change Verification	0	0	0	2	6	1	2	2	4	2	5	2	26
Alternative Fuel System Retrofit	0	0	0	0	2	1	1	0	1	0	1	3	9
Part Unavailability Compliance Time Extension	5	0	0	0	0	0	0	0	0	0			5
Test Result Dispute	0	0	0	0	1	0	0	0	0	0			1
Total By Month	18	17	21	16	31	18	42	87	57	93	167	114	681

Figure 19 Clean Truck Check Referee year-to-year inspection totals (Mar 2025–Feb 2026): 681 inspections across categories, with monthly volume rising sharply as the program scales.

Heavy-Duty Diesel Vehicle Deterioration: Impact of Vehicle Age and Emission Control Technology on NOx Emissions

Amber Allen, Andrew Coleman, Darrell Sonntag, Gary Bishop — Brigham Young University and University of Denver

Scope of the Study

Heavy-duty diesel NOx control has evolved through three technology generations: engine control for 2000-and-older engines, exhaust gas recirculation (EGR) for 2001+ engines, and selective catalytic reduction (SCR) systems for 2009/2010+ engines. Recent California data show fleet-wide NOx emissions increasing, and the aging of SCR-equipped trucks could be a contributor, since very high NOx at newer ages can indicate SCR tampering and SCR systems may deteriorate with age. The central question was how SCR and non-SCR control technologies perform as they age. The study drew on the EPA engine certification database (updated quarterly, containing manufacturer, model, year, and control technology) and roadside remote-sensing measurements using two methods — FEAT and OHMS — both of which capture license-plate images linked to chassis information (state, model year, weight) and engine information (manufacturer, model, model year). Campaigns spanned multiple years and locations in California and Utah (Cottonwood, Peralta, Perry, Stockton, West Valley City), covering engine-control, EGR, and SCR+EGR vehicles across a wide age range.

Results

Fleet-average emissions analyzed by age showed a clear pattern: ages 0–6 had significantly less NOx, ages 6–8 saw a significant increase, and ages 8–12 exhibited a significant increase with high variability. Comparing technologies, SCR-equipped trucks emitted the same or higher NOx than EGR-only vehicles at the same ages; both SCR and EGR-only vehicles initially emitted less NOx than engine-control vehicles at younger ages, but at later ages their emissions surpassed those of engine-control vehicles where overlapping data existed. By manufacturer, an aging trend was observed across all manufacturers for 2009–2018 engine model years (2019–2021 model years were harder to interpret), and 2009–2015 Cummins engines showed generally higher predicted mean emissions by age, consistent with a recall of 2010–2015 Cummins engines. On lifetime emissions, real-world data indicated that at ages 1–12 SCR-equipped trucks emit 20–75% less NOx than non-SCR trucks, with an overall lifetime reduction of about 16% relative to engine-control and EGR vehicles. By contrast, MOVES estimates an 80% lifetime reduction for SCR-equipped vehicles relative to engine-control vehicles and a 57% reduction relative to EGR vehicles, and MOVES lifetime estimates for engine-control vehicles were significantly higher than the real-world-derived estimates.

Key Conclusion

Fleet-average NOx from SCR-equipped trucks becomes comparable to or higher than that of non-SCR trucks after several years of aging (around age 6), and this high NOx from older SCR-equipped trucks erodes the benefit of their initially lower emissions. The authors expect real-world NOx to rise with age more than the MOVES model predicts, meaning the deterioration of SCR-equipped trucks will lead to smaller atmospheric NOx reductions than the National Emissions Inventory anticipates. More data are needed to fully understand the true impacts of aging on NOx from SCR-equipped heavy-duty diesel trucks, but the findings carry important implications for inventory accuracy and the durability expectations built into emission models.

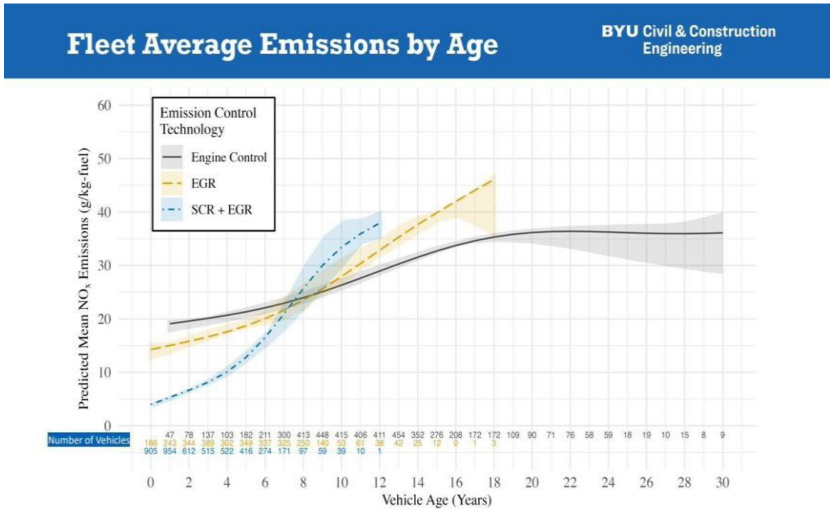

Figure 20 Fleet-average NOx by vehicle age and control technology: SCR+EGR (blue) starts lowest but rises steeply, surpassing engine-control (gray) and approaching/exceeding EGR (orange) after ~age 6–8.

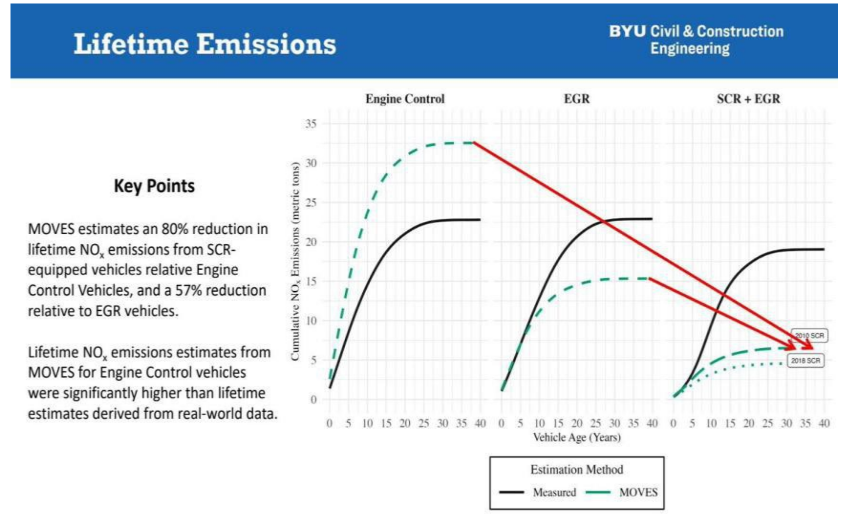

Figure 21 Measured vs MOVES lifetime cumulative NOx: MOVES (green dashed) overstates engine-control emissions and assumes far larger SCR benefits than real-world measurements (black) support.

A Comparison of On-Board Diagnostics Results with On-Road RSD, Mass Transient IM240, and FTP Exhaust Results

Rob Dawson, Jim Sidebottom, Bin Liu, Jim Kemper — Colorado

Scope of the Study

Set against Colorado's air-quality status, the study compares the ability of three testing methods to identify high NOx emitters: the OBD test, the mass-transient IM240 test, and the remote-sensing-device (RSD) network. Colorado's OBD test exempts the first seven model years and applies pass/fail to vehicles in their 8th through 11th model year (for 2024, model years 2014–2017), with readiness rules on monitors; in 2024 it ran 366,666 initial tests with 21,229 failed for a commanded MIL. The IM240 is a mass, transient, 240-second test performed beginning in the 12th model year, with exhaust fails given two full back-to-back tests (eight minutes of transient loaded-mode testing before a fail); in 2024 it ran 518,031 initial tests with 20,807 failed for excessive emissions. The RSD network has clean-screened vehicles from the periodic test since 2003, operating up to 21 units per day and producing 4.7 million valid observations from 145 sites in 2024, with a random 2% holdback given full tests. A high-altitude AVL FTP test cell provides detailed but lower-volume comparisons, and dedicated lab studies recruited vehicles failing IM240, OBD, or both for FTP, IM240, SHED, and PEMS testing.

Results

The comparison consistently showed OBD missing many high emitters. In 2024 lane data, of 1,496 Tier 2 vehicles failing IM240 for NOx, 826 (55%) would have passed Colorado's OBD program, with an average NOx of 3.08 g/mi — 44 times certification and 29 times a generic OBD fail threshold; 99.9% of these had mass rates at least 19 times the OBD fail threshold. Errors of omission have cumulative effects across calendar years (1,433 in 2023 rising to a growing in-airshed total), and most such vehicles probably continue operating in the airshed. In a 125-vehicle lab study (calendar years 2011–2014, Tiers 1 and 2), 28 vehicles passed IM240 but failed the FTP and 25 passed OBD but failed the FTP; IM240 identified 91.3% of excess FTP NOx versus OBD's 72.9%, and IM240 identified 99.5% of excess HC versus OBD's 85.8%. RSD high-NOx vehicles frequently passed OBD, and an IEEE/Carnegie Mellon analysis of Colorado matched-pair data found OBD accuracy of 87% but a 50% false-pass rate for NOx over-emitters — a concern given the disproportionate environmental impact of NOx.

Key Conclusion

While the authors emphasize they are not claiming manufacturers are out of compliance, and that IM240 errors of commission are rare, each dataset has strengths and weaknesses yet all point to the same trend: OBD appears to miss a large fraction of high and very-high emitters. It seems unlikely Colorado can meet its air-quality goals while missing roughly 30–50% of the high-emitting fleet each year. The authors encourage additional research into this issue, noting that high apparent OBD "accuracy" rates are misleading because most vehicles pass and most are genuinely low emitters, masking the test's poor sensitivity to the relatively few but heavily polluting over-emitters.

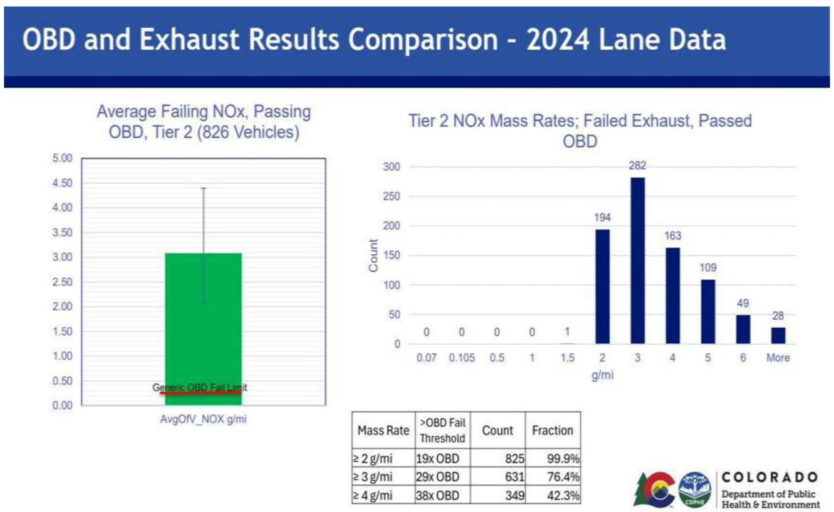

Figure 22 2024 lane data: of Tier 2 vehicles failing IM240 for NOx, 826 (55%) passed OBD, averaging 3.08 g/mi NOx — about 44× certification and 29× the generic OBD fail threshold.

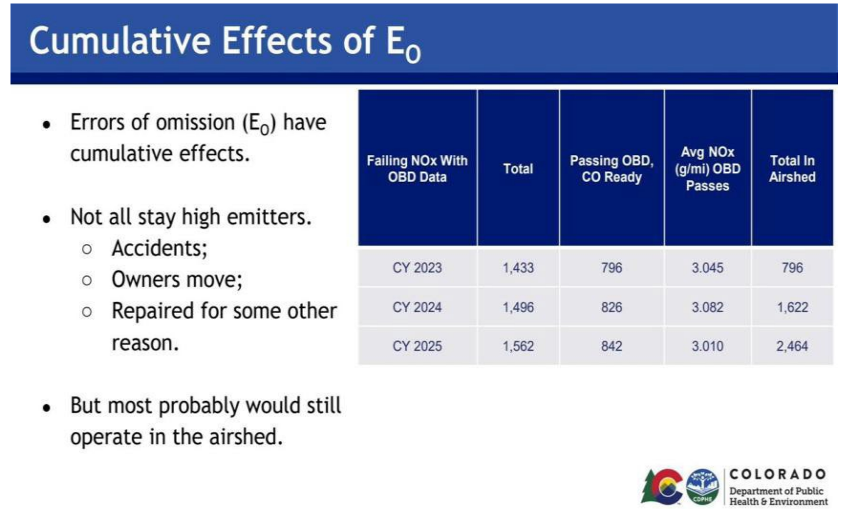

Figure 23 Errors of omission accumulate across calendar years; most high-NOx vehicles passing OBD continue operating in the airshed rather than being repaired or removed.

Alternative Power Determination Strategies for Replicating "Real-World" Off-Road Emissions Testing

Edwin Diaz, Tony Nassar, Chas Frederickson, Stephen Berdahl, Hyun Ji (Julie) Lee, Tao Huai, Mark Fuentes — California Air Resources Board

Scope of the Study

Off-road in-field PEMS testing is uniquely challenging: there is no standard OBD connection or ECU CAN message system, no unified installation protocol and limited space for PEMS installation, no standard test site analogous to a road or highway, and consequent difficulty calculating brake-specific emissions (g/bhp-hr or g/kW-hr) as required by 40 CFR 1065.650. Set within CARB's long history of heavy-duty and off-road compliance programs leading toward Tier 5, the study's overall goal was to conduct PEMS emissions testing on off-road equipment with limited or no engine ECU data during real-world operation, including Not-To-Exceed evaluation under 40 CFR 1039.515. Two objectives followed: to identify and evaluate methods for determining the power used by off-road equipment during in-field operation (interpreting the 40 CFR 1065 calculation methods and assessing the plausibility of brake-specific calculations without ECU data), and to identify and assess methods for NTE evaluation for equipment with limited or no ECU data. Three brake-power methods were compared — ECU channels (engine speed and torque), measured fuel rate combined with a Brake-Specific Fuel Consumption (BSFC) value, and a chemical-balance approach that derives fuel rate from exhaust composition then applies the fuel-rate method.

Results

Testing used a single AC dynamometer with a 2017 model-year, 7.01 L, 269 BHP Tier 4 Final diesel engine, running triplicate Cold NRTC, Hot NRTC, and RMC cycles with engine-dyno reference instrumentation (speed encoder, torque transducer, exact fuel meter, exhaust molar flow) and an AVL PEMS measuring CO, CO2, NO, NO2, THC, and CH4. Work values calculated from laboratory-measured BSFC were extremely close to the engine-dyno reference — about 0.2% error on the Cold NRTC, 0.6% on the Hot NRTC, and 0.3% on the RMC. Work values calculated using Executive Order (EO) BSFC — a single value representative of the engine family — were within roughly 8% of the dyno reference across all three cycles (7.2% Cold NRTC, 4.5% Hot NRTC, 6.4% RMC), with the largest error on the Cold NRTC. The difference between EO-based work and dyno work stems from the assumption that BSFC stays constant throughout the cycles, whereas the EO BSFC (228.4 g/kWh) is a single representative value for an engine family that may have several configurations with differing lab BSFC values (213.5–241.7 g/kWh across cycles).

Key Conclusion

Work values from laboratory BSFC tracked the engine-dyno reference to within about 0.6% for all three cycles, while EO-based BSFC produced about an 8% difference. Despite that gap, the EO-based BSFC provides a reasonable screening-level estimate of engine work for equipment lacking ECU data, since the discrepancy is attributable to assuming constant BSFC. Next steps include studying additional methods to calculate torque without using a BSFC, conducting proof-of-concept testing in the field, identifying and assessing methods for NTE evaluation with limited or no ECU data, and validating additional sensors to enable further testing types — collectively advancing the ability to perform regulatory-grade off-road emissions testing on equipment that lacks accessible ECU data.

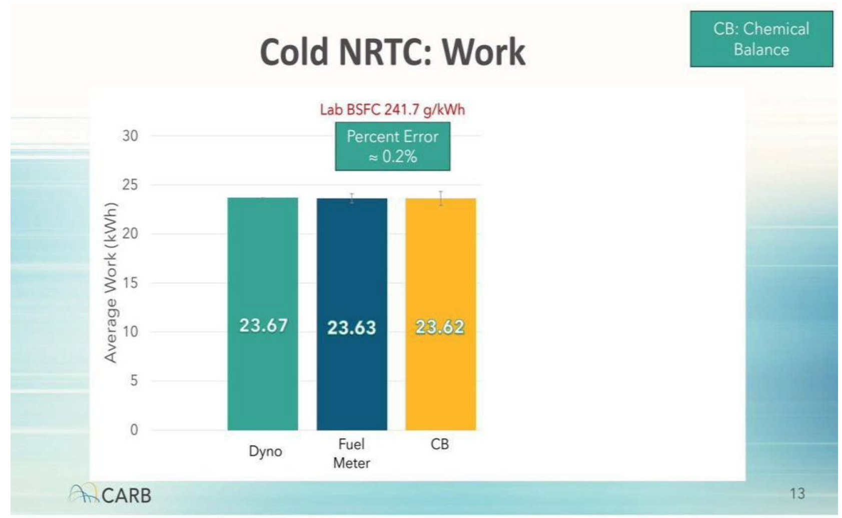

Figure 24 Cold NRTC work: laboratory-BSFC and chemical-balance methods match the engine-dyno reference within ~0.2%, while EO-BSFC methods differ by ~7.2%.

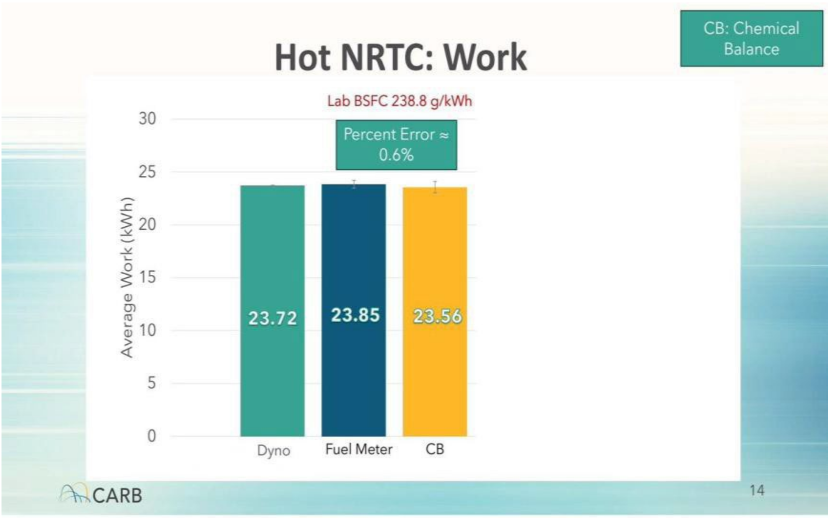

Figure 25 Hot NRTC work comparison: laboratory-BSFC methods remain within ~0.6% of the dyno reference; EO-BSFC methods (single family value of 228.4 g/kWh) differ by ~4.5%.

Co-Benefit Effect of Air Pollutants and GHGs Emission Abatement by Net-Zero Strategy in Taiwan

Jiun-Horng Tsai, I-Chen Yeh — National Cheng Kung University, Taiwan

Scope of the Study

Taiwan (about 36,000 km² and 23 million people) had 22.83 million vehicles in 2024, including 14.38 million motorcycles, 8.44 million gasoline vehicles, 870 thousand diesel trucks, and 804 thousand EVs and e-motorcycles. On-road vehicles contributed about 13.4% of national PM2.5, 41.1% of NOx, and 24.5% of NMHC emissions (2023), plus roughly 13% of national greenhouse-gas emissions. Taiwan adopted a 2050 Net-Zero Roadmap, revised in 2025, with a midterm target of 36–40% GHG reduction by 2035 and a transport-sector strategy including commercial-vehicle electrification, decarbonization, and sustainable aviation fuel. The study estimated the potential 2035 abatement of criteria pollutants (PM2.5, NOx, NMHC) and CO2 from the on-road sector under the net-zero strategy, proposed advanced measures to increase reduction potential, and evaluated co-benefits. Emissions were estimated for 2024 and projected for 2035 using vehicle numbers and mileage, emission and deterioration factors, EV numbers, biofuel consumption, electricity carbon intensity, and public-transport loading, with four enhanced measures: Scenario A (raising EV share for motorcycles and passenger cars), Scenario B (accelerating phase-out of old diesel trucks and buses), Scenario C (increasing biofuel application), and Scenario D (raising public-transport loading).

Results

Total on-road mileage was projected to decline 9.4% by 2035, with old vehicles almost entirely phased out. Emission factors for PM2.5 and NOx fall significantly due to stricter standards and a higher share of renewable electricity, and emissions of PM2.5, NOx, and NMHC drop substantially — though diesel trucks and buses remain the major NOx source by 2035. GHG emissions from on-road vehicles and public transport fall around 50% by 2035, helped by a greater share of passenger mileage shifting to public transport and lower electricity emission factors. Examining the four enhanced measures, EV measures (A) and public-transport measures (D) reduce NOx from motorcycles and gasoline vehicles, while the diesel-truck program (B) reduces emissions from diesel trucks and buses; biofuel measures (C) reduce NMHC and PM2.5 across vehicles but can increase NOx. For co-benefits, EV and public-transport measures could significantly co-benefit abatement of PM2.5, NMHC, and GHGs; the diesel-truck program also shows co-benefits; and the biofuel measure presents both a positive effect (PM2.5, NMHC) and a negative effect (NOx). All enhanced measures abate more GHG emissions.

Key Conclusion

No single measure could significantly abate all criteria pollutants (PM2.5, NOx, and NMHC) and GHG emissions simultaneously from Taiwan's on-road vehicles under the 2050 Net-Zero Pathway. However, implementing the enhanced measures together could abate more of the various air pollutants and GHGs respectively. Taiwan still faces the challenge of attaining PM2.5 and ozone air-quality standards over the next decade, so further research is needed to develop a strategy that achieves the co-benefit effect of simultaneous air-pollutant and GHG abatement — recognizing that biofuel in particular creates a trade-off by lowering particulate and hydrocarbon emissions while raising NOx.

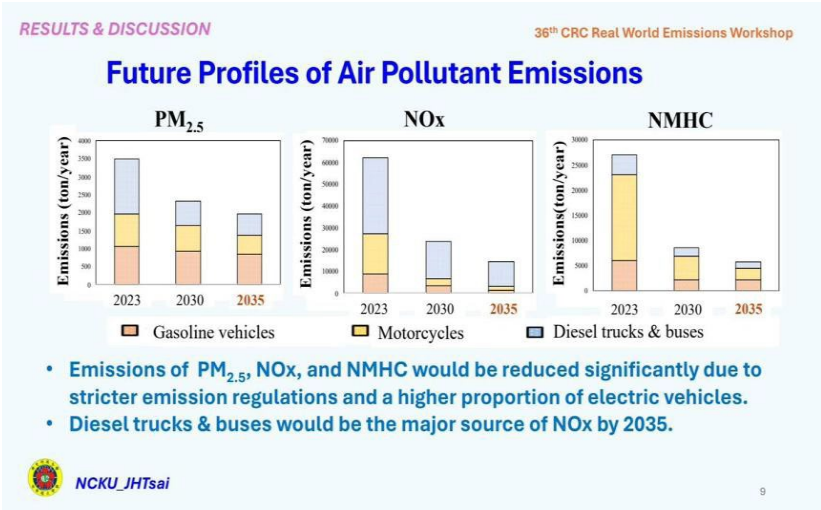

Figure 26 Projected PM2.5, NOx, and NMHC emissions for 2023, 2030, and 2035 fall sharply with stricter standards and more EVs; diesel trucks and buses remain the dominant NOx source by 2035.

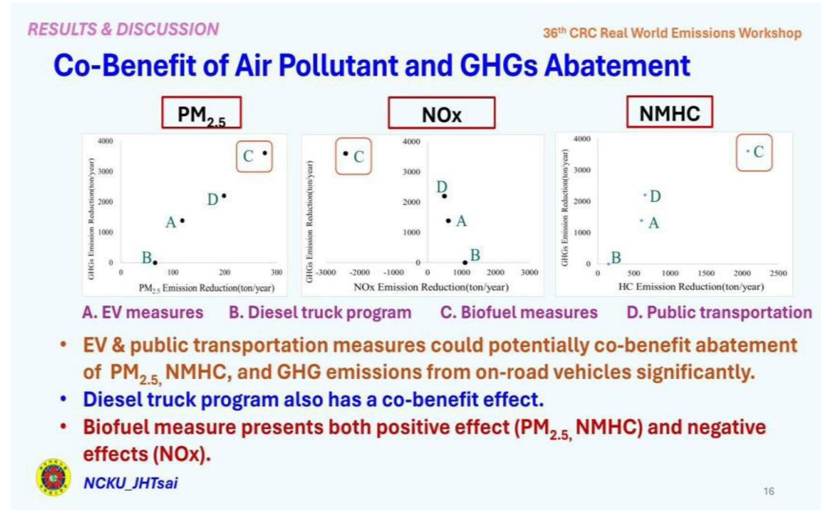

Figure 27 Co-benefit analysis of the four enhanced measures: EV (A) and public-transport (D) measures co-benefit PM2.5, NMHC, and GHGs; biofuel (C) helps PM2.5/NMHC but increases NOx

.

Section 4. Fuels, Aftertreatment, and Alternative Energy

An Update on the Assessment of the Long-Term Impact of Contaminant Metals and Phosphorus on Low NOx Aftertreatment

Christopher Sharp — Southwest Research Institute

Scope of the Study

Maintaining the ASTM specifications for biodiesel (D6751, introduced 2002) is an ongoing effort that has required repeated updates as engine technology and demand evolve. Two current market trends drive new technical work: decarbonization is increasing demand for higher biodiesel and renewable-diesel blends (B50, B100), and new MY2027+ emission regulations will significantly change diesel engines and their aftertreatment via Ultra Low Emission Diesel Engines (ULEDE). Current diesel aftertreatment achieves about 96–97% NOx reduction; 2027+ ULEDE systems target 99.5% reduction, with tailpipe FTP/RMC NOx tightening from 200 to 35 mg/hp-hr and full useful life extending from 435,000 to 650,000 miles. The central question is whether ASTM specifications need modification for higher blends in ULEDE engines. A B100 ULEDE Steering Committee of OEMs, suppliers, and labs operates like CRC, with quarantined data later released for ASTM consideration. The strategy uses the Diesel Aftertreatment Accelerated Aging Cycle (DAAAC) protocol — an EPA-accepted aging method under 40 CFR Part 1065.1131-1145 targeting a 10x acceleration — with ULSD doped with metals and phosphorus to determine definitively whether metals or phosphorus, rather than B100 combustion nuances, drive NOx-performance loss.

Results

The demonstration used a 2017 Cummins X15 engine with advanced low-NOx aftertreatment (dual SCR, dual dosing) and cylinder deactivation, aged via DAAAC. Market levels from the NREL B100 quality report informed dosing: 2024 mean values were 0.449 ppm Na+K (over 80% below 0.5 ppm), 0.343 ppm Ca+Mg (over 90% below 0.5 ppm), and 0.796 ppm phosphorus (over 85% below 1 ppm), so the committee chose to begin "high" at 2 ppm total metals and 1 ppm phosphorus. The first run (System 1, 2 ppm metals / 1 ppm phosphorus) generated results at 435k and 650k miles; NOx conversion was affected more than the zero-metals Stage 3RW reference at 650k, ending the test. The second run (System 2, 1 ppm metals / 0.5 ppm phosphorus) split the difference. At 435k miles, NOx conversion loss showed a clear dose response: Stage 3RW lost 0.15% (FTP), 0.66% (LLC), 0.18% (RMC); System 2 lost 0.27%/0.70%/0.18%; and System 1 lost 0.36%/0.95%/0.33%. The 1/0.5 ppm system showed no statistical difference from the reference (FTP was at the edge), but the 2/1 ppm system did. Metals and phosphorus affected the light-off SCR and the diesel oxidation catalyst more than the petrodiesel reference, and at 650k with System 1 these impacts were large enough to cause tailpipe NOx-conversion loss and degraded DOC active/passive regeneration.

Key Conclusion

A measurable dose response to metals and phosphorus was observed at these levels — described as "a good thing" because it provides valid dose-response curves for both internal OEM modeling and ASTM specification-setting. At 435k miles the effects were relatively small, with the downstream SCR compensating for upstream LO-SCR and DOC impacts, but at 650k with higher metals/phosphorus the effects caused real NOx-margin loss on FTP and LLC. Catalyst post-mortem testing (segmenting cores axially, with metallography at ORNL) is matching performance changes to poison deposition. Next steps include completing System 2 testing at 650k, additional post-mortem analysis, and investigating practical production-control test methods for metals and phosphorus (alternatives to ICP-MS); these results, combined with test-method capability, regulatory needs, and industry deliberation, will inform proposed ASTM metals and phosphorus specifications for B100 use in ULEDEs and lower blends.

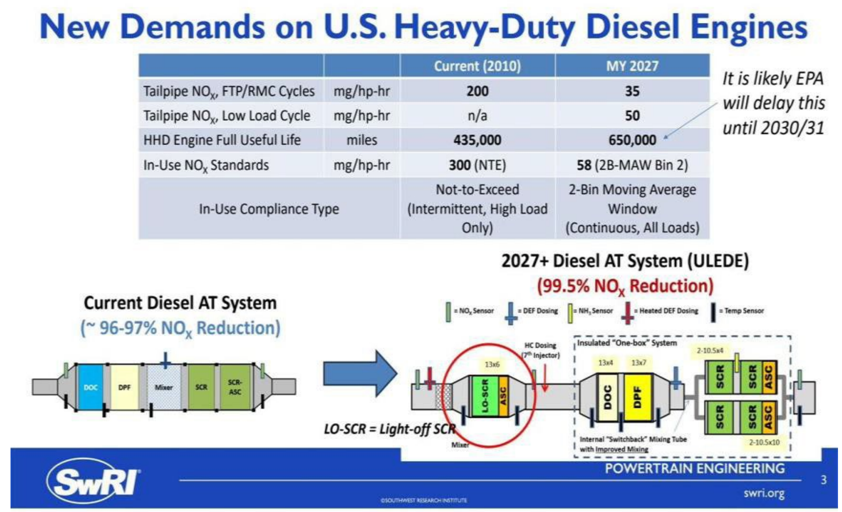

Figure 28New demands on heavy-duty diesel engines: MY2027 tightens FTP/RMC NOx from 200 to 35 mg/hp-hr and extends full useful life to 650,000 miles, requiring 99.5% NOx-reduction ULEDE systems.

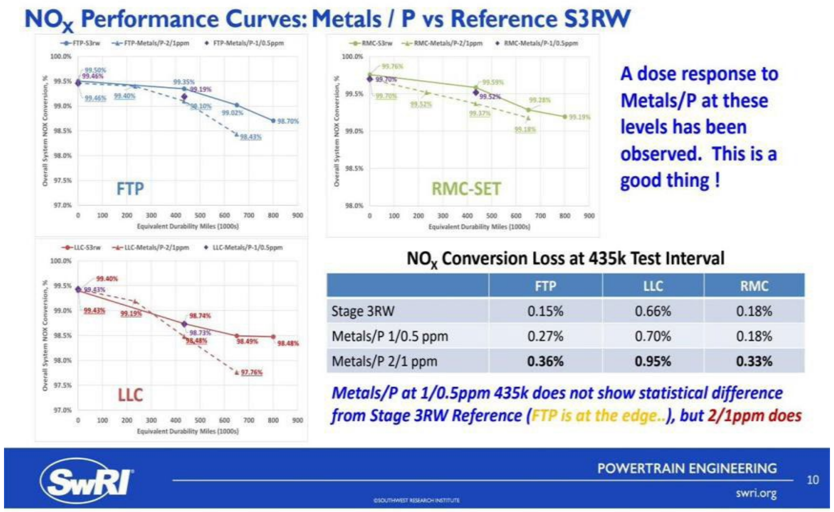

Figure 29 NOx conversion loss at 435k miles shows a clear dose response: 2/1 ppm metals/phosphorus (System 1) differs from the Stage 3RW reference, while 1/0.5 ppm (System 2) does not.

Impacts of B100 on Emission Stability in Heavy-Duty Systems

Simone Costa, Reto Schegel, Priftis Konstantinos — FPT Industrial (Iveco Group)

Scope of the Study

With growing interest in biofuels such as B20 and B100 to meet global sustainability targets, FPT Industrial — the powertrain brand of Iveco Group — evaluated the long-term impacts of B100 on Stage V aftertreatment systems, focusing on emission stability and component aging. Biodiesel's chemical composition differs from standard B7 diesel, with generally higher oxygen, alkaline-earth-metal, and phosphorus content, which alters combustion characteristics. Testing was conducted on two identical FPT Stage V aftertreatment systems built around the FPT Cursor 9 Stage V engine with a production DOC + SCR-on-Filter (SCRoF) architecture from a combine application; one system was fueled with standard B7 and the other with pure B100. The B100 was a special blend designed to deliver, within an 800-hour TME091 aging cycle, the full-useful-life (8,000-hour) amount of poisoning elements (Na, K, Ca, Mg, and P). The standardized aging cycle operated at high speed (2,000–2,200 RPM), low-to-mid load, with aftertreatment temperatures between 275 and 425 °C, while comprehensively monitoring SCRoF performance, oil quality, and backpressure.

Results

Emissions remained stable along the cycles relative to NOx, but the diesel oxidation catalyst showed stronger aging characteristics with B100, and B100 led to significantly faster oil degradation than B7. The primary impact of poisoning was a decrease in NO2 production from the DOC, and post-mortem (PMA) analysis revealed the highest concentration of poisoning elements in the DOC. Backpressure analysis showed the pressure drop across the SCRoF system at rated power increasing with B100 while decreasing with B7. Oil analysis (both systems starting with fresh Shell 10W-40) showed faster aging on B100 in terms of calcium, fuel-in-oil increase, and oxidation. The most obvious difference between systems was the significantly higher ash loading of B100 samples, producing not just a longer ash plug at the rear of the SCRoF but a thick ash layer on the wall even in the middle of the filter. From a performance standpoint the DOC was hurt most, followed by the SCRoF, while the SCR/AMOX was not impacted; the SCRoF impact did not directly affect NOx performance, whereas DOC aging affected NO2 values.

Key Conclusion

After 800 hours of aging, the B7 system showed minimal DOC aging while the B100 system showed significantly more pronounced DOC aging; SCRoF aging was minimal for both, though the B100 SCRoF pressure-drop increase was significantly higher. After this fuel-consumption-based aging cycle — which carried no thermal-aging effect — the aging of both systems remained within acceptable limits versus NOx and emission limits. However, the DOC aging from B100 fuel raises concerns for full-useful-life capability once the additional impacts of thermal aging are taken into account, signaling that B100 durability validation must extend beyond chemical poisoning to include thermal effects before full-life acceptance.

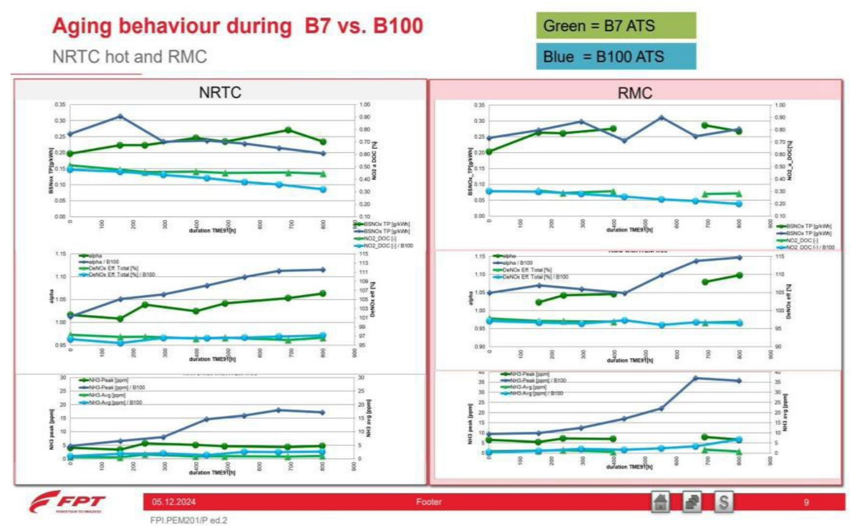

Figure 30 Aging behavior on NRTC-hot and RMC cycles, B7 (green) vs B100 (blue) aftertreatment systems, tracking emission stability over the 800-hour accelerated cycle.

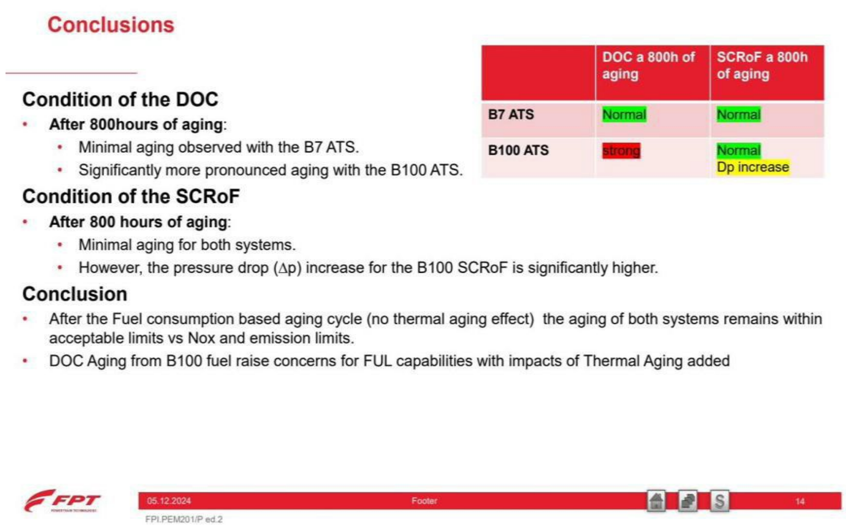

Figure 31 Post-mortem condition summary: B100 produced strong DOC aging and higher SCRoF pressure-drop increase, while B7 aging stayed normal — raising full-useful-life concerns once thermal aging is added.

Bio and Renewable Diesel Fuel Effects

Dr. Rob Middleton, Prof. Andre Boehman (University of Michigan); Dr. Andrea Strzelec (USCAR); Dr. Courtney Videchak (MARC-IV)

Scope of the Study

This work, drawing on Courtney Videchak's dissertation and the CRC AVFL-46 and DOE projects, studies how to leverage low-carbon diesel alternatives to maximize life-cycle greenhouse-gas reductions while managing the well-known emissions trade-offs of these fuels. Relative to conventional diesel, biodiesel (B100) and renewable diesel (R100) differ in oxygen content, energy content, density, cetane number, and aromatic/sulfur content, producing different effects on CO2, PM, NOx, fuel consumption, and engine efficiency — and a B50R50 blend could combine their benefits. Four key questions framed the study: how an engine responds to simply dropping the fuel into the tank; how much the engine's response can be improved through calibration; what the life-cycle GHG emissions are; and what the broader fleet impacts are. Experiments used a 2020 Ford 6.7L Powerstroke V8 diesel with an open Bosch ECU (engine-out measurements, no active aftertreatment), reducing operating points to six representative steady-state "mini-map" points and optimizing eight fuel-injection and air-path parameters in ASCMO to minimize CO2 and maximize efficiency while maintaining NOx parity with conventional diesel and operating within stability limits.

Results

Creating an optimized biodiesel calibration evaded the biodiesel-NOx effect, though interactions between brake-specific CO2 and NOx limited the optimization benefits — no operating condition met all of the diesel-baseline constraints simultaneously. For biodiesel as a drop-in, all operating conditions degraded (increased) NOx, while the optimized calibration improved most conditions. Renewable diesel could be used as a drop-in replacement with no calibration changes, with optimization improving GHG at a NOx penalty; for R100 drop-in, no operating conditions showed a statistically significant change from baseline. B50R50 behaved between biodiesel and renewable diesel and was also a viable drop-in replacement. Each renewable fuel improved the NOx–PM trade-off curves relative to diesel, but a trade-off persisted between tank-to-wheel GHG improvements and achieving NOx parity. On broader impacts, fuel economy varied within 1.5 mpg and driving distance within 60 miles across fuels and calibrations; renewable-fuel costs ran $1,000–$2,000 higher annually for 20,000 miles, but the inherent carbon-intensity benefit dropped the social cost of carbon by over $1,400. Over 10 years, adoption by 5.75 million medium- and heavy-duty vehicles (40% of the U.S. fleet) was estimated to mitigate 500+ million tons of CO2 and avoid $90+ billion in climate damages.

Key Conclusion

Renewable fuels can substantially reduce life-cycle greenhouse gases as drop-in replacements, with renewable diesel and B50R50 requiring no calibration changes and biodiesel benefiting from optimization to evade its NOx penalty. The persistent trade-off between tank-to-wheel GHG gains and NOx parity means calibration choices matter. A key experimental limitation was that only engine-out emissions were measured with no aftertreatment system; the next step is aftertreatment testing through collaboration with DOE and CRC (AVFL-46), installing diesel oxidation catalysts, particulate filters, and SCR to better understand how fuel changes propagate to tailpipe emissions — results the authors noted will be presented in a future workshop.

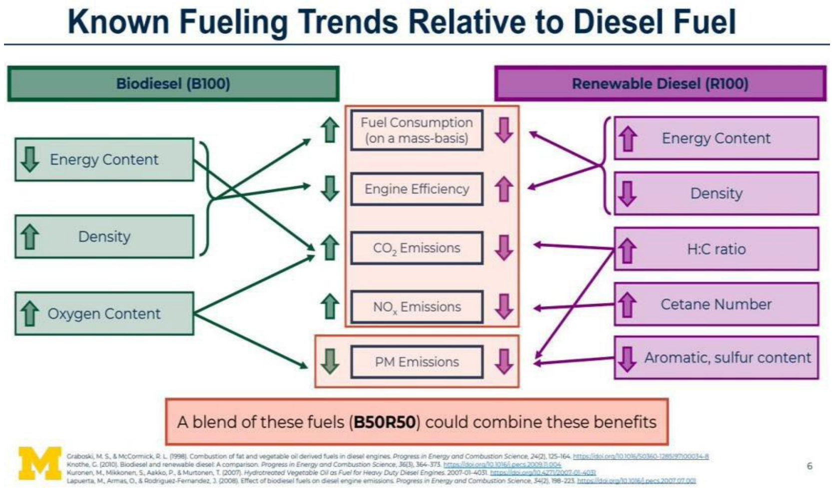

Figure 32 Known fueling trends relative to diesel: biodiesel (B100) and renewable diesel (R100) differ in oxygen/energy content, density, and cetane, producing offsetting effects on CO2, PM, NOx, and efficiency; a B50R50 blend can combine benefits.

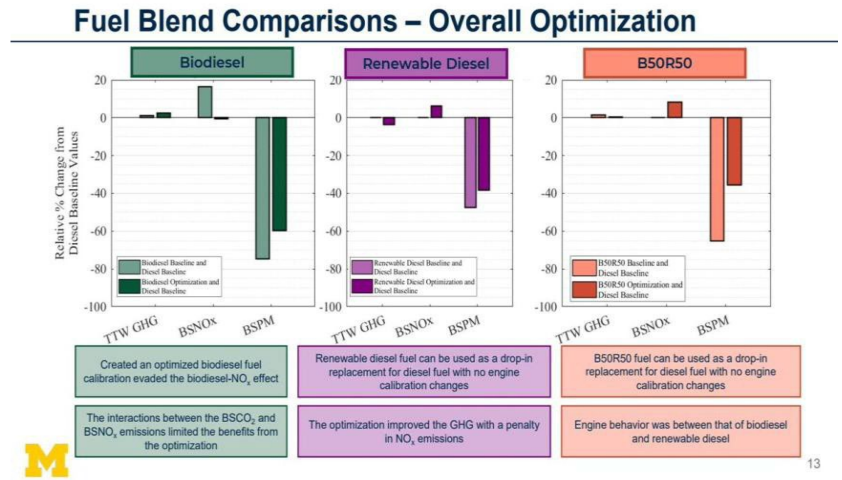

Figure 33 Fuel-blend optimization results: optimized biodiesel evades the NOx effect, while renewable diesel and B50R50 work as drop-in replacements; CO2–NOx interactions limit overall optimization gains.

Designing Comprehensive and Lifecycle-Based Independent Verification Program for Low Carbon Hydrogen and Derivatives

Hong Jin, Ph.D. — AmSpec Group

Scope of the Study

Low-carbon hydrogen — defined by significantly lower lifecycle GHG emissions than conventional production — is critical to mitigating emissions, but its "colors" (grey, blue, green, pink, turquoise, white) reflect very different production pathways and carbon intensities, and definitions differ between the EU and US. Hydrogen is essential for energy independence and manufacturing, used heavily in refineries (43 Mt in 2023) and industry (ammonia, methanol), and offers significant carbon-reduction potential for transportation per the Argonne GREET model. The industry faces challenges including reliance on government incentives, regulatory uncertainty and tariffs, and technology development and scale-up needs. The presentation reviewed current certification schemes and proposed a comprehensive lifecycle-based verification program. It noted that most schemes focus solely on carbon and differ in system boundaries and rigor: Australia's Guarantee of Origin (well-to-gate, Scope 1 and 2 only), CertifHy's phased EU RFNBO approach (well-to-gate through well-to-wheel with tightening time-matching), Korea's Clean H2 scheme, India's program, and the Inter-American Development Bank's voluntary CertHiLAC. It also highlighted that hydrogen product classifications and grades (ISO 14687:2019) and ammonia fuel standards remain inconsistent or under development.

Results

The proposed AmSpec Hydrogen Verification Program centers on three key elements: product quality control (hydrogen product analysis, production-facility inspection, review of safety SOPs), environmental impact (lifecycle carbon footprint, water-use volume and intensity, environmental permits, air emissions, water quality, waste disposal), and green/blue hydrogen validation (renewable-energy sources for green, natural-gas feedstock and CCUS for blue, chain-of-custody documents, and carbon-reduction thresholds set by certification schemes). Ancillary services span product testing/inspection/safety, lifecycle assessment and carbon accounting (Scope 1, 2, 3 GHG inventory; LCFS, 45Q, 45Z incentives; CBAM compliance; EPD certification), and monitoring/reporting/verification, supported by ISO 17025, ANSI, and LCFS certifications. The verification workflow runs from initial conformity assessment (selecting schemes and standards, developing pass/fail criteria, initial audit) through conformance and certificate issuance, product identification via a verification mark and central portal, and annual assessment with witness testing, permit review, carbon-intensity validation, and a five-year re-audit. Emerging issues include CBAM full implementation in 2026 with no de minimis exemption and country-specific default carbon intensities (e.g., US 26.640 versus UK/Canada/Qatar 10.820 tCO2e/t H2), California LCFS amendments phasing in third-party sustainability certification through 2031, and EU ETS rules requiring high carbon prices for green-hydrogen competitiveness.

Key Conclusion

Low-carbon hydrogen is critical to mitigating GHG emissions, and an "all-of-the-above" strategy offers the most effective path for the industry to thrive — innovations delivering substantial cost savings, consistent product quality, and seamless integration with existing infrastructure will prevail. Independent verification is essential to uphold transparency, consistency, and reliability during product custody transfer, thereby reducing commercial risk. Dedicated effort is needed both to improve existing standards and to develop new ones for emerging applications such as ammonia as a marine fuel, where standardization (e.g., ISO/AWI 23397 and IMO interim guidelines) is still maturing.

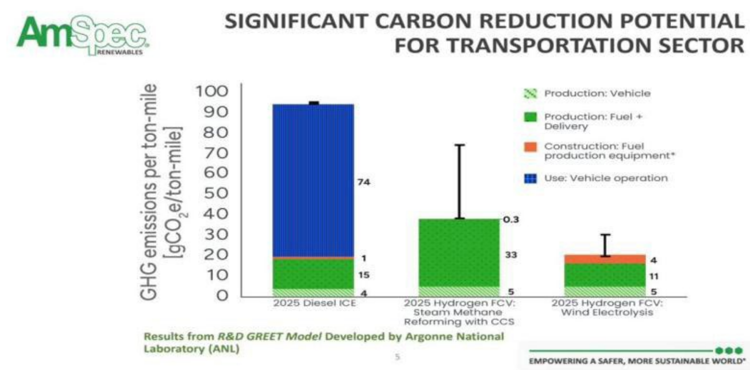

Figure 34 Significant carbon-reduction potential of low-carbon hydrogen for transportation, from the Argonne National Laboratory R&D GREET model.

Figure 35 Not all certification schemes are equal: most focus solely on carbon and differ in boundaries (well-to-gate vs well-to-wheel), time-matching, and thresholds across Australia, the EU/CertifHy, Korea, India, and Latin America.

Particle and Gas Emissions from Lithium-Ion Batteries During Thermal Runaway Fires

Imad Khalek, Ph.D. — Southwest Research Institute

Scope of the Study

Lithium-ion batteries power a wide range of devices — electric scooters, bikes, EVs, laptops, smartphones, and energy-storage facilities. Thermal runaway is a chain reaction triggered by internal overheating that can lead to an uncontrollable release of heat, flammable gases, and toxic emissions, and electric scooters are especially relevant given their lightweight, high-energy-density batteries and propensity for thermal runaway under unsafe conditions. The study provided a detailed characterization of gaseous and particulate emissions from three lithium-ion (NMC) scooter batteries (12 Ah, 36 V, 0.43 kW), each containing 50 cylindrical cells, subjected to thermal runaway by overcharging after bypassing the battery management system that would normally prevent overcharge; batteries were instrumented with internal thermocouples. The experimental setup drew flow from a blast chamber through a tunnel for venting and abatement, with FTIR sampling directly from the duct and the remaining instruments (VOC by GC-FID, PM2.5 gravimetric, MSS soot, DMS500 sizing) sampling downstream of a diluter at roughly 36:1 dilution, with a PM2.5 cyclonic separator upstream of filter collection.

The setup also included firefighter gear and cab-fabric swatches to study contamination and cleaning.

Results

Significant battery weight loss of 44–63% of initial weight was observed after the fires were extinguished. Over an average 200 seconds of thermal runaway, the most toxic gaseous species were CO and formaldehyde: CO reached up to 500 times the OSHA 8-hour 50 ppm limit and 125 times the NIOSH 15-minute 200 ppm limit, while formaldehyde reached 150 times its 8-hour 0.75 ppm limit and 56 times its 15-minute 2 ppm limit. VOC emissions were dominated by electrolytes (47–75% of total VOC) representing various carbonates; ethylene reached 446 times the OSHA 8-hour 1 ppm limit and 30 times the 15-minute limit, and 1,3-butadiene reached 26 times its 15-minute limit. PM2.5 mass concentration near the diluted fire was 12,000–17,000 times higher than the proposed EPA ambient PM2.5 standard of 9 $\mu g/m^3$, with soot/elemental carbon at 3–6% and dilute number concentrations comparable to an old-model-year diesel engine. Metallic elements dominated PM2.5 at 16–23% (rising to 34–49% if lithium is counted as Li_2O), led by lithium, then cobalt, manganese, nickel, and copper. Particles showed a small nuclei mode (16–28 nm) and an accumulation mode (109–154 nm); although filterable by an N95 mask, even a perfect mask would still expose the wearer to significant particle concentrations. On PPE, CO_2-based cleaning outperformed water cleaning, both removing over 99% of deposited metals.

Key Conclusion

Three NMC scooter batteries overcharged to induce thermal runaway emitted toxic gases (CO, CH_4, HCN, HF, formaldehyde), VOCs (ethylene, acetylene, butadiene), PM2.5, and metallic particles (Li, Ni, Cu, Mn, Co), all far exceeding OSHA limits, with PM2.5 levels 12,000–17,000 times the proposed EPA ambient standard and most particles in the respirable range below 500 nm. The study highlights the extreme toxic emissions from lithium-ion battery thermal runaway and the serious exposure risks they pose. For protective equipment, cleaning PPE swatches with water or CO_2 was highly effective (over 99%), with CO_2 cleaning outperforming water and two-cycle cleaning suggested to further reduce residual metals, while clean cab fabric such as leather retained fewer metals than traditional fabric.

Gaseous Species Measured by FTIR

- On average, over 200 seconds of thermal runaway, the most toxic species were:
  - CO and formaldehydes. CO concentration can reach 500 times the OSHA 8-hour 50 ppm limit, and 125 times the NIOSH 15-Minute limit of 200 ppm
  - Formaldehydes can reach 150 times the 8-hour 0.75 ppm limit, and 56 times the 15-minute of 2 ppm.

Mass by FTIR	Formula	Test 1 (g)	Test 2 (g)	Test 3 (g)
CARBON DIOXIDE	CO_2	71.724	770.790	574.400
CARBON MONOXIDE	CO	16.634	98.990	34.693
NITRIC OXIDE	NO	0.010	0.462	0.393
NITROGEN DIOXIDE	NO_2	<0.001	<0.001	0.009
HYDROGEN FLUORIDE	HF	0.003	0.014	0.018
HYDROGEN CHLORIDE	HCl	<0.001	<0.001	0.108
HYDROGEN CYANIDE	HCN	<0.001	0.046	0.018
FORMALDEHYDE	CH_2O	0.568	2.241	0.683
METHANE	CH_4	0.977	5.704	1.703

Figure 36 Gaseous species by FTIR over ~200 s of thermal runaway: CO reached up to 500× the OSHA 8-hour limit and formaldehyde 150×, among the most toxic species measured.

PM Metallic Elements Collected on the Filters

- Lithium dominated the emissions followed by Cobalt, Manganese, Nickel and Copper
- Metallic elements dominates $PM_{2.5}$ in the range of 16% to 23%
- If we assume Li as Li_2O, the % weight will reach 34% to 49% of total $PM_{2.5}$ concentration
- These metals could be highly toxic depending on their chemical composition.

Elements	Test 1, mg/m^3	Test 2, mg/m^3	Test 3, mg/m^3
Cobalt	0.9	1.3	1.8
Copper	0.7	1.2	1.6
Lithium	19.5	14.9	15.2
Manganese	1.4	1.6	2.3
Nickel	2.3	3.1	4.8
Sum of Metals	24.8	22.1	25.7
$PM_{2.5}$	159.5	111.1	111.9
% of PM2.5	16%	20%	23%

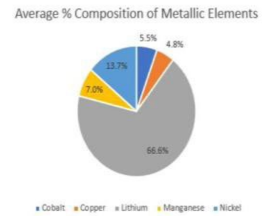

Figure 37 Metallic elements collected on PM filters: lithium dominates, followed by cobalt, manganese, nickel, and copper; metals make up 16–23% of PM2.5 (up to 34–49% as Li2O).

Comparison of Lifecycle GHG Emissions — Propane vs Electric Forklifts from a Marginal and Average Emissions Perspective

Satish Guda — Propane Education & Research Council

Scope of the Study

Using an ecosystem-and-butterfly-effect analogy, the study challenges the common framing that full electrification is the solution, arguing that while battery-electric vehicles are zero-emission at the tailpipe they are not zero-emission on a lifecycle basis, so the source of the electron matters. Generation sources and carbon-intensity scores vary by state and balancing authority, fossil fuels still dominate generation, and states import and export electricity based on demand over regional transmission. The key concept is marginal emissions — the additional emissions produced to meet the next increment of demand — which can be affected by dispatch decisions made at another location miles away, so it is important to model the dynamic variations of the system in time rather than relying on a static snapshot. PERC commissioned an S&P study (2023) that modeled hourly generation and emissions for California (CAISO), NYISO, and ISO-NE using 2019 pre-COVID data, assuming a 1% hourly demand increase in a target location while the rest of the interconnection held demand constant, then analyzed change in demand versus change in emissions on an hourly and marginal basis. This was applied to a 365-day forklift case study comparing a propane forklift against a lead-acid battery-electric forklift on an 8-8-8 charge/cool/work cycle.

Results

A snapshot example (1% load increase on June 3, 2019 at 2 PM) showed a California load change of 335 MWh producing a total WECC emissions change of 185 short tons, giving a marginal emission rate of 0.55 short ton/MWh — capturing all transmission-flow effects. California concentrates 80% of demand under CAISO, imports about a quarter of its electricity, has no in-state coal, and draws out-of-state generation dominated by gas, hydro, and coal (coal being 15% of total WECC generation). Using carbon-intensity scores from CARB LCFS, EPA eGRID, and the S&P marginal analysis, results across California, New York, and New England compared electric forklifts (annual-average versus hourly-average versus marginal data) against propane forklifts in all "flavors" (conventional, renewable from animal tallow at 43.5 gCO2eq/MJ, and from used cooking oil at 20.5), including improved-efficiency and hybridized propane variants. California's marginal grid emissions were higher than the annual-average state generation by 44%, the annual-average balancing authority by 26%, and the hourly-average balancing authority by 48%. Charging a battery between midnight and 8 AM yielded the highest marginal emissions, with variation of 2x or 3x depending on viewpoint.

Key Conclusion

Battery-electric forklifts may not result in significant emissions reductions in every scenario, sometimes shifting emissions from one point to another rather than reducing them. Hourly marginal emissions are critical and must be considered when policy decisions are made on energy sources. Running on renewable propane reduced emissions versus the marginal numbers by 11% (tallow) to 58% (used cooking oil), rising to 25%/65% for improved-efficiency engines and 55%/79% for hybridized engines. Employing renewable fuels, engine-efficiency improvements, and hybridization can achieve reductions on par with or better than full electrification. The growing electricity demand from AI data centers will significantly raise marginal emissions and grid stress, and if policy support were extended to internal-combustion and hybridization technologies comparable to what ZEVs receive, similar or greater emissions reductions could be achieved in the time- and cost-sensitive material-handling market.

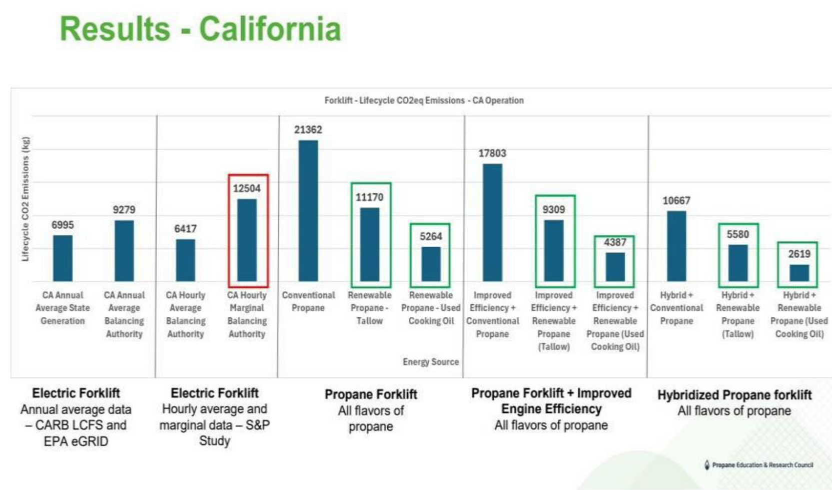

Figure 38 California 365-day forklift results: electric forklift lifecycle CO2e under annual-average, hourly-average, and marginal grid data, versus propane in all flavors plus improved-efficiency and hybridized variants.

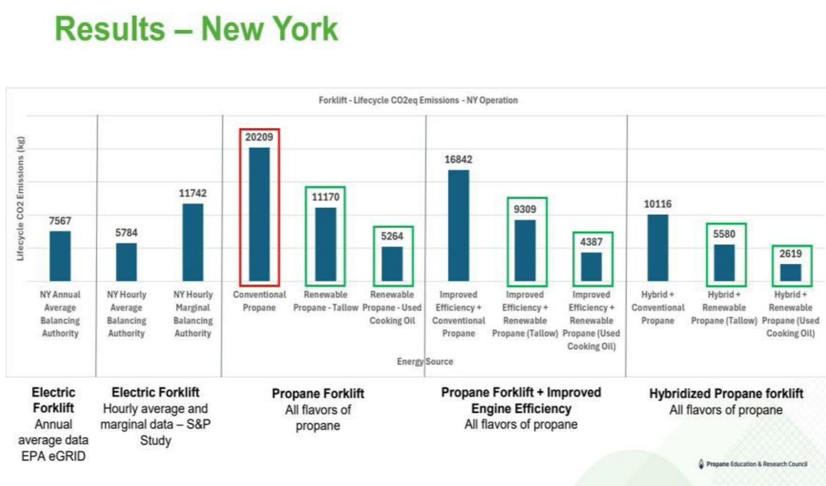

Figure 39 New York results comparison: the same forklift powertrain options show how marginal grid emissions and renewable propane reshape the lifecycle comparison across balancing authorities.

Section 5. Onboard Sensing, In-Use Measurement, and Real-World Activity

Preliminary Results of Sensor-Based Onboard Sensing Analysis and Reporting from Fleets During a Two-Month Timeframe

Grace Johnson, George Scora, Zisimos Toumasatos, Georgios Karavalakis, Thomas D. Durbin, Kent Johnson (CE-CERT); Seungju Yoon, Georges Saliba (CARB)

Scope of the Study

In-use emissions vary substantially with vehicle operation: across 189 tests of model-year 2010–2016 SCR-equipped vehicles between 2010 and 2019, 43% of activity occurred between 0–25 mph, representing 40% of NOx mass. The study contrasts three measurement approaches by accuracy and setup effort: laboratory testing (2% margin of error, but one day of data takes weeks or months to set up), in-use PEMS measurement (5%, one day takes 4–6 hours), and onboard sensing (10%, but one year of data takes under an hour to set up). A key limitation of PEMS is that emissions change between days on the same vehicle, yet PEMS data typically present a single day's measurement. To address this, the Onboard Sensing Analysis and Reporting (OSAR) system was developed for continuous annual monitoring of diesel and natural-gas technologies; it began as a consortium-led initiative and has grown to over nine funded programs. OSAR includes NOx, PM, GPS, CAN, and other sensors with auto start/shutdown to capture cold starts and all truck operation, packaged so that installers add exhaust bungs, install sensors and a wire harness, with no on-site calibration needed and data good for a year or more.

Results

The diesel analysis covered eight heavy-duty diesel fleets (model years 2013–2023, average 2021), comprising a transfer-truck fleet, six goods-movement fleets, and one off-road-equipment fleet, with about 10 vehicles per fleet and roughly two months of OSAR data per vehicle, filtering out SAE max/min ECU and sensor values to avoid sensor dropout and applying criteria of 20-minute and 23 bhp-hr minimums. Vehicle emissions-factor histograms (summed NOx over summed work across all trips), fleet NOx comparisons against the NTE limit, and scatter plots of NOx versus aftertreatment temperature with a work gradient revealed substantial daily variability within and across fleets. On model-year trends, newer diesel and natural-gas engines showed in-use emission factors closer to emission standards. Overall, 84% of diesel vehicles tested fell on average under the NTE limit, 91% of natural-gas vehicles fell under the 1.5x 0.02 g/bhp-hr Optional Low NOx standard, and 96% fell under the 0.058 g/bhp-hr Bin 2 federal off-cycle level.

Key Conclusion

Onboard sensing can help identify higher-emitting vehicles and capture the day-to-day variability that single-day PEMS testing misses, while remaining inexpensive and fast to deploy at scale. The majority of tested vehicles met the relevant standards on average — 84% of diesels under the NTE limit and 91% of natural-gas vehicles under the Optional Low NOx standard — and newer model-year engines' in-use emission factors increasingly match emission standards. With about 40 OSAR systems ready for installation requiring no on-site calibration, the approach offers a practical path to continuous, fleet-wide, year-long emissions monitoring.

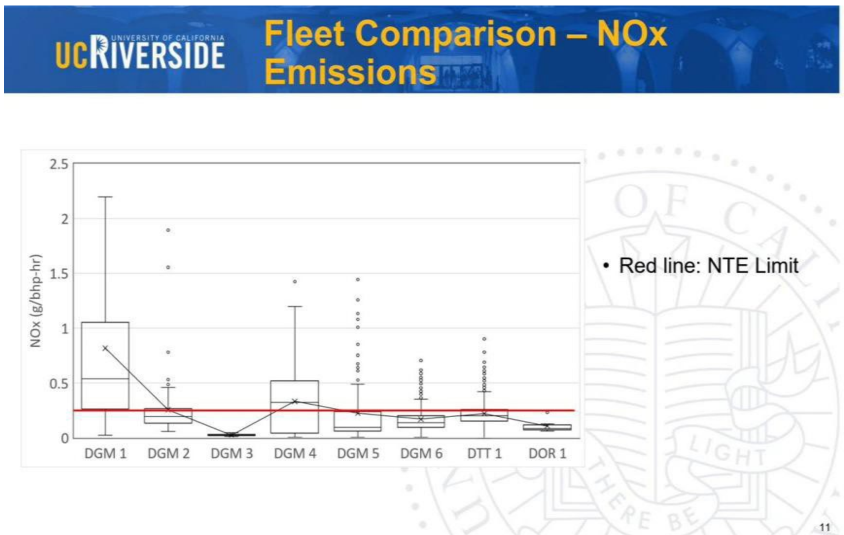

Figure 40 Fleet comparison of NOx emissions against the NTE limit (red line); onboard sensing reveals both fleet-level differences and substantial daily variability within fleets.

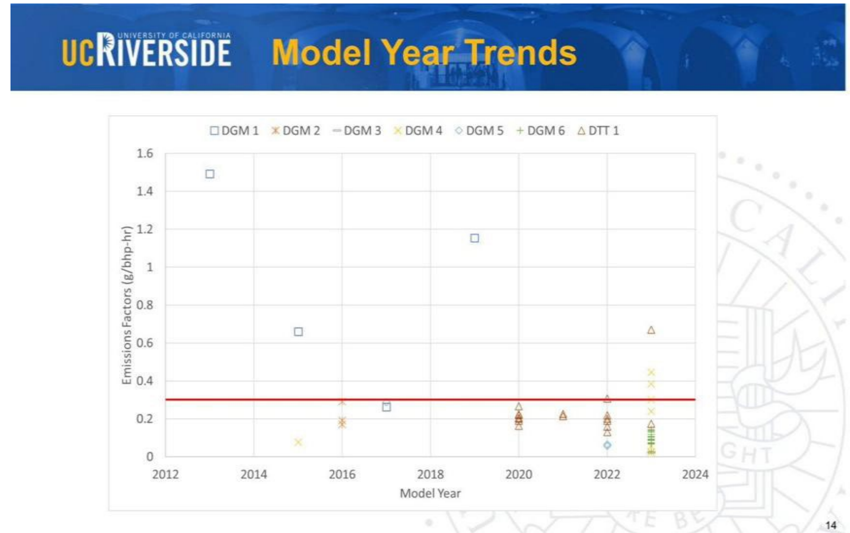

Figure 41 Model-year trends: newer diesel and natural-gas engines show in-use emission factors converging toward emission standards across the tested fleets.

Comprehensive Emissions Measurements and Their Impacts: OMEGA

Kent Johnson et al. (UC Riverside CE-CERT) and Karl Ropkins (University of Leeds)

Scope of the Study

The OMEGA project (Objective Measurement, Monitoring, and Mitigation of Emissions from Goods Movement and Impacts on Air Quality) combines OSAR onboard sensing with remote-sensing technologies to characterize the heavy-duty goods-movement fleet and demonstrate how clean the mobile fleet can perform. The framing draws on the status of the mobile-fleet NOx inventory and a custom scenario analysis: 95% of the heavy-duty NOx reductions between 2025 and 2045 would come from replacing older vehicles with 2027-certified low-NOx vehicles running on diesel or compressed natural gas, and a complete transition to zero-emission vehicles after 2027 would provide only an additional 5% reduction. Heavy-duty vehicles also provide competitive carbon solutions, since over 50% of California diesel is renewable, renewable diesel offers roughly 70% (or more) of the carbon benefit of grid electricity, and renewable natural gas has a negative carbon intensity — biofuels thus provide carbon benefits equivalent to electrifying 35–50% of California's heavy-duty and off-road engines, and 70–100% of off-road equipment. Measurement methods included OSAR, remote sensing at speed (HEAT/EDAR), and PEAQS roadside screening.

Results

Remote sensing at speed using the HEAT/EDAR system over a two-week April sampling saw 49,000 vehicles trigger the scanner (mostly light-duty), including 8,800 Class 8 tractor-trailers and 3,430 smaller heavy-duty trucks, enabling emission-factor estimation for thousands of trucks per day. The PEAQS unit, screening trucks accelerating from a stop, screened 622 heavy-duty trucks over April 16–17, 2024, pulling over 54 (8%) for full inspection and issuing citations for OBD failures, missing emission-control labels, malfunction indicator lights, Statewide Truck and Bus violations, and excessive opacity. A 200-vehicle PEMS project found diesel NOx of 0.05–2.3 g/hp-hr (decreasing with model year) and natural-gas NOx below 0.1 and down to 0.02 g/hp-hr. OSAR natural-gas results showed 71% of vehicles below 0.02 g/bhp-hr over the two-month interval and 97% below 0.06. Remote sensing flagged high emitters at speed, with 32% of observations above 1 g/hp-hr (averaging 3.49), 13% above 3 g/hp-hr, and 2% above 10 g/hp-hr, while OSAR preliminary data showed diesel emissions approaching natural-gas levels.

Key Conclusion

Modern low-NOx combustion is a positive, competitive solution, and heavy-duty vehicles also provide competitive carbon solutions through renewable fuels, with the custom scenario indicating that replacing older vehicles with 2027-certified low-NOx diesel and natural-gas vehicles delivers the overwhelming majority of future NOx reductions. The central message to OEMs, fleets, and truckers is that ensuring new technology continues to work in-use is more important than ever given how clean the mobile fleet can perform — requiring robust monitoring and evaluation, with open questions about whether inspection and maintenance can do this alone. Onboard sensing (OSAR), remote sensing at speed (HEAT), and roadside screening (PEAQS) provide complementary tools, with continued attention needed to natural-gas PM/PN, NH3 management, and CH4.

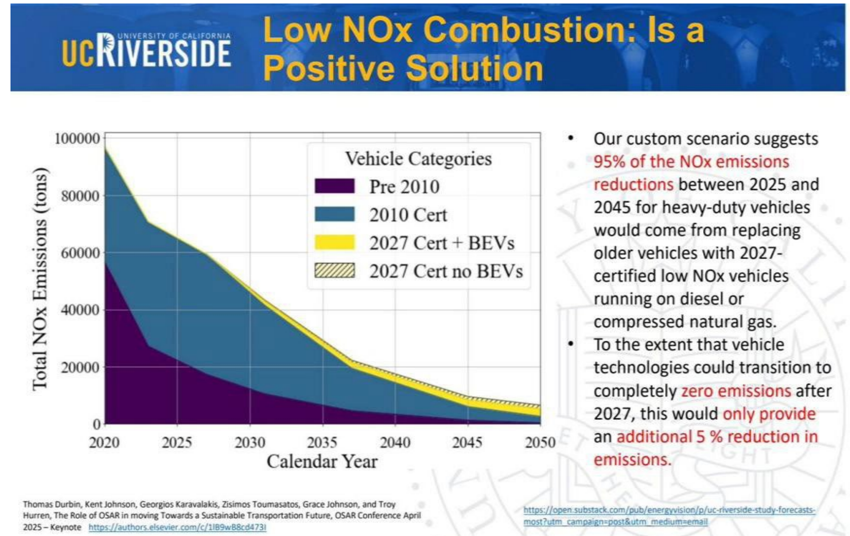

Figure 42 Custom scenario: ~95% of 2025–2045 heavy-duty NOx reductions come from replacing older vehicles with 2027-certified low-NOx diesel/CNG; full ZEV transition adds only ~5%.

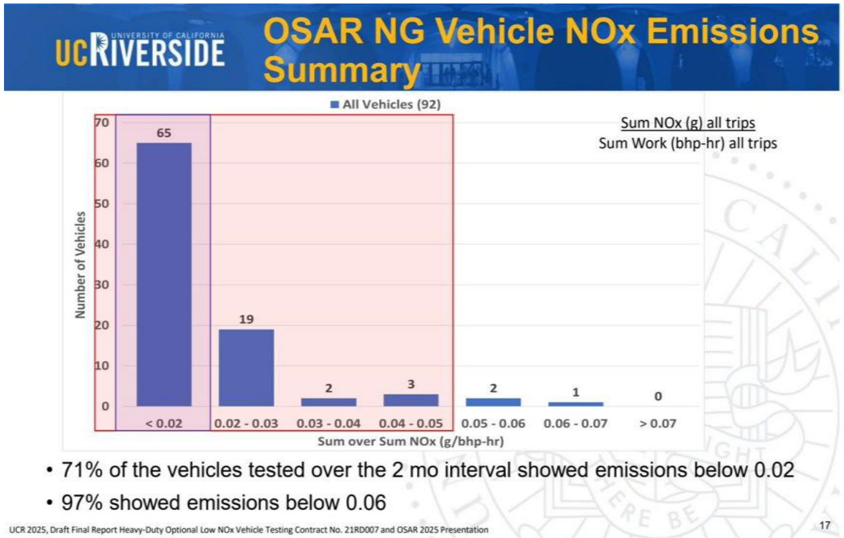

Figure 43 OSAR natural-gas NOx summary: 71% of vehicles fell below 0.02 g/bhp-hr over the two-month interval and 97% below 0.06 g/bhp-hr.

Real-World and Laboratory-Based Emissions Assessment of Modern Heavy-Duty Diesel Vehicles in California: Insights from the Truck and Bus Surveillance Program (TBSP)

Yucheng He, Mo Chen, Sara Forestieri, Jiachen Zhang, Brett Hoffstadt, Hee Je Seong, Xu Wang, Shaohua Hu, Tao Huai, David Quiros — California Air Resources Board

Scope of the Study

Further emissions reduction is needed for the South Coast to meet federal standards, and heavy-duty vehicles are a major NOx contributor. The Truck and Bus Surveillance Program (TBSP) systematically evaluates HDV diesel-truck emissions and has supported California's on-road emission inventory model, EMFAC, since EMFAC2017. The study reflects implemented regulations as of 2022: the U.S. EPA 2007 Heavy-Duty Highway Diesel Rule (0.20 g/bhp-hr NOx from model year 2010, requiring SCR and diesel particulate filters), the 2008 Truck and Bus Regulation, the 2010 Heavy-Duty OBD Regulation, and the 2021 Omnibus regulation tightening standards from model year 2024 toward 0.05 to 0.02 g/bhp-hr. TBSP tested 65 trucks on a chassis dynamometer and 21 using PEMS, covering model years 2010–2019 and reporting roughly 1,000 dynamometer tests and 300 PEMS tests. Dynamometer equipment included an exhaust flow meter, Horiba MEXA One (CO_2, CO, NO/NOx, THC), AVL SESAM FTIR (N_2O, NH_3), and a Sierra partial-flow

PM system; PEMS routes covered urban local (19 mph average), highway (56 mph), highway downhill (59 mph), and highway uphill (56.4 mph).

Results

Dynamometer NOx results, organized by engine model-year group with average speed increasing across cycles, and PEMS trip-average NOx results both demonstrated that newer model-year engines have improved aftertreatment performance. A micro-trip analysis — defining a micro-trip as the period between a vehicle start and the next stop, merging segments shorter than 0.25 miles and separating those longer than 3 miles — was developed and used in the EMFAC2025 heavy-duty emission-rate update. Comparing dynamometer cycle-average emissions with PEMS micro-trip-average emissions for a drayage truck visiting the ports of Los Angeles and Long Beach, telematics showed that speeds below 10 mph account for only about 3% of drayage VMT and speeds below 5 mph less than 1%, raising the practical question of how to model emission rates for very low speeds. For both dynamometer and PEMS data, cycle-average and micro-trip-average emissions exhibited a negative linear correlation with average vehicle speed.

Key Conclusion

The study provides a comprehensive overview of criteria-pollutant emissions from diesel heavy-duty vehicles using both laboratory-based dynamometer testing and on-road measurements, and the resulting dataset has been used as a key input for EMFAC2025, improving the model's representativeness of real-world conditions. For both measurement approaches, cycle-average and micro-trip-average emissions show a negative linear correlation with average vehicle speed, and newer model-year engines demonstrate improved aftertreatment technology performance. The TBSP program will continue to test more vehicles and provide data for EMFAC updates; it represents a critical benchmark that is not replaceable for assessing emissions performance.

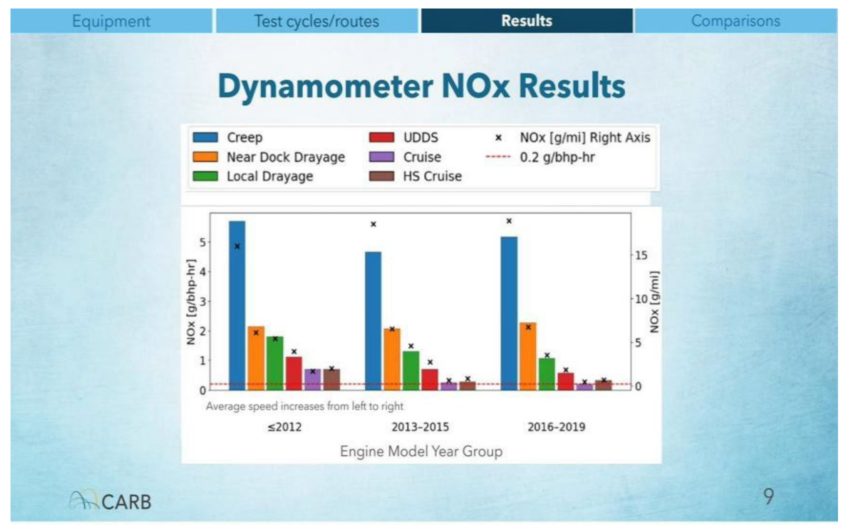

Figure 44 Dynamometer NOx results by engine model-year group, with average cycle speed increasing left to right; newer model years show clearly improved aftertreatment performance.

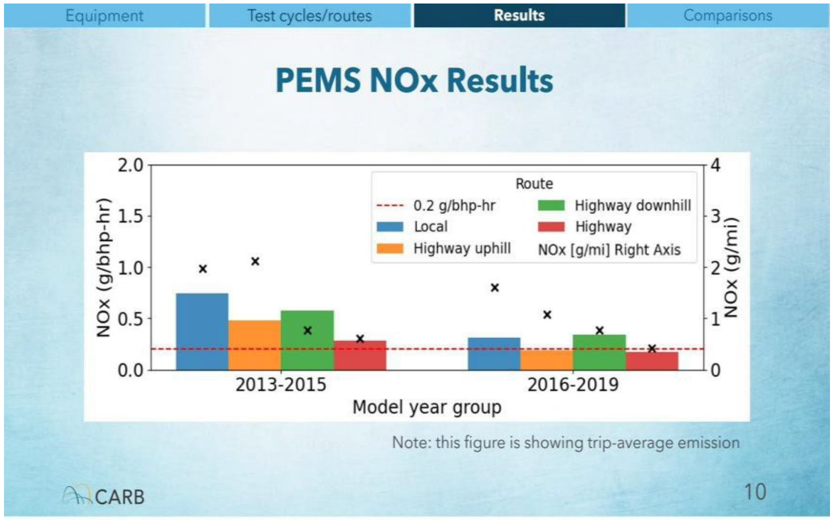

Figure 45 PEMS trip-average NOx results across urban, highway, downhill, and uphill routes for two model-year groups, reinforcing the speed dependence and model-year improvement.

Emissions from High-Speed Driving on California Roadways: Insights from a Large Spatial Dataset

Bharat Jayaprakash, Will Northrop (University of Minnesota); Lucas Algrim, Waqas Quadri, Satya Sardar (CARB)

Scope of the Study

Building on the principle that speed mitigation and traffic smoothing reduce fuel consumption and emissions, and on EMFAC2025 emission factors for high-speed driving, the study quantifies high-speed-driving emissions across California using a large spatial dataset and models an intervention that limits speeds to posted limits. The dataset (Wejo) covered four days, one in each season, with roughly 30 million trips per day, recording time, speed, geohash, elevation, speed limit, road type, ambient temperature, and vehicle class for General Motors 2015–2020 model vehicles across the entire United States. Over 8 million trips in California were mapped to representative EMFAC vehicle classes. Speeding on highways and arterial roads was analyzed as a percentage of vehicle-miles-traveled, with statewide average VMT above 65 mph around 21.7–26%. An intervention algorithm then reduced the speed of all California trajectories to posted speed limits, after which EMFAC2025 emission factors were applied to quantify the savings.

Results

The percentage of emissions from speeds above 65 mph varied by pollutant, and the cumulative share of emissions versus cumulative share of VMT (ordered by speed bin across all vehicle classes) showed that CO, ROG, PM2.5, and NOx exhibit a higher, non-linear share of emissions above 65 mph — meaning high-speed driving contributes disproportionately to these pollutants relative to its share of distance traveled. When speed was limited to posted limits across all California trajectories, significant savings were achieved: 13.8% for NOx, 37.4% for CO, 2.1% for CO2, 16.8% for ROG, and 17.0% for PM2.5. The spatial mapping revealed that speeding concentrates along major interstate and U.S. highways shown across the state network, allowing the geographic distribution of high-speed emissions to be visualized for each pollutant.

Key Conclusion

High-speed driving above 65 mph accounts for a disproportionate, non-linear share of CO, ROG, PM2.5, and NOx emissions relative to its VMT share, and limiting speeds to posted limits across California's fleet would yield substantial reductions — most notably 37.4% for CO, around 17% each for ROG and PM2.5, and 13.8% for NOx, with a more modest 2.1% for CO2. The large spatial dataset enables both statewide quantification and geographic targeting of where high-speed-driving emissions are concentrated, supporting speed-management and traffic-smoothing strategies as effective emissions-reduction levers.

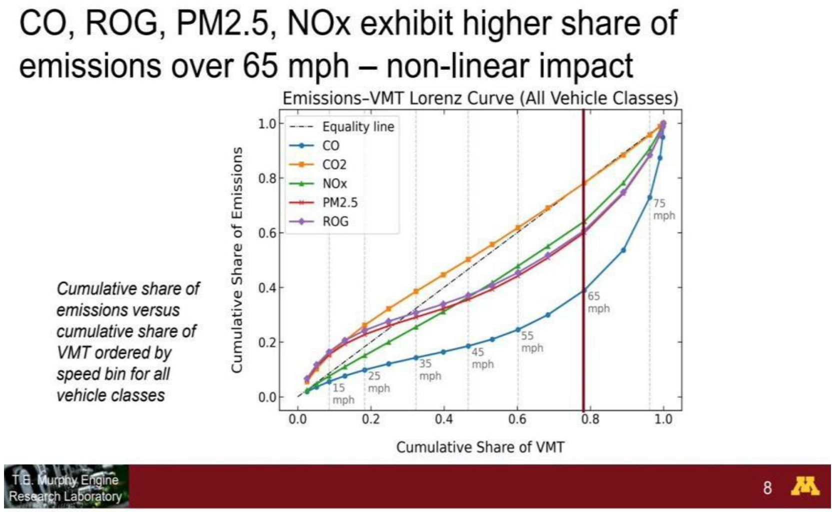

Figure 46 Emissions–VMT Lorenz curves (all vehicle classes): CO, ROG, PM2.5, and NOx show a disproportionate, non-linear share of emissions from speeds above 65 mph.

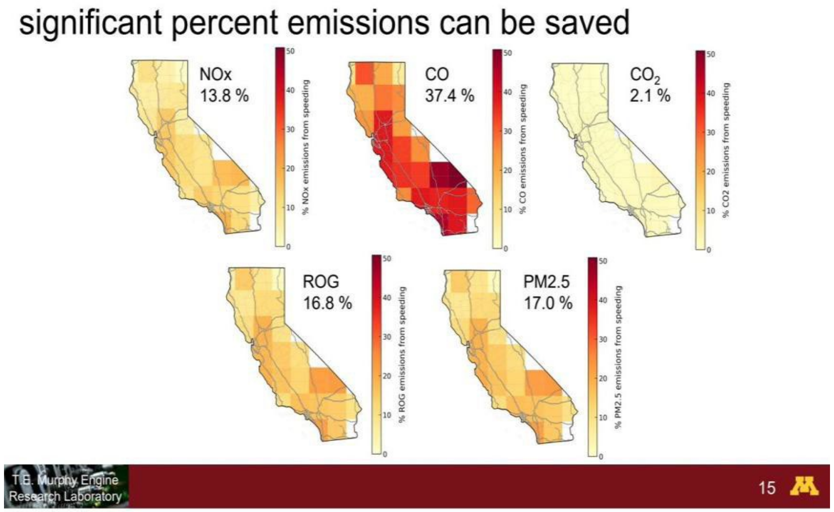

Figure 47 Savings achievable by limiting speeds to posted limits across California: 13.8% NOx, 37.4% CO, 2.1% CO2, 16.8% ROG, and 17.0% PM2.5.

Measurement and Estimated Effects of Engine Enrichment on In-Use Light-Duty Vehicle Emissions

Benjamin Ellies — U.S. EPA, National Vehicle and Fuel Emissions Laboratory

Scope of the Study

Gasoline engine enrichment — supplying excess fuel beyond that needed for stoichiometric combustion — is a control strategy commonly used by vehicle manufacturers that results in higher tailpipe emissions. In 2025, EPA began a test program at its National Vehicle and Fuel Emissions Laboratory to better understand how enrichment affects in-use driving emissions, with three goals: develop a repeatable chassis-dyno test methodology for enrichment emissions measurement, evaluate the data for potential application in EPA's MOVES model, and observe enrichment controls behavior via OBD. The dyno setup used a 4WD chassis dynamometer and Horiba bench measuring HC, CO, and NOx (bag and modal), NH3 (tailpipe modal via a MEXA-ONE-QL-NX analyzer), and soot (via AVL MSS in the tunnel), with OBD data collected through the J1979 data port. Testing modes included steady-state (quantitative, for emissions rates) and US06 cycle testing (qualitative, for enrichment modes and engine controls). Eleven vehicles (model years 2022–2025) were tested, spanning GDI, PFI, and dual injection designs, engine sizes from 1.2 to 5.7 L, and a mix of turbocharged and naturally aspirated engines across vehicle classes and weights.

Results

In steady-state testing, the dyno operated in constant-speed mode with dynamic load, driven at 20–80 mph holding pedal positions for 15–45 seconds, with averages calculated for each data field. Over 1,000 steady-state averaged points were plotted against vehicle specific power (VSP, in kW/ton — power at the wheels divided by test weight, a parameter used in MOVES modeling), using a piecewise curve fit based on average lambda: a linear fit for stoichiometric operation and a quadratic fit for pollutants in the enrichment zone. The average onset of enrichment occurred at about 33 kW/ton. CO rose clearly in the enrichment zone as a function of VSP, while soot showed more scatter due to the transient nature of soot formation and required a different calculation approach. As expected, NOx did not present a clear trend with enrichment, and CO showed no observable correlation outside the enrichment zone.

Key Conclusion

The work established a repeatable chassis-dyno methodology for quantifying enrichment emissions as a function of vehicle specific power, with the average enrichment onset around 33 kW/ton, suitable for potential application of emissions rates in MOVES. NOx did not trend clearly with enrichment, and soot emission rates may need further thought about how to represent them as a "rate" given their transient formation. Potential future work includes testing more vehicles (adding high-sales-volume models and considering hybrids with adjusted methods), analyzing the data for MOVES emissions-rate application, assessing enrichment during on-road testing, and characterizing in-use towing frequency.

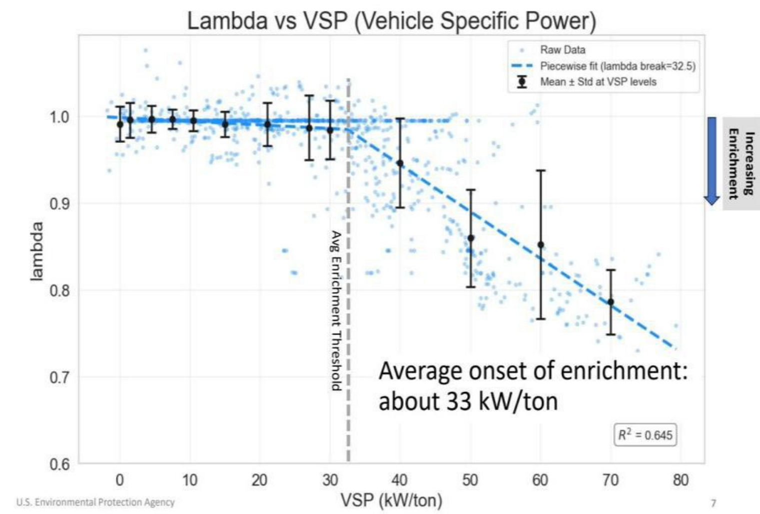

Figure 48 Lambda vs vehicle specific power: enrichment (lambda below 1) begins on average around 33 kW/ton, defining the enrichment threshold used for the emissions-rate analysis.

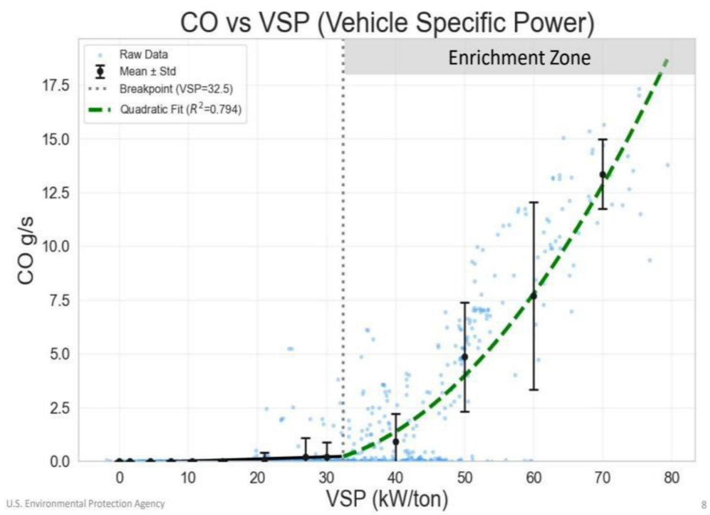

Figure 49 CO emissions rise sharply with VSP in the enrichment zone, fit with a quadratic curve; this characterizes the elevated tailpipe emissions enrichment produces.

Assessing Sources of Variability in Fuel Use and Emission Rates for Station-to-Station Passenger Rail Segments

Tongchuan Wei, H. Christopher Frey, Nikhil Rastogi — North Carolina State University

Scope of the Study

The objective was to demonstrate a methodology for quantifying passenger-rail fuel use and emission rates at the mesoscale, station-to-station segment level, and to identify key sources of variability. The study focused on Amtrak's Piedmont passenger-rail service between Raleigh and Charlotte, North Carolina — 173 miles, 190 minutes each direction, with 9 stations. Over-the-rail measurements used portable emission measurement systems capturing CO_2, CO, HC, NOx, and PM, alongside GPS receivers, a manifold-absolute-pressure sensor, an RPM sensor, an intake-air-temperature sensor, and a locomotive activity recorder on the prime-mover engine exhaust duct. The work covered 12 measured combinations of locomotives, consist types, and fuels (single locomotive consist, double-powered tandem, single- and double-powered push/pull configurations, using ultra-low-sulfur diesel and a 20% biodiesel blend). Locomotive power demand — the tractive power to overcome resistive forces, a function of speed, acceleration, track grade, and curvature — was estimated at 1 Hz using a detailed physics-based equation and used to quantify variability.

Results

The team built the Piedmont RAIL-ACE model (Rail Analytics for In-use Locomotives — Activity, fuel Consumption, and Emissions), a locomotive-power-demand-based fuel-use and emissions model using a 12-second backward moving average of power demand to account for operating history, calibrated per locomotive/consist/fuel combination on measured one-way trips and validated by leave-one-out cross-validation. Across 8 station-to-station segments and 45 measured one-way trips meeting data-completeness criteria, 4,320 segment-level simulation runs estimated segment-average fuel use and emission rates. Analysis of variance identified the significant sources of variability. Inter-run variability was 15–35% for fuel economy and 16–45% for NOx for a given segment and direction, indicating strong sensitivity to operational dynamics. Inter-directional variability reached up to 40%, linked to positive elevation gain — the direction with lower elevation gain consistently had lower fuel use and emissions. By ANOVA, positive elevation gain was the dominant factor (F-ratio 198 for fuel economy, 261 for NOx, 232 for PM), followed by average speed and positive acceleration, with several interaction effects also significant.

Key Conclusion

Inter-run variability in fuel use and emission rates differs by segment and direction, indicating energy-saving and emission-reduction potential of 15–45% through improved train operations. Inter-directional variability is pronounced (up to 40%), particularly for segments with large differences in positive elevation gain between directions; for a given segment, the direction with lower elevation gain tends to have lower fuel use and emissions. Inter-segment variability is primarily driven by positive elevation gain (infrastructure), average speed (operations), and positive acceleration (operations), which directly affect locomotive power demand. High-fuel-use-and-emission segments can be identified using RAIL-ACE, informing operational strategies and infrastructure investments for energy saving and emission reduction.

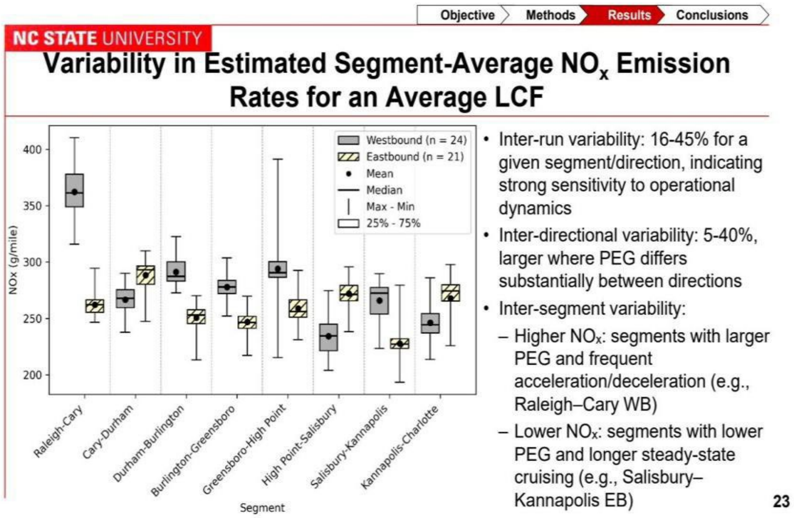

Figure 50 Variability in estimated segment-average NOx emission rates: inter-run variability 16–45% and inter-directional variability 5–40%, largest where positive elevation gain differs between directions.

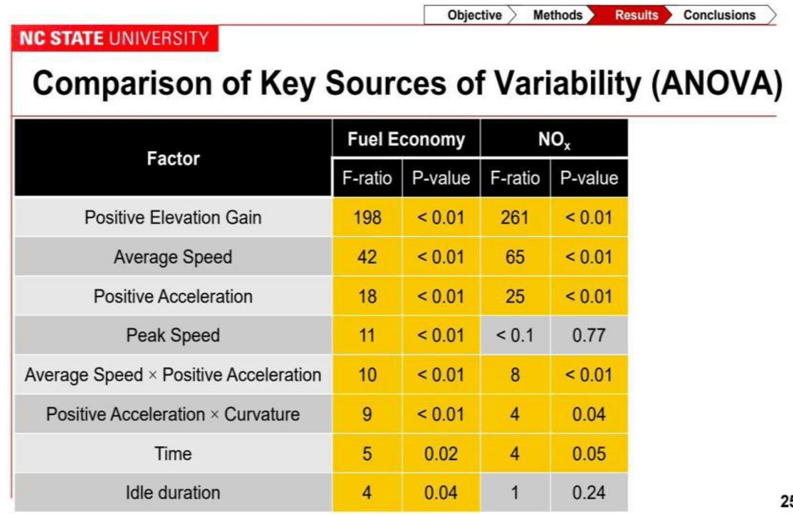

Factor	Fuel Economy		NO_x	
	F-ratio	P-value	F-ratio	P-value
Positive Elevation Gain	198	< 0.01	261	< 0.01
Average Speed	42	< 0.01	65	< 0.01
Positive Acceleration	18	< 0.01	25	< 0.01
Peak Speed	11	< 0.01	< 0.1	0.77
Average Speed × Positive Acceleration	10	< 0.01	8	< 0.01
Positive Acceleration × Curvature	9	< 0.01	4	0.04
Time	5	0.02	4	0.05
Idle duration	4	0.04	1	0.24

Figure 51 ANOVA of variability sources: positive elevation gain dominates (F-ratio 198 for fuel economy, 261 for NOx), followed by average speed and positive acceleration.

Mobile Hydraulic Dynamometer Evaluation

Cavan McCaffery, Axel Freund, Xiangyi Li, Thomas Montes, Robin Lang, Daniel Zaragoza, Edward O'Neil, Edwin Diaz et al. — California Air Resources Board

Scope of the Study

The Mobile Hydraulic Dynamometer (MoHyD) is a mobile, standalone instrument that uses the hydraulic system of off-road equipment to load the engine, streamlining engine-dyno-style testing using in-use PEMS. Rated to 400 hp, it can load and operate an engine without removing anything from the equipment, electronically controlling pedal position via CAN, PWM, or analog to mimic engine-dynamometer operation over cycles such as the nonroad transient cycle (NRTC), ramped modal cycle (RMC), and field cycles. The objectives were to understand MoHyD control and continue cycle improvements, verify MoHyD testing for engine control by comparison to a reference, and understand emission characteristics. Building on prior work showing MoHyD precise at targeting load and RPM setpoints, this study evaluated MoHyD setpoints against engine-dyno setpoints, with torque setpoints created by targeting hydraulic pressure and RPM setpoints by targeting CAN engine speed. Testing in April 2024 at CARB's Riverside lab integrated UC Riverside's Mobile Emissions Laboratory with the MoHyD-PEMS setup, with engine-dyno-plus-PEMS reference testing in October 2025, running triplicate Cold NRTC, Hot NRTC, and RMC cycles and measuring diluted exhaust with a CVS.

Results

MoHyD controlled engine speed consistently but biased high on engine torque during the NRTC, so cycle work was higher as a result. On the RMC, low-torque points were higher for MoHyD due to auxiliary loads (cooling fan, driving belts, pumps, alternator) while high-torque points were lower due to cooling-fan restriction (resolvable with an additional fan); on the Cold NRTC, MoHyD managed transient torque fluctuations but low-torque points were again elevated by auxiliary loads, with room to improve torque setpoints. On emissions, CO2 agreed within 11% on the NRTC and within 3% on the RMC, while brake-specific fuel consumption differences ranged from about 3% to 15%. For NOx, there was no statistically significant difference between the Cold NRTC and RMC diluted emissions, but Hot NRTC differences were attributed to SCR temperature: the SCR during the MoHyD hot NRTC started about 40 °C hotter, possibly because it was hotter at the end of cold-start testing due to torque differences and retained more heat inside the chassis.

Key Conclusion

MoHyD's speed control setpoints and feedback are optimized for stability and accuracy, and it handles dynamic certification cycles effectively, remaining robust under transient conditions. Further refinement of torque setpoints for certification cycles is possible, requiring procedural changes for deriving torque and pressure setpoints in an iterative process that can be improved using this data. On emissions performance, CO2 and NOx were comparable to the engine dynamometer, with improvements available by running correct cycle setpoints and accounting for SCR temperature during soak — supporting MoHyD as a practical tool for engine-dyno-equivalent off-road testing without removing components.

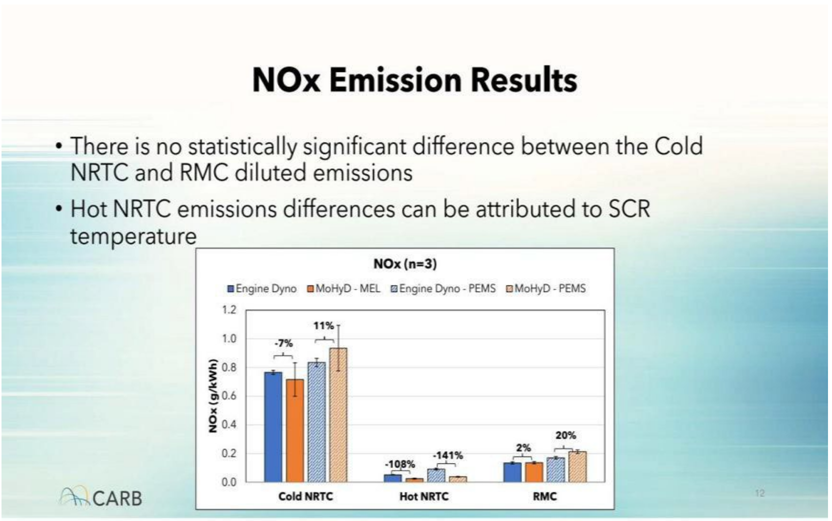

Figure 52 NOx emission results: no statistically significant difference between MoHyD and engine dyno on Cold NRTC and RMC; Hot NRTC differences trace to SCR temperature.

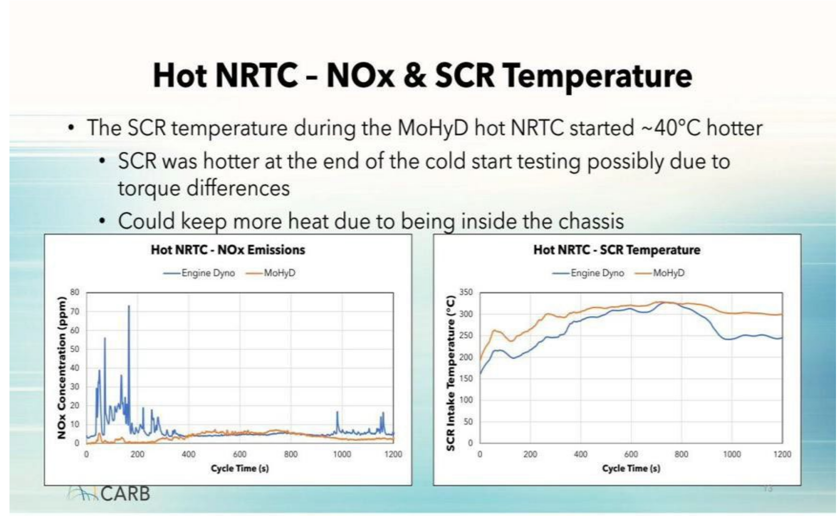

Figure 53 Hot NRTC NOx and SCR temperature: the MoHyD SCR started ~40 °C hotter, explaining the Hot NRTC NOx difference versus the engine dynamometer reference.

Leveraging Off-Road Engine ECU Data to Evaluate Operating Patterns and Power Prediction

Ehsan Soleimanian, Stephen Berdahl, Hyun (Julie) Lee, Tao Huai, Mark Fuentes — California Air Resources Board

Scope of the Study

Off-road equipment is essential across agriculture, construction, ports, and power generation, but it is the leading source of NOx and PM among all mobile sources in California, has no OBD regulation (complicating in-use emission testing), and exhibits highly diverse duty cycles that make operating behavior and emission patterns difficult to characterize. As CARB pursues an off-road in-use compliance program, phases out older high-polluters, and promotes cleaner fuels, this study used real-world operational data to predict instantaneous engine power for off-road equipment. The goals were to analyze real-world operating patterns across vehicle categories and characterize variability from different chassis, and to develop data-driven power-prediction models using measurable engine parameters and evaluate them on unseen duty cycles and engines. The dataset comprised 35 vehicles (multiple types and engine families, 4.4–18.1 L displacement, 115–620 hp) across 840 trips (each 20–200 minutes), with ECU data including engine speed, torque, and fuel rate.

Results

Operating behavior varied with intended function and duty cycle, and the same engine behaved very differently depending on the chassis it was installed in. Engine-speed (RPM) distributions differed markedly by category: scrapers, loaders, and backhoes used the entire RPM range for mixed-intensity work, excavators showed bimodal duty cycles (much time at low RPM with spikes at high RPM during digging), and other vehicles fell in between. Operating power also varied widely across categories. Because engine speed and power are critical for regulatory emission calculations but many off-road vehicles lack OBD or full ECU access, a predictive model was built to estimate power from limited measurable inputs (engine speed via a sensor, fuel rate via a flow meter, and engine rated power), training three machine-learning models (Random Forest Regression, LightGBR gradient boosting, and a neural network) on 672 trips (80%) and validating on 168 (20%). All three performed strongly; Random Forest Regression was selected, achieving an overall R^2 of about 0.98, though performance differed among categories. Weaker per-vehicle cases traced to decoupling between fuel rate and power on certain trips (e.g., high power at submaximal fuel rate, or high fuel rate without corresponding power), reflecting dynamic-lag effects such as turbocharger and ECU response. On previously unseen vehicles tested via MoHyD (backhoes and excavators), the model maintained strong performance across Cold NRTC, Hot NRTC, and RMC cycles (R^2 0.90–0.99, MAE under 5 kW, RMSE under 7 kW).

Key Conclusion

Off-road engines exhibit substantial diversity in operating patterns across equipment categories and duty cycles, even within similar engine families. A data-driven modeling framework was developed to estimate engine power from a constrained set of measurable parameters, and the trained Random Forest Regression model generalizes to previously unseen engines and trips, enabling enhanced emissions characterization for off-road equipment lacking OBD systems. Model performance was not dependent on vehicle type; rather, variability was linked to individual trips. Future work may incorporate additional operational features — such as transient-behavior indicators and load proxies — to further improve predictive accuracy under highly dynamic conditions.

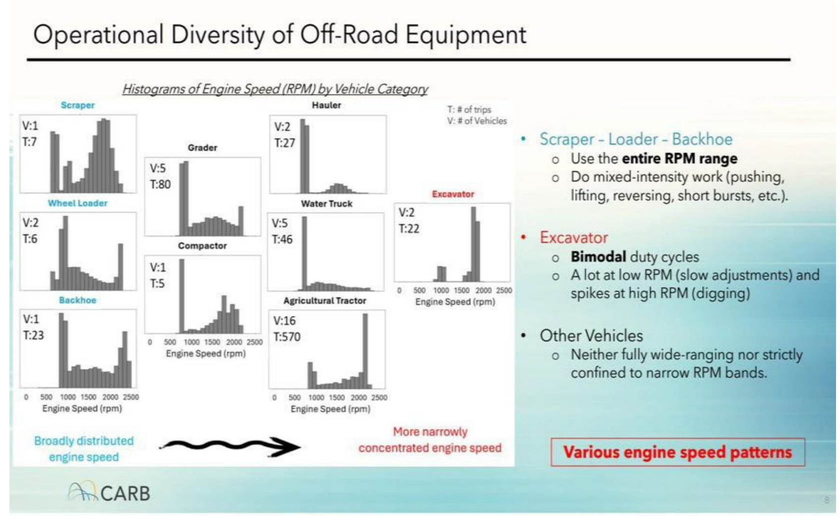

Figure 54 Operational diversity: engine-speed (RPM) histograms by vehicle category differ widely — scrapers/loaders/backhoes use the full range, excavators are bimodal — even for the same engine family.

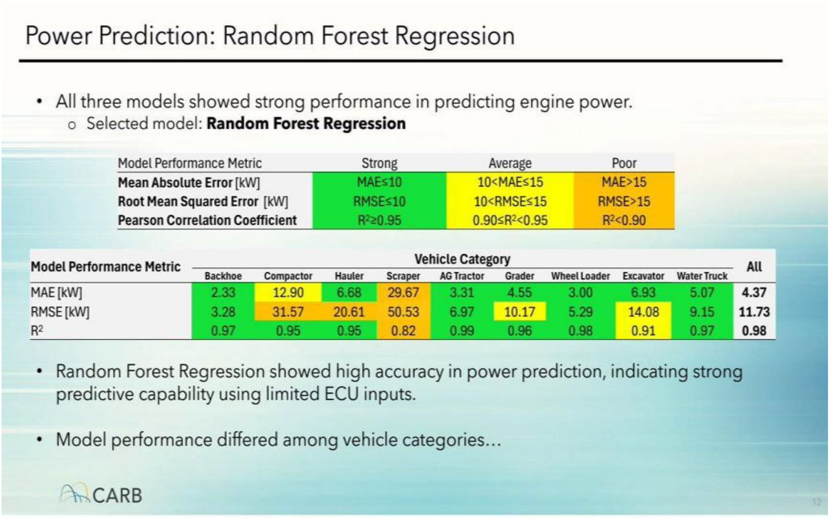

Figure 55 Random Forest Regression power-prediction performance by vehicle category: overall R² ~0.98 using only engine speed, fuel rate, and rated power as inputs.1

Section 6. Advanced Emissions Measurement and Instrumentation

Contamination Effects in Near-Zero PM Filter Weighing

Sergio Perez, Eric Miller, Benjamin Mensen, Daniel Barnes, Jingzhe Zhang, Atharva Desai, Yusuf Khan — Cummins Inc.

Scope of the Study

Engine manufacturers set design targets more stringent than the standard to account for deterioration and measurement variation, so for 2027+ PM targets the challenge is measuring accurate and repeatable PM filter weights at very low levels — a maximum of 30–40 µg of net filter mass corresponds to a PM design target of 2 mg/bhp-h. Testing guidelines in 40 CFR Part 1065 ensure consistent PM formation: 1065.546 verifies a minimum dilution ratio of 5 to 7 for PM batch sampling, and 1065.170 specifies a filter face velocity of 90–100 cm/s; 1065.516 considers a sample system contaminated if filter weight exceeds 20 µg. The objective was to evaluate zero-PM emissions-measurement capability and identify potential PM added onto the gravimetric filter due to handling, loading, and tunnel blanks. The test plan progressed through four stages of increasing complexity (pre/post weights with conditioning; loading into cassettes; loading into the PM filter holder and cycling; and simulated NRTC airflow), conducted before and after facility improvements (Study 1 versus Study 2).

Results

Reference filter data established the measurement floor: across 16,317 measurements, the mean was 0.018 µg with a standard deviation of 1.94 µg, a distribution centered near zero with no systematic bias and well below the regulatory tolerance of ±10 µg, with about 92% of delta measurements within ±3 µg and 99% within ±5 µg. Study 1 (before improvements) showed incremental PM loading proportional to test complexity, with the shift toward higher loading producing a mean of 13 µg — nearly 50% of the net design filter-weight target — though a separate low-handling site showed no systematic loading and repeatable measurements due to its smaller operation, newer equipment, and minimal handling. Improvements then upgraded the microbalance, improved air handling, tightened temperature/humidity control, completed annual preventive maintenance, and instituted controlled, careful handling outside the weigh room. Study 2 (after improvements) showed no systematic PM-loading trend across all test phases and increased repeatability; aside from one instance of high loading, data across all test types showed acceptable loading (under 3 µg mean for most phases). Comparing studies, Test A and Test B variability tightened significantly (reduced standard deviation), Test C loading dropped after handling and weigh-room improvements, and Test D loading dropped more than 10 µg.

Key Conclusion

Because 2027+ PM design targets require minimal loading on PM filters, contamination from handling and the sample system poses a real risk: Study 1 showed significant PM loading from handling and system contamination, with a mean of about 13 µg. After targeted weigh-room and handling improvements, Study 2 showed minimal PM loading (under 3 µg mean for most phases) and substantially improved repeatability. The measurement capability now supports PM targets for 2027 and beyond with the improvements in place, demonstrating that near-zero PM measurement is achievable provided handling, loading, and system contamination are rigorously controlled.

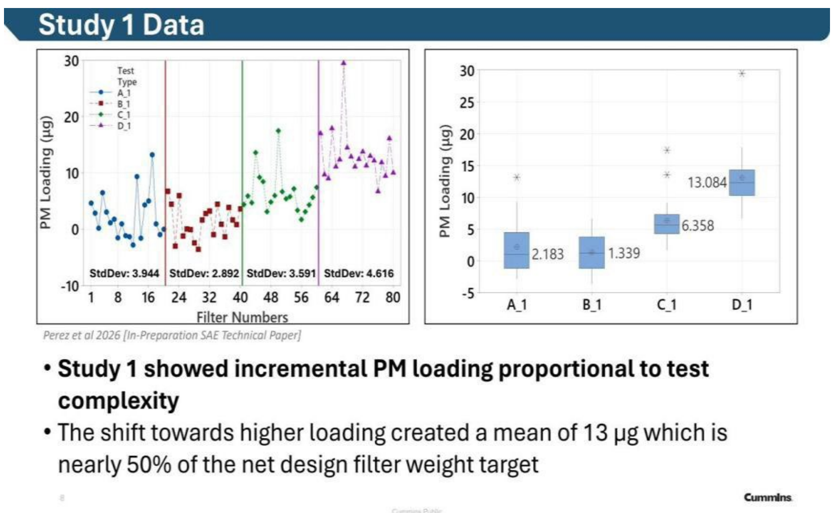

Figure 56 Study 1 (before improvements): incremental PM loading proportional to test complexity, with a mean of ~13 µg — nearly 50% of the net design filter-weight target.

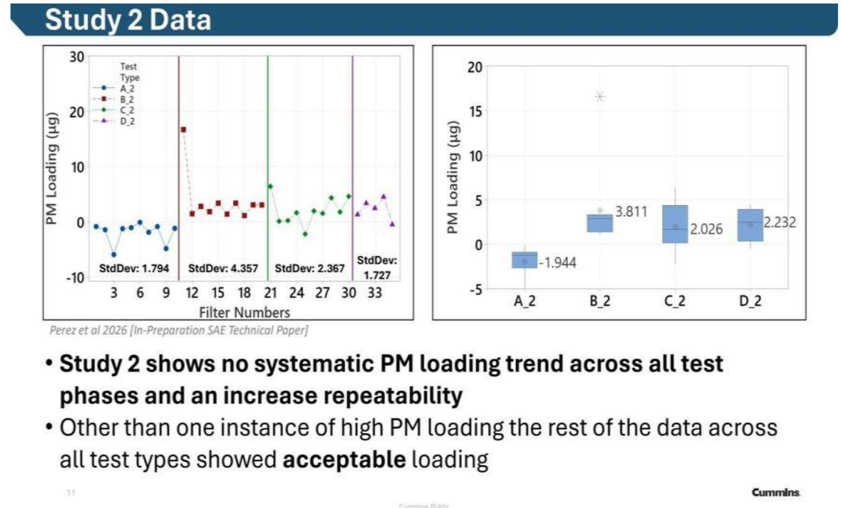

Figure 57 Study 2 (after improvements): no systematic PM-loading trend across test phases and improved repeatability, with under 3 µg mean for most phases.

Euro 7 Emissions Measurement Challenges

Troy Hurren, Yusuf Khan, Sergio Perez, Atharva Desai, Niklas Schmidt, Eric Miller — UC Riverside and Cummins Inc.

Scope of the Study

Euro 7 introduces more regulated species, lower emission limits, and new measurement techniques (QCL-based analyzers, FTIR, and catalytic strippers for particle number), with the overarching objective of reliably measuring all regulated species — NOx, PM, N2O, NMOG/formaldehyde, PN10, NH3, CH4, and CO — at low concentrations. The presentation systematically reviewed the measurement challenges for each species. For NOx, the Euro 7 limit of 200 mg/kWh is a 57% reduction from Euro VI but about 7.5 times higher than the US EPA 2027 standard, so NOx is not a significant measurement challenge and Euro 7 allows alternate analyzers (FTIR and IRLAM/QCL) in addition to chemiluminescence. Datasets spanned three diesel engines, five test cells, and 133 test cycles. The work examined how lower limits stress measurement repeatability and background control, how new species require new techniques, and where regulatory definitions remain unsettled.

Results

For PM, the Euro 7 limit of 8 mg/kWh is a 20% reduction from Euro VI; repeatability is poor under 10 µg but acceptable (10–15%) for net mass of 25–45 µg, and partial-flow-system tunnel background becomes critical as limits fall — when tunnel-blank mass rose from about 5 µg to 18 µg, net filter mass rose from about 25–30 µg to nearly 50 µg, a linear additive bias. For N2O (Euro 7 limit 200 mg/kWh), both FTIR and QCL are allowed; FTIR and a Horiba analyzer agreed closely, with the challenge being capturing transient N2O formation during catalyst warm-up below 300 °C. For particle number, Euro 7 requires solid PN down to 10 nm instead of 23 nm, expecting higher variability from sampling losses; the volatile particle remover requires a catalytic stripper (giving about 7% lower counts), and urea and crankcase particles are significant contributors, with sub-23 nm particles averaging 25–58% (diesel) and 19–51% (NG). For NH3, mass-based reporting (Euro 7 limit 60 mg/kWh) is complicated because NH3 slip is driven by SCR dosing and catalyst temperature rather than fuel or exhaust flow, and sample-line adsorption/desorption causes response lag that distorts brake-specific results; technical committees are still debating mass versus concentration standards. CH4 (500 mg/kWh, unchanged) is now regulated for all heavy-duty engines and both cycles. For NMOG, the Euro equation reduces for non-oxygenated fuels to essentially NMHC plus formaldehyde, requiring an additional HCHO measurement, though committees push for the simpler EPA approach. CO (1500 mg/kWh, a 62.5% reduction) poses no significant challenge for engines already meeting Euro VI, but a new verification requirement addresses N2O interference on the CO NDIR analyzer.

Key Conclusion

Euro 7's lower limits and additional species create substantial measurement challenges that demand careful analyzer selection and verification. The most significant include capturing transient N2O during catalyst warm-up, controlling partial-flow tunnel background for low-level PM, handling sub-23 nm particle number with catalytic strippers amid urea and crankcase contributions, and managing NH3 response lag that makes brake-specific reporting sensitive to alignment error. NOx and CO are comparatively manageable for engines already meeting Euro VI. Across species, the presentation underscores that reliable low-concentration measurement — not just lower limits themselves — is the central engineering challenge of the Euro 7 transition.

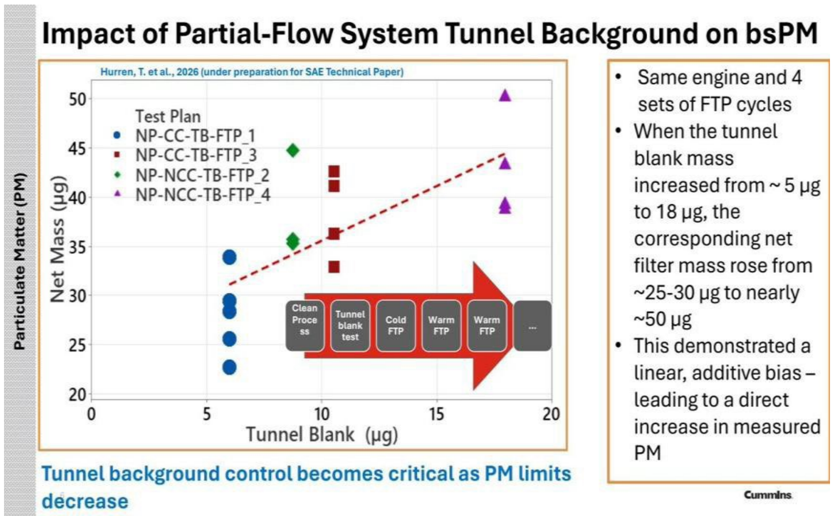

Figure 58 Partial-flow tunnel background drives bias at low PM: as tunnel-blank mass rose from ~5 to 18 µg, net filter mass rose from ~25–30 µg to nearly 50 µg — a linear additive effect.

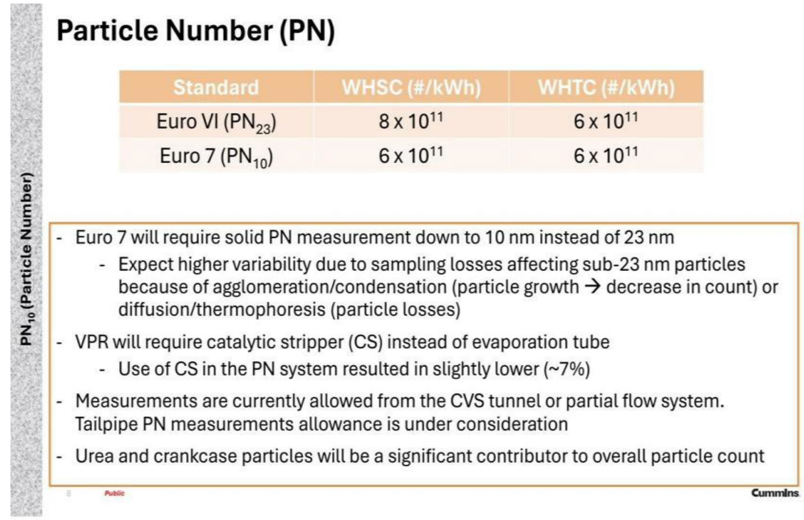

Figure 59 Particle number under Euro 7 moves from PN23 to PN10 (10 nm); urea and crankcase particles contribute significantly, with sub-23 nm particles 25–58% (diesel) and 19–51% (NG).

Evaluation of the Infra-Red Laser Absorption Modulation (IRLAM) Analyzer Compared to Conventional Laboratory Instruments

Troy Hurren, Thinnesh Ragupathy, Atharva T. Desai, Yusuf Khan, Benjamin Mensen et al. (Cummins Inc.) with Montajir Rahman et al. (HORIBA)

Scope of the Study

IRLAM is HORIBA's patented Infra-Red Laser Absorption Modulation analyzer, a QCL-based instrument using a multi-pass Herriott cell and feature-extraction algorithm that offers narrow-wavelength, high-directivity, small-volume (fast-response), long-optical-path measurement that is computationally moderate. It comes in a lab-testing-grade form (IRLAM XL-NX, measuring NO, NO2, N2O, and NH3) and a lab/in-use PEMS-grade form (IRLAM CUBE, adding CO, CO2, and an HC FID), and received EPA approval as an alternate test procedure in February 2025. The objective was to evaluate IRLAM nitric-oxide (NO) performance relative to the regulatory-reference chemiluminescence detection (CLD) across multiple engines, test cells, and sampling configurations under real-world exhaust conditions. The test matrix spanned 3 engines, 5 test cells (3 raw and 2 CVS), 22 test sequences, and 110 cycles, with a sequence of conditioning and official transient cycles, Cold-Hot Emissions Tests (CHET), and Ramped Modal Cycles, analyzing only post-conditioning data.

Results

IRLAM demonstrated near-unity linear agreement with CLD across the full brake-specific NO dynamic range, with a regression of $y = 0.99x + 2.82$ and $R^2 = 0.99$ when data were pooled across multiple engine platforms and both raw and CVS sampling configurations; all but one data point fell within the control-limit agreement band. A validation framework assessed three levels of variability: within-sequence repeatability per test cell, within-test-cell variability per cycle type, and across-test-cell reproducibility per cycle type. IRLAM exhibited within-sequence repeatability comparable to CLD during back-to-back transient testing, with an overall average coefficient of variation of 2.1% and a mean inter-instrument difference of 0.21%. Within-test-cell variability remained consistent with CLD across cycle types, with an average inter-instrument %CV difference of 0.9%. Despite relocation across independent test cells, IRLAM reproducibility remained comparable to CLD, with an average inter-instrument variability difference of 0.8% across cycle types. On an EPA 2027+ ultra-low-NOx natural-gas engine (under 35 mg/bhp-hr), both IRLAM XL-NX and CUBE agreed with CLD within ±3 mg/bhp-hr on the CHET composite cycle, with only one data point exceeding control limits across 18 CHETs.

Key Conclusion

IRLAM demonstrates accuracy, repeatability, and reproducibility comparable to the reference chemiluminescence detector for NO measurement across multiple engines, test cells, and sampling configurations — including challenging ultra-low-NOx natural-gas conditions where it agreed within ±3 mg/bhp-hr. With near-unity linear agreement (R^2 = 0.99) and inter-instrument variability differences well under 1%, IRLAM is validated as a credible alternate to CLD. Next steps extend validation to additional nitrogen species (N_2O and NH_3) using the lab-grade XL-NX, evaluate CO and CO_2 using the in-use-grade CUBE, and continue validation under evolving ultra-low-NOx regulatory frameworks across diesel, gasoline, and natural-gas platforms.

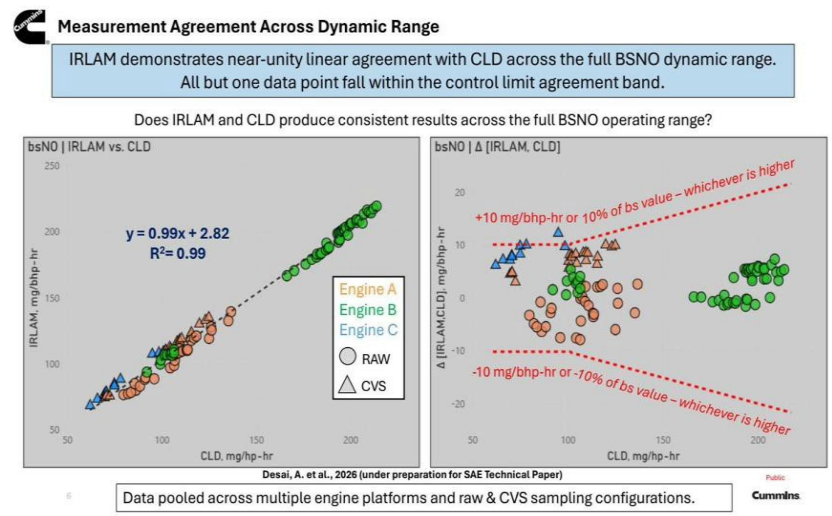

Figure 60 Measurement agreement across the dynamic range: IRLAM shows near-unity linear agreement with reference CLD (y = 0.99x + 2.82, R^2 = 0.99), pooled across engines and raw/CVS sampling.

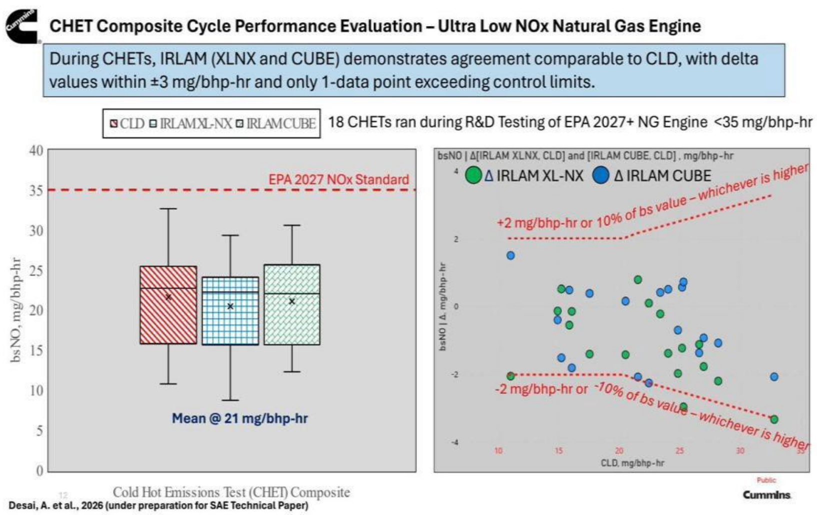

Figure 61 On an EPA 2027+ ultra-low-NOx natural-gas engine, IRLAM XL-NX and CUBE agree with CLD within ±3 mg/bhp-hr on the CHET composite cycle (18 CHETs).

Measurement and Reporting Challenges of Automobile NH3 and Best Practices

Montajir Rahman, Joshua Israel (HORIBA USA); Kenji Hara, Naoki Nagura (HORIBA Japan); Simone Eichmann (HORIBA Europe); Yusuf Khan (Cummins Inc.)

Scope of the Study

Ammonia forms in diesel engines within the SCR catalyst from urea/AdBlue (urea decomposing to NH3 and reacting with NOx to reduce it; overdosing during cold start leads to NH3 slip) and in gasoline engines as a by-product in the three-way catalyst via a two-step reaction through intermediate hydrogen. While the main source of NH3 is agriculture, automobile NH3 emissions are significant in urban areas, and ammonia can also be a synthetic non-carbon fuel itself. NH3 is challenging to measure because of three physical characteristics: high polarity causing adsorption and desorption at surfaces, high water solubility causing it to dissolve in liquid water and cold spots, and high reactivity causing NOx reduction and salt formation. These produce increased response time and hang-up effects, with countermeasures including reducing surface area, increasing flow rate, selecting good materials, and keeping surfaces clean and dry. The presentation reviewed U.S. and California regulations and detailed best practices for sampling and measurement.

Results

Under U.S. regulations, 40 CFR 1066 and 1065 currently do not include NH3 standards and Tier IV does not require it, though 1065 provides measurement guidance and EPA recommends ammonia slip below 10 ppm averaged over the test cycle; California limits verified in-use diesel technology to no more than 25 ppm by volume at the tailpipe averaged over any test cycle. A contaminated sample line caused a temporal lag from adsorption/desorption that distorted results, shifting the true NH3 peak and producing roughly a 25% difference in brake-specific NH3, with the Euro 7 brake-specific requirement more sensitive to alignment error than the Euro VI cycle average. On filter material, a standard hydrophilic filter (86R) absorbed water and produced a long NH3 response time (T90 of 153 s), whereas a hydrophobic filter (88RH) prevented absorption and gave the fastest response (T90 of about 7 s, matching no filter). On sample-line material, NH3 adsorption/desorption depended strongly on internal surface material and condition: PTFE for sampling below 190 °C, electropolished stainless steel above 190 °C (sulfinate coating improving response), avoiding copper, and always using a filter ahead of the line. Vacuum sampling outperformed ambient sampling with slightly faster response, lower contamination chance, and a sharper absorption spectrum.

Key Conclusion

Accurate NH3 measurement depends heavily on sampling-system design and condition because PM and heavy hydrocarbons cause slow response in extractive analyzers and contaminated lines distort results by roughly 25%. Best practices include a short heated sample probe (190 °C recommended, under 0.3 m, mounted upward with no cold spots), a frequently replaced hydrophobic heated filter (88RH) placed as close as possible to and above the sample point, a short heated stainless-steel or PTFE transfer line (6 m or less at 110–190 °C, under 130 °C under vacuum), and a heated analyzer (110–190 °C, under 130 °C under vacuum), with raw/tailpipe extractive sampling and filtration recommended. These measures ensure faster, more consistent NH3 response — increasingly important as Euro 7 introduces brake-specific NH3 requirements sensitive to timing alignment.

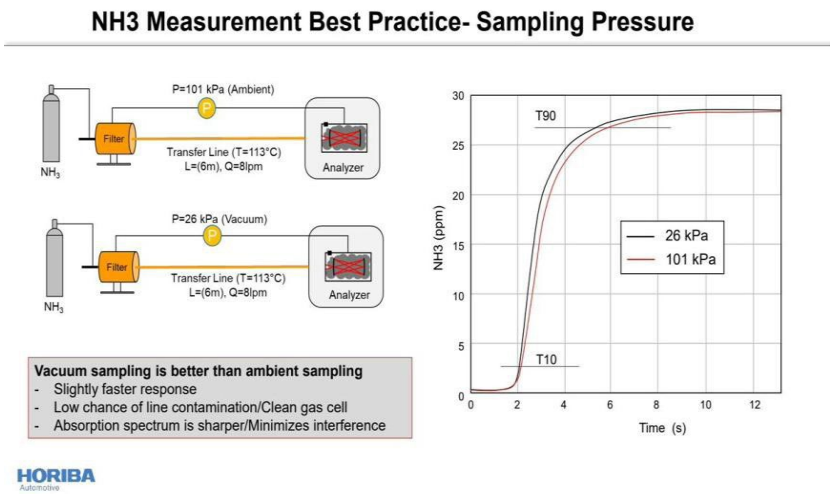

Figure 62 Sampling pressure best practice: vacuum sampling (26 kPa) gives a slightly faster NH3 response than ambient (101 kPa), with lower contamination risk and sharper absorption spectrum.

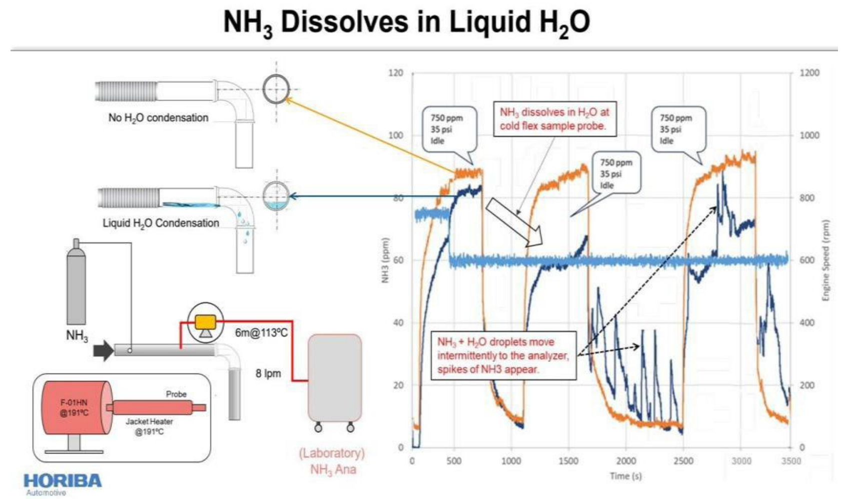

Figure 63 NH3 dissolves in liquid water and adsorbs at surfaces; heated routing with no condensation or cold spots is essential to avoid response lag and hang-up.

Emission Measurement Benchmarking in Ultra-Low-NOx Conditions: Sensors

Yang Li, Tyler Rash — Cummins Inc.

Scope of the Study

Increasingly stringent NOx standards and extended-useful-life requirements are key drivers shaping NOx-sensor performance expectations and validation strategies, and the challenges of sensor accuracy, durability, and long-term stability grow more significant as regulatory thresholds tighten. Aftertreatment-inlet NOx-sensor accuracy is especially important because it directly influences aftertreatment control strategies and dosing, affecting NOx conversion efficiency and tailpipe NOx. The study characterized current and next-generation NOx sensors for accuracy, signal noise, cross-sensitivity, and response under dynamic conditions, and assessed whether on-application sensor errors are predictable by measuring sensitivity to temperature and lambda on a gas bench. The primary characterization used the Sensor Exerciser and Test Instrument (SETI), a gas bench with a 20–550 °C temperature range, isobaric flow sweep capability, 20–250 SLPM flow, about 0.2-second response measurements, and independently controlled H_2, CH_4, C_3H_8, CO, CO_2, N_2, O_2, H_2O, NO, NO_2, and NH_3 concentrations, with FTIR, O_2, and NDUV NOx reference analyzers.

Results

Current and next-generation sensors showed similar cross-sensitivity to NO_2 and NH_3. The next-generation sensor exhibited increased signal noise during steady states, though the real-world impact remained unclear. Under dynamic conditions with fast O_2 and slow H_2O changes (7.5% to 19.5% O_2, 0 ppm NOx), the next-generation sensor showed apparent NOx spikes/dips of ±20 ppm even under zero-NOx conditions; testing fast H_2O with and without fast O_2 demonstrated that the sensor's erroneous NOx response was primarily associated with rapid O_2 change. A test matrix hypothesized that sensor NOx response is a function of temperature, air-fuel ratio, and NOx, and bench data were used to develop a lookup table predicting sensor behavior in real-world applications. In on-engine testing at the aftertreatment inlet, current and next-generation sensors performed similarly, with measured and predicted values tracking reference trends and low normalized errors; predictions helped both generations but worked better for the next-generation sensor. In a transient cycle at the aftertreatment outlet, both sensors read higher NOx than the reference (with truncating negative values adding further positive bias), and the next-generation sensor was helped by the flow-bench test while the current sensor was affected by uncaptured factors.

Key Conclusion

Current and next-generation sensors showed similar cross-sensitivity in measuring NO2 and NH3, and for both the erroneous NOx response to fast lambda changes was mostly due to O2-concentration change. The next-generation sensor exhibits more noise and dynamic peaks/dips, which may only matter on an integrated basis for especially transient cycles and could worsen at ultra-low-NOx thresholds if negative values are truncated. SETI bench results can potentially predict NOx-sensor deviations in real-world applications, with particularly good agreement for the next-generation sensor; the prediction for the current sensor is less accurate and requires further investigation of temperature-gradient and flow-rate effects. Correction and prediction schemes may need to change from one sensor generation to the next.

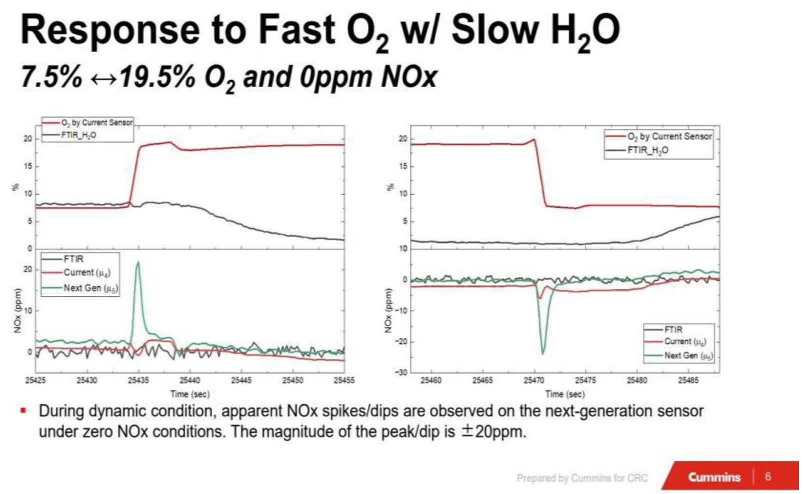

Figure 64 Response to fast O2 with slow H2O (zero NOx): the next-generation sensor shows apparent NOx spikes/dips of ±20 ppm driven primarily by rapid O2 change.

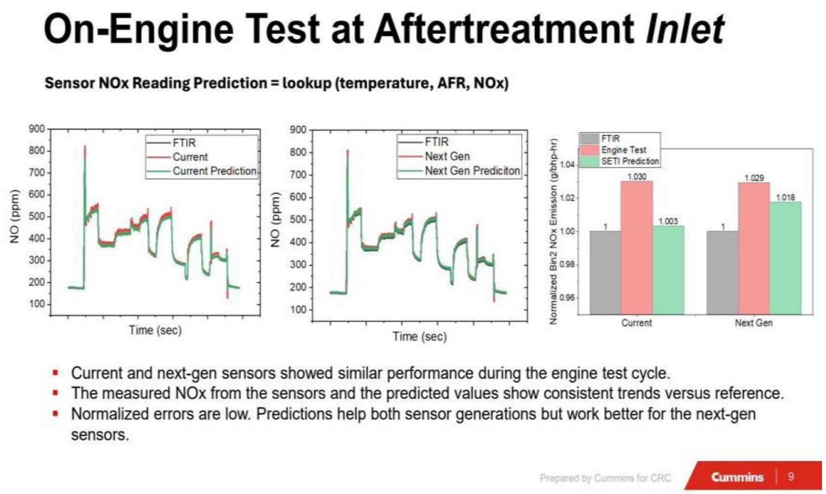

Figure 65 On-engine test at the aftertreatment inlet: measured and SETI-predicted (temperature, AFR, NOx lookup) sensor values track the reference, with prediction working best for the next-generation sensor.

The Importance of Real-World Emissions in an Electrifying World: A Manifesto for Radical Simplification

Nick Molden — Emissions Analytics; Imperial College London

Scope of the Study

Challenging the assumption that electrification alone will solve emissions, the presentation argues that the world is stuck in a mixed-powertrain reality for a long time, with continued decline in internal-combustion emissions, battery-electric emissions that are "not zero, just different," and customer confusion stemming from no consistent way to compare combustion and electric vehicles. Car ratings and labelling cannot simultaneously achieve simplicity, accuracy, and comprehensiveness. The talk surveys growing emissions sources that do not fit easily within in-use inventories — manufacturing, end-of-life, static tyre off-gassing (evaporative emissions), and in-use brake and tyre wear affecting mainly soil and water — and notes that California air quality is not improving as expected: despite years of VOC control, South Coast Air Basin ozone remains stubborn, and recent work attributes ozone formation largely to biogenic VOCs (26.6%), traffic VOCs (21.2%), volatile chemical products (19%), and plant decomposition (14.9%). It then asks whether tyres could be a major, understudied factor and tests which single metric best predicts environmental impact.

Results

Tyre-wear emissions comprise particles and gases, but gaseous emissions from tyres are understudied and poorly characterized, with only a handful of referenced studies, some nearly 50 years old. The VOCs and SVOCs come from plasticizers and processing oils (aromatic, naphthenic, or TDAE oils), vulcanization and curing chemicals (sulfur-containing VOCs), and tackifiers and resins, with specific compounds traced to particular tyre-chemistry sources. A box model for Los Angeles (assuming a 1 km boundary layer, well-mixed air, 25 °C, 2.3 million vehicles, and literature ozone and secondary-organic-aerosol formation potentials) produced an ozone estimate of 322 ppb (versus a summer 2024 maximum of about 50 ppb) and secondary organic aerosol of 7.6 μg/m³ (versus a 2024 maximum of about 30 μg/m³). While most likely an overestimate due to model assumptions, these results indicate that tyre VOC emissions may be a non-negligible and so-far overlooked source. Testing candidate predictors of impact — noise, infrastructure, and safety — the clear winner was vehicle mass, with 83% of problematic emissions strongly correlated to mass; nothing else came close.

Key Conclusion

Vehicle mass is the single best predictor of real-world environmental impact right now, with 83% of problematic emissions strongly correlated to mass. In a multi-powertrain world, less complexity rather than more is better for consumers to drive good behaviors, and a mass-based metric allows radical simplification of both car labelling and taxation during the complex transition to electrified cars — suggesting that, for now, emissions might be expressed per kilogram rather than per kilometre. The approach has acknowledged limitations (vehicles that are not cars, Goodhart's Law where interventions reduce weight but not emissions, lightweighting, hydrogen, and the Jevons paradox) and need not work forever, but offers a pragmatic simplification for the current transition.

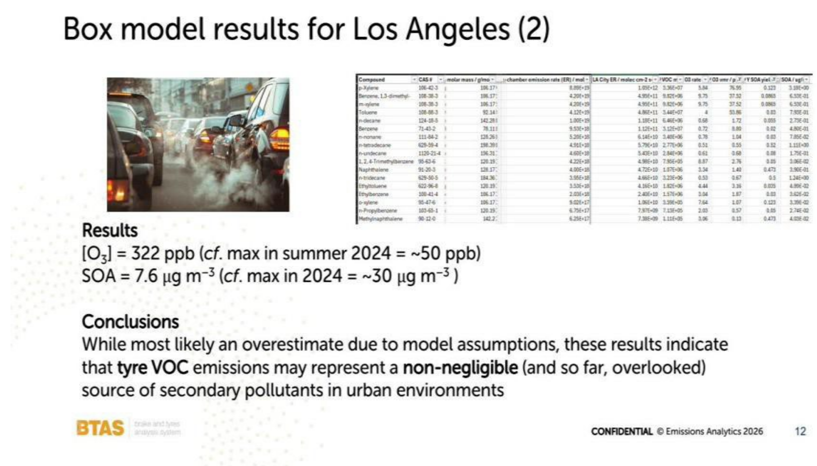

Figure 66 Los Angeles box-model results: tyre-derived VOCs yield modeled ozone of 322 ppb and SOA of 7.6 μg/m³ — likely overestimates, but indicating a non-negligible, overlooked source.

Comparing Brake Emissions and Cycle Characteristics of the WLTP-Brake and California Brake Dynamometer Cycle (CBDC)

Sampsa Martikainen, Michael Peter Huber, Tobias Zimmermann, Harald Mayrhofer, Christoph Weidinger (AVL List GmbH); Selina Wassermann, Heinz Bacher (BMW AG)

Scope of the Study

With brake-emission test cycles entering global regulation (UN GTR 24 and UN R 179 taking effect around 2028–2030), the study compares two cycles: the WLTP-Brake cycle, developed by UNECE GRPE/PMP for regulatory testing and designed to represent global WLTP driving characteristics with 10 trips and defined cooling phases, and the California Brake Dynamometer Cycle (CBDC), developed through CARB and ERG brake-emission studies for research and emission-inventory modeling (EMFAC) with three segments representing urban, rural, and highway operation. The brake-emission test system used an enclosure with PM10 and PM2.5 sampling, air-flow measurement, an air-conditioning system, solid and total particle-number measurement (10 nm to 2.5 µm), and a dynamometer rated to 476 kW, 2,250 Nm, and 2,500 rpm. The work evaluated cycle key characteristics, execution quality, brake-torque control performance, brake-temperature behavior, and resulting emission factors.

Results

Comparing cycle characteristics, the CBDC has more braking events (485 versus 303), a higher average speed (44 versus 29 km/h), higher maximum deceleration (3.89 versus 2.18 m/s^2), lower maximum specific friction work per event (374 versus 633) but higher total specific friction work (20,923 versus 15,983 J/kg), and a higher braking time share (15.6% versus 10.8%). The CBDC introduces more dynamic braking behavior — variable deceleration within braking, continuously changing torque demand, and brake-pumping sequences (brake, cruise, brake, cruise) — making torque tracking more demanding, whereas WLTP uses constant deceleration and constant brake torque. Cycle execution quality met UN GTR 24 / UN R 179 criteria with deviation well within the 5% tolerance and repeatability of 0.18%, and brake-torque control showed fast rise time, very small systematic deviations, and minor overshoot (CBDC slightly more demanding but stable). The CBDC produced higher disc temperatures due to longer and more frequent braking sequences, higher friction work, fewer cooling phases, and greater thermal accumulation. Consequently the CBDC produced higher PM emission factors per distance (+53%, +59%, +12% across metrics), with normalization per friction work reducing the differences (+28%, +33%, and approximately unchanged); potential PM drivers include temperature, braking dynamics, and braking speed.

Key Conclusion

The CBDC shows more dynamic braking behavior — variable deceleration and brake pumping — than the WLTP-Brake cycle, and leads to higher brake temperatures and higher PM emissions, with the per-distance differences narrowing once normalized per friction work. Despite the CBDC's more demanding torque tracking, the dynamometer achieved high-fidelity cycle execution for both cycles, demonstrating that both the WLTP-Brake cycle and the CBDC can be executed with excellent control performance. The comparison clarifies how cycle design choices translate into measured brake PM, informing both regulatory testing (UN GTR 24 / UN R 179 / Euro 7) and California emission-inventory modeling.

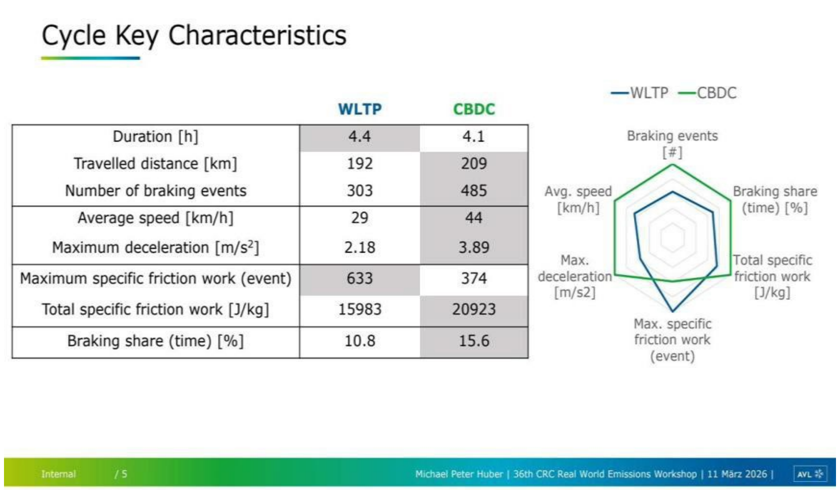

	WLTP	CBDC
Duration [h]	4.4	4.1
Travelled distance [km]	192	209
Number of braking events	303	485
Average speed [km/h]	29	44
Maximum deceleration [m/s²]	2.18	3.89
Maximum specific friction work (event)	633	374
Total specific friction work [J/kg]	15983	20923
Braking share (time) [%]	10.8	15.6

Figure 67 Cycle key characteristics: CBDC has more braking events (485 vs 303), higher average speed (44 vs 29 km/h), and higher total specific friction work (20,923 vs 15,983 J/kg) than WLTP.

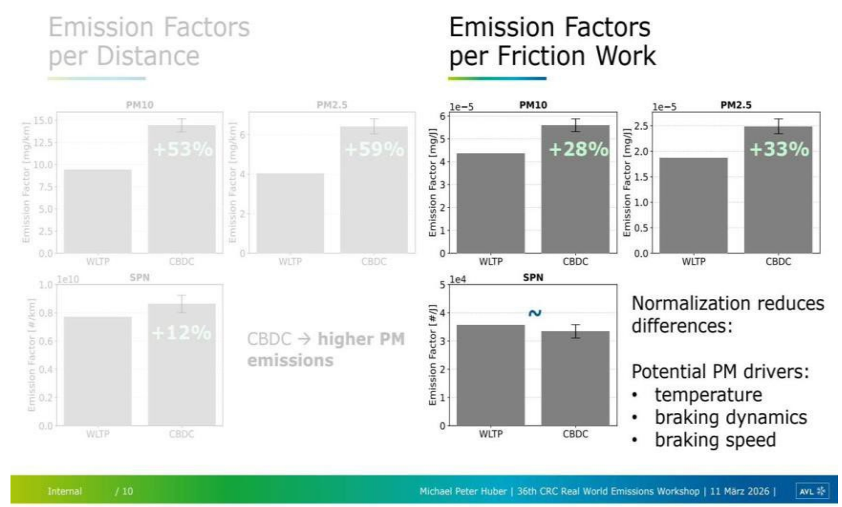

Figure 68 Emission factors: CBDC produces higher PM per distance (+53%, +59%, +12%); normalizing per friction work narrows the differences (+28%, +33%, ~unchanged).

Section 7. Non-Exhaust Emissions: Tyre, Brake, and Rail Wear

A Real-World Optimized Collection System for PM10 and PM2.5 Tyre Wear Particles

Zissis Samaras — e:misia and Aristotle University

Scope of the Study

With non-exhaust emissions gaining focus as exhaust controls improve — road transport accounts for about 10% of PM in Europe, and tyre-wear particles contribute up to 20% of road-transport PM2.5 and 30% of PM10 (EU27, 2020) — the study targets accurate measurement of airborne tyre-wear particles under real-world conditions. The challenge is that airborne tyre-wear particles in the real world are internally mixed with road particles (tyre and road wear particles) and externally mixed with particles from other sources (road dust, brake particles, resuspension, soot), so real-world collection is feasible only as multi-source particles, requiring both an efficient sampling system and separation of tyre-wear particles from other sources. The methodology generates particles by testing a vehicle in typical driving conditions on asphalt for a wide selection of tyres, collects them with a sampling nozzle behind the wheel, and analyzes them for PM/PN with post-test chemical analysis. Methodological refinements addressed each challenge: a closed circuit with a cleaned surface and a fully enclosed braking system, a system and materials designed to maximize particle capture, a nozzle optimized via CFD, and background subtraction with post-test chemical apportionment.

Results

Particle generation used real-driving conditions on asphalt with profiles based on UN R117 metrics, more than 20 different tyres, over 200 km per tyre, and an overnight circuit-cleaning procedure (three hours of vacuum sweeping and three hours of water cleaning) with a fully enclosed brake system on the test wheel. The collection nozzle was a single front-wheel unit (FWD vehicle) mounted on the wheel hub for high efficiency during cornering, made of antistatic non-abrasive materials, using isokinetic sampling with a 0.04 m^2 CFD-optimized inlet, positioned 20 mm above the ground and 20 mm behind the tyre at a sampling flow of about 230 m^3/h. ANSYS Fluent CFD simulations (realizable k-ε turbulence) predicted an average nozzle mass-based collection efficiency of about 60% for PM10, with larger particles more prone to inertial loss. Particle analysis used cyclones with 47 mm quartz filters for PM10 and PM2.5, an ELPI for total and (with a thermodenuder) solid particle number, and continuous background measurement. Emission factors were calculated mainly as the ratio of PM mass to tyre mass loss, corrected for system aspiration/transport efficiency (about 60%) and for non-tyre particles using pyrolysis GC/MS chemical markers. Preliminary results (assuming a 40% tyre-wear share of multi-source particles and 60% collection efficiency) gave emission factors around 1.3% of mass loss for PM10 and 0.4% for PM2.5.

Key Conclusion

The study presents a novel approach for accurately generating, collecting, and analyzing tyre airborne emissions (PM10 and PM2.5) under real-world driving in a closed circuit, with a robust vehicle-integrated sampling system, appropriate materials to maximize capture and limit losses, CFD-optimized nozzle positioning and geometry, and physical plus chemical post-test analysis to separate tyre-wear particles. Preliminary results show a small share of airborne particles relative to tyre mass loss, consistent with literature findings. Next steps include an improved methodology for handling background and ambient particles, statistical analysis to calculate overall uncertainty, and calculation of tyre-wear emission factors based on 23 different tyres — work funded by Tyres Europe to generate primary data for tyre airborne emission factors.

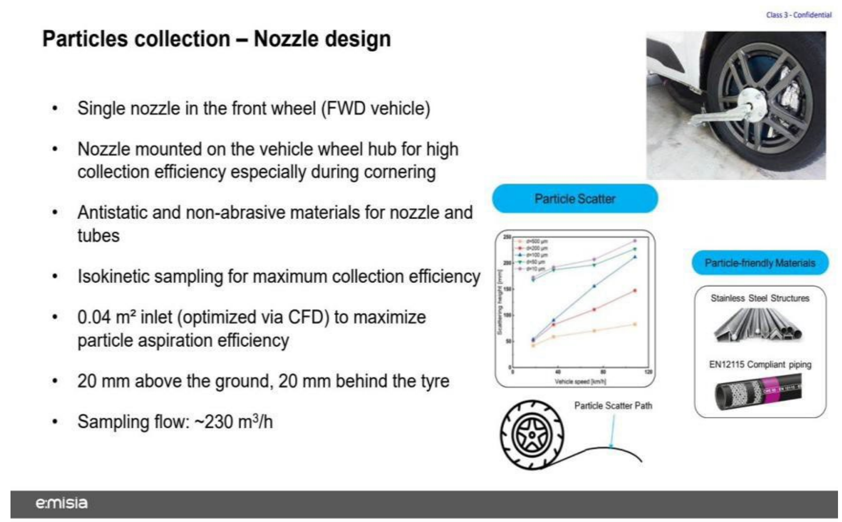

Figure 69 CFD-optimized collection nozzle: single front-wheel hub-mounted unit, antistatic materials, isokinetic sampling, 0.04 m² inlet, 20 mm above ground and behind the tyre, ~230 m³/h flow.

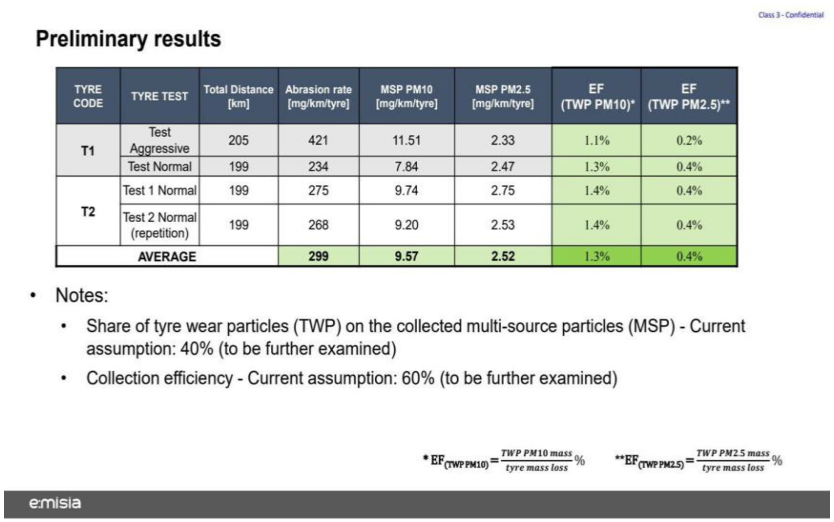
Class 3 - Confidential

Preliminary results

TYRE CODE	TYRE TEST	Total Distance [km]	Abrasion rate [mg/km/tyre]	MSP PM10 [mg/km/tyre]	MSP PM2.5 [mg/km/tyre]	EF (TWP PM10)*	EF (TWP PM2.5)**
T1	Test Aggressive	205	421	11.51	2.33	1.1%	0.2%
	Test Normal	199	234	7.84	2.47	1.3%	0.4%
T2	Test 1 Normal	199	275	9.74	2.75	1.4%	0.4%
	Test 2 Normal (repetition)	199	268	9.20	2.53	1.4%	0.4%
AVERAGE			299	9.57	2.52	1.3%	0.4%

- Notes:
  - Share of tyre wear particles (TWP) on the collected multi-source particles (MSP) - Current assumption: 40% (to be further examined)
  - Collection efficiency - Current assumption: 60% (to be further examined)

$* EF_{(TWP\,PM10)} = \frac{TWP\ PM10\ mass}{tyre\ mass\ loss}\%$ $\quad$ $** EF_{(TWP\,PM2.5)} = \frac{TWP\ PM2.5\ mass}{tyre\ mass\ loss}\%$

e:misia

Figure 70 Preliminary tyre-wear emission factors: PM10 around 1.3% and PM2.5 around 0.4% of tyre mass loss (assuming 40% tyre-wear share and 60% collection efficiency).

Light-Duty Vehicle Tire-Wear Particle Emissions

Elizabeth DeFrance, Zisimos Toumasatos, Georgios Karavalakis — UC Riverside CE-CERT

Scope of the Study

The study measured tyre-wear particle emissions from light-duty vehicle tyres using a vehicle-integrated sampling system positioned behind the wheel. It tested six tyre configurations, all sized 245/75R17: a new and an aged tyre from Manufacturer 1 (the aged tyre having over 60,000 miles), plus new tyres from Manufacturers 2, 3, 4, and 5, spanning all-season (45,000–70,000 mile ratings) and one summer tyre. All tyres underwent triplicate testing on a 60 mph US06x3 cycle lasting 48 minutes over 34 miles, with 162 braking events, an average speed of 43 mph, and a maximum of 80 mph. The measurement setup captured real-time particle size distributions and real-time emissions, with particle-number and particle-mass emission factors derived, supplemented by X-ray fluorescence (XRF) analysis of tyre-wear metals, PM2.5 morphology, and liquid chromatography-mass spectrometry (LC/MS) of tyre-derived chemical compounds.

Results

PM2.5 and PM10 for the Manufacturer 1 new tyre were higher than for the Manufacturer 1 aged tyre, indicating that a newer tyre shed more mass under these conditions.

Comparing against the EMFAC inventory estimate, Manufacturer 3 fell below EMFAC while all other tyres were above it. XRF analysis of the collected tyre wear found iron accounted for 75–85% of metals (ranging from 84.79% for the Manufacturer 1 aged tyre down to 75.13% for Manufacturer 5), while zinc accounted for only 0.06–0.4%; in the tyre tread material itself, however, zinc dominated at 70–88% and iron was only 1.2–3.8%, reflecting how the collected airborne particles differ in composition from the bulk tread. LC/MS quantified compounds including 5-MBTR, 2-OH-BTH, DPG, HMMM, and others in ng/mi, showing that in the aged tyre 6PPD, 6PPD-quinone, and other compounds were depleted compared with the new tyre of the same manufacturer.

Key Conclusion

Tyre-wear particle emissions varied by manufacturer and tyre age, with the Manufacturer 1 new tyre emitting more PM2.5 and PM10 than its aged counterpart and most tyres exceeding the EMFAC estimate (only Manufacturer 3 fell below it). Iron dominated the metals in the collected particles (75–85%) while zinc was minor (0.06–0.4%), even though zinc dominates the bulk tread — an important distinction for source apportionment. The LC/MS results showing depletion of 6PPD, 6PPD-quinone, and related compounds in the aged tyre are particularly relevant given growing environmental concern over 6PPD-quinone, indicating that tyre age affects not just the quantity but the chemical character of emitted particles.

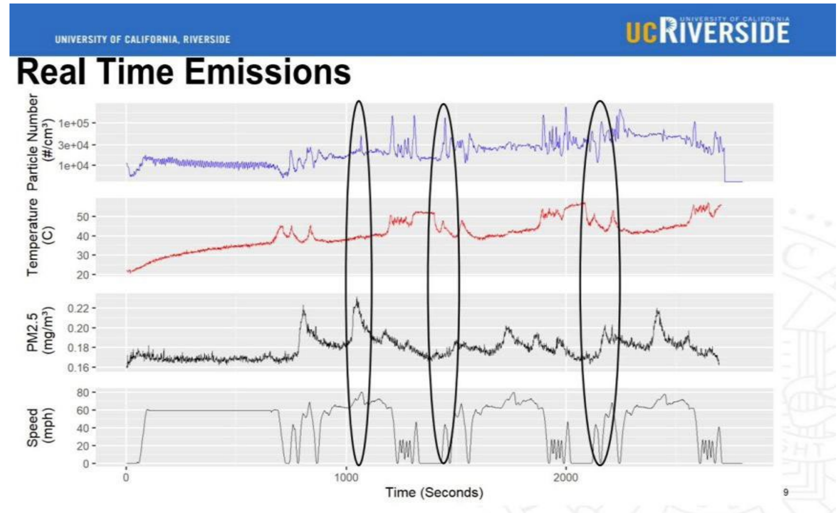

Figure 71 Real-time emissions over the US06x3 cycle: PM2.5 and PM10 concentrations tracked with vehicle speed, temperature, and braking across the 162-event test.

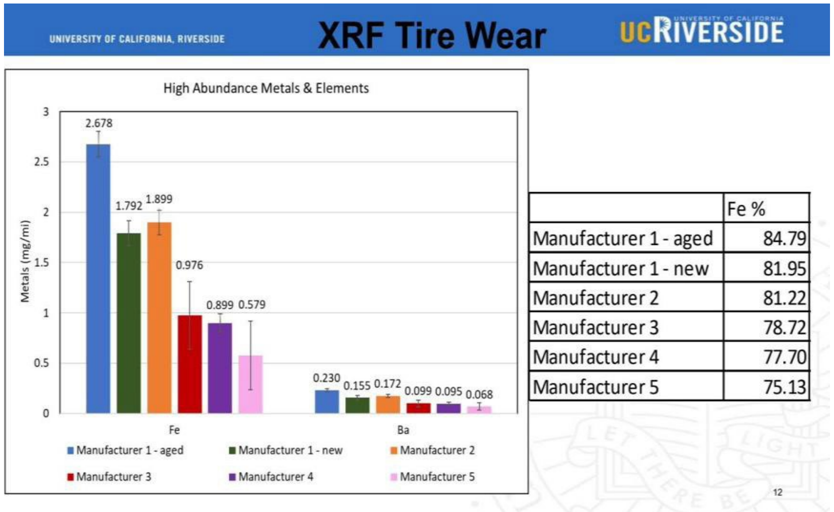

	Fe %
Manufacturer 1 - aged	84.79
Manufacturer 1 - new	81.95
Manufacturer 2	81.22
Manufacturer 3	78.72
Manufacturer 4	77.70
Manufacturer 5	75.13

Figure 72 XRF tire-wear analysis: iron accounts for 75–85% of metals in the collected particles across manufacturers, while zinc is a minor fraction (0.06–0.4%).

Impacts of Vehicle Weight and Speed on EV Brake-Wear Emissions, and the Impact of Regenerative Braking

Michelia Dam, Okjoo Park, Seungju Yoon, Yilin Ma, Wilson Chau, Shishan Hu, Gary Mikailian, Jorn Herner — California Air Resources Board

Scope of the Study

Amid growing concern over non-exhaust PM emissions, these paired presentations measured brake-wear particle emissions for compact and mid-size internal-combustion (ICEV), hybrid (HEV), and battery-electric (BEV) light-duty vehicles, with regenerative braking as a potential co-benefit subject to a considerable knowledge gap around driving cycles, brake and tyre materials, vehicle technologies, and regenerative braking. Objectives were to measure brake-wear particle concentrations in CARB's RL-SHED (Running Loss Sealed Housing for Evaporative Determination) chassis dynamometer for gasoline, hybrid, and battery-electric vehicles; compare concentrations between gasoline and electric vehicles; investigate energy recovery through regenerative braking; and explore potential reductions by vehicle weight and speed. Sampling occurred near the brake pad, behind the tyre, and at the rear brake, using real-time PM and PN instruments (DRX, APS, CPC, EEPS), brake-pad thermocouples, a CAN data logger for the brake signal, and a Hioki power meter for regenerative energy. Six test vehicles (MY 2022–2024) spanned ICEV, HEV, and BEV powertrains with front, all-wheel, and rear drivetrains, tested over a cycle group including idle, NYCC (low-speed stop-and-go), FTP (city driving), and US06 (aggressive driving) phases.

Results

Braking duration and frequency were higher in low-speed cycles. Compared with ICEVs, the tested BEVs reduced PM2.5 particle-mass concentrations and total particle number by more than 80%, despite the BEVs' heavier weight, and brake-pad weight loss followed the same trend as the real-time PM measurements. Brake PM2.5 emission reductions by vehicle class showed improvement in reduction potential even as vehicle weight increases, comparing new (MY 2022–2025) SHED results against EMFAC inventory data from older vehicles (HEV 2016, BEV 2020). By speed, BEVs achieved greater reductions than HEVs in all speed bins for both compact and mid-size vehicles, with reductions highest at mid-speeds where friction braking is used more relative to regenerative braking; mid-size HEV and ZEV vehicles had negligible reductions in the lowest and highest speed bins. Examining regenerative braking, particle-concentration peaks aligned with the brake-switch-on signal for ICEVs, while HEVs and BEVs applied friction braking under conditions of minimal or zero regenerative torque. The regen fraction (regenerative energy divided by braking kinetic energy) was 0.2–0.4 for HEVs and 0.4–0.6 for BEVs, with vehicle B2 showing the highest recovery; the HEV's maximum regenerative torque reached about 200 Nm versus about 1,500 Nm for the BEV. Higher brake-pad temperatures corresponded to higher particle emissions, and HEVs and BEVs showed substantially lower brake-pad temperatures due to regenerative braking.

Key Conclusion

Brake-wear particle concentrations measured at the RL-SHED chassis dynamometer showed that within the same vehicle class, BEVs emit substantially lower particle emissions than ICEVs — more than 80% lower for PM2.5 and total PN — despite their heavier weight, and new vehicles show increasing reduction potential even as weight rises. Regenerative braking is most efficient at medium speeds, where emissions reductions are highest because friction braking would otherwise dominate; vehicle B2 showed the highest regeneration performance. Higher brake-pad temperatures correspond to elevated particle emissions indicating friction-brake application, and HEVs and BEVs exhibit substantially lower brake-pad temperatures. Conducting EMFAC measurement methods on modern EVs is needed for future inventory updates, since current EMFAC relies on older-vehicle data.

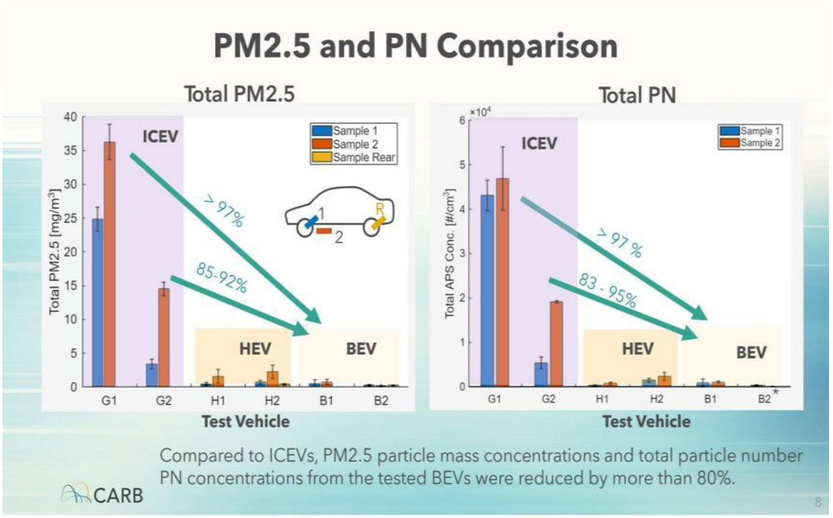

Figure 73 PM2.5 and PN comparison by powertrain: tested BEVs reduced PM2.5 mass and total particle number by more than 80% versus ICEVs, despite heavier weight.

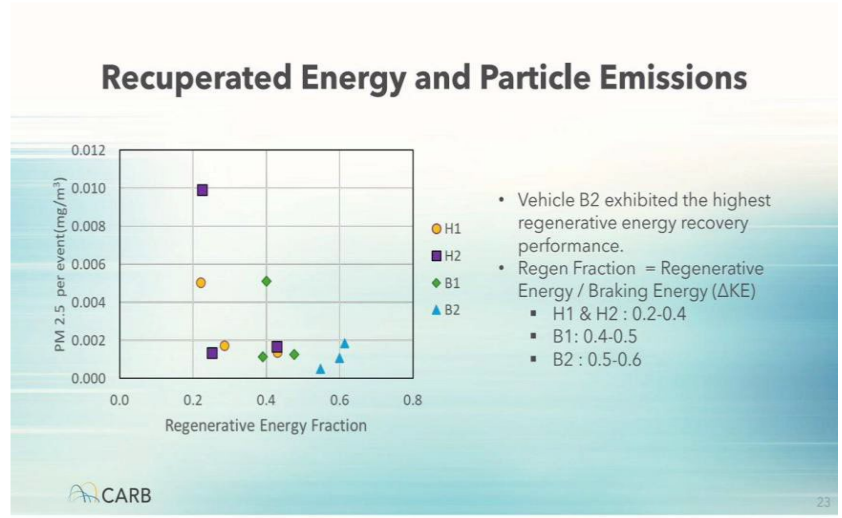

Figure 74 Recuperated energy and particle emissions: BEV B2 showed the highest regen fraction (0.5–0.6); higher regenerative energy recovery corresponds to lower brake-wear particle emissions.

Quantifying Real-World Impacts of Non-Exhaust Particulate Matter: The HEI Experience and What's Next

Eva Tanner, Allison Patton, Hanna Boogaard, Greg Evans, Meredith Franklin, Christopher Griffiths et al. — Health Effects Institute

Scope of the Study

The Health Effects Institute (HEI) provides impartial science to inform decisions fostering a healthier environment. After a systematic review and meta-analysis of selected health effects of long-term exposure to traffic-related air pollution found that few studies evaluated exposure to and health effects of non-exhaust particulate matter, and after a workshop identified research gaps and needs — improving characterization of non-exhaust PM emissions, reaching consensus on which measurements best represent them for exposure and health studies, and better characterizing human exposures and health effects — HEI funded three studies. These were led by Chris Griffiths in London (the IONA study), Greg Evans in Vancouver and Toronto, and Meredith Franklin in Southern California, together spanning fixed-site monitoring, mobile monitoring, laboratory and field tyre measurements, hot-spot measurements, and evidence integration.

Results

The IONA study measured PM2.5 and PM10 mass and composition, particle-number concentration, and NO2, conducting source apportionment at three sites: busy stop-go traffic produced the highest NO2 and brake wear, high-speed continuous traffic produced the highest PM and tyre/road wear, and urban background had the lowest traffic pollution; in a randomized crossover trial of 44 mild-to-moderate nonsmoking asthmatics exercising at the sites, preliminary results suggested decreases in lung function and increased airway inflammation. The Evans study characterized hourly and long-term non-exhaust PM patterns (rush-hour peaks, with 2017–2023 concentration trends varying by location), found larger differences between exhaust and brake wear near heavy traffic, identified tyre age and particle size as important, and evaluated methods to differentiate exhaust from non-exhaust PM. The Franklin study estimated exhaust and non-exhaust PM exposures and examined associations with children's lung function across multiple ages, finding reductions in lung function with exposure to some exhaust and non-exhaust PM components (decreased lung function with iron and copper, no associations with zinc), modestly attenuated after adjusting for traffic noise and green space. Across studies, non-exhaust contributed 2–7% of PM2.5 and 6–21% of PM10 from brake and tyre wear, plus 22–28% of PM10 from road dust.

Key Conclusion

The research program provides important evidence on non-exhaust PM exposures and associated respiratory outcomes, with reports published in April (Franklin) and later in the year (Griffiths, Evans). Strengths included complementary state-of-the-art exposure-assessment methods across four urban areas, high-quality study designs, comprehensive analyses applying novel methods, and both population and individual exposure assessment. Limitations included an inability to completely disentangle the air-quality and health effects of non-exhaust PM from other PM sources, and the possibility that specific non-exhaust markers may not generalize. Future research should further characterize non-exhaust emissions and their relative importance amid multiple sources, continue evaluating population-level impacts, and synthesize the literature. HEI plans a synthesis manuscript and further work, partnering in the new NEXUS non-exhaust air pollution partnership led by Chris Griffiths, Ian Mudway, and Greg Evans.

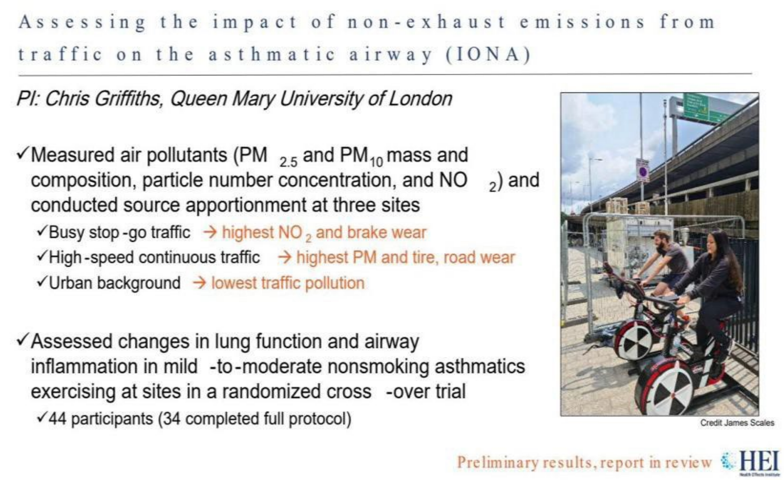

Figure 75 The IONA study (London): source apportionment at three sites — busy stop-go traffic gave the highest NO2 and brake wear; high-speed continuous traffic gave the highest PM and tyre/road wear.

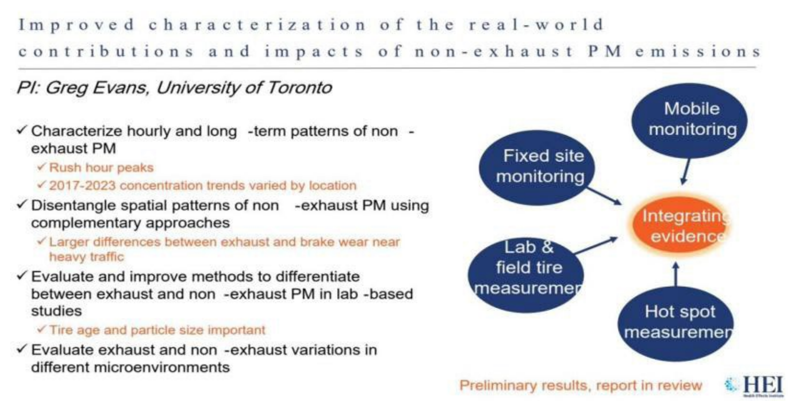

Figure 76 The Evans study (Toronto): characterizing hourly non-exhaust PM patterns and spatial differences using fixed-site, mobile, tyre, and hot-spot measurements with evidence integration.

Characterizing Train Brake and Wheel Wear Activity in California

John Koupal, Heather Perez, Jie Yan (ERG); Tongchuan Wei, George List, Christopher Frey (NC State); Zisimos Toumasatos, Georgios Karavalakis (UC Riverside); Carlos Agudelo (LINK Engineering); Stephan Dorsch (Deutsche Bahn); Okjoo Park, Seungju Yoon (CARB)

Scope of the Study

CARB Project 23RD010 will measure PM emissions from train brake and wheel-rail wear (BWWW) in California, with ERG and NC State developing the activity framework and simulation modeling and LINK, Deutsche Bahn, and UC Riverside conducting emissions testing and chemical analysis. An inventory framework is needed to assess the train BWWW inventory at state and local levels, providing a relative sense of important sources, developing a framework for applying test results to inventory, informing test-matrix design, and remaining refinable as new data arrive. An initial proof-of-concept estimate for California train brake PM combined a preliminary inventory of freight, passenger, and commuter braking activity across the California network with published studies on train tread and disc-brake emissions, set against 2022 locomotive PM2.5 exhaust. The presentation focused on developing representative track alignments — characterized by distance, speed limit, grade, and curvature — for simulation modeling, needed separately for freight, passenger, and commuter operation.

Results

Two options were considered for choosing track alignments: selecting a sample of existing alignments (real, history-aware, but possibly unrepresentative) or constructing representative alignments analogous to vehicle emission-test-cycle development (efficiently matching the overall network but not real and not history-aware). Freight-network attributes were mapped including speed limit, deceleration/acceleration points, gross tonnage, speed-limit reductions, freight density, and grade — with PM emissions on disc brakes high for downgrades maintained at constant speed, though dynamic braking use is likely high on downgrades. An example freight alignment (Cajon Pass) profiled speed limit against elevation. For passenger and commuter rail, station locations and spacing were analyzed; the Ventura and Orange County lines have the same number of stations per 50-mile alignment (9) but different speed-limit profiles and station spacing that may affect emissions. The modeling incorporates the OneTrain simulator (part of the A-STEP / Achieving Sustainable Train Energy Pathways tool developed by NC State, Virginia Tech, Ohio State, and Deutsche Bahn under an ARPA-e project), which simulates train dynamics as a distributed mass of cars and locomotives, captures grade, curvature, and speed limit at high spatial detail (e.g., 100 feet), and records second-by-second tractive effort, braking effort, and energy recapture across regenerative, dynamic, and friction braking modes.

Key Conclusion

A simulation-based framework combining representative track alignments, train dynamic modeling (OneTrain within the A-STEP tool), and emissions testing (UC Riverside, LINK, Deutsche Bahn) will translate emissions-test results into a state and local train brake and wheel-wear inventory for California, refinable as new data become available. Work is in progress on identifying alignments for simulation, refining speed, grade, and curvature estimates, incorporating the NC State train dynamic simulation model, and defining the emissions test matrix. By capturing how grade, curvature, speed limits, and braking-mode choices (regenerative, dynamic, friction) drive brake and wheel-rail wear, the framework will provide a relative sense of important sources and a structured method for applying test results to the inventory.

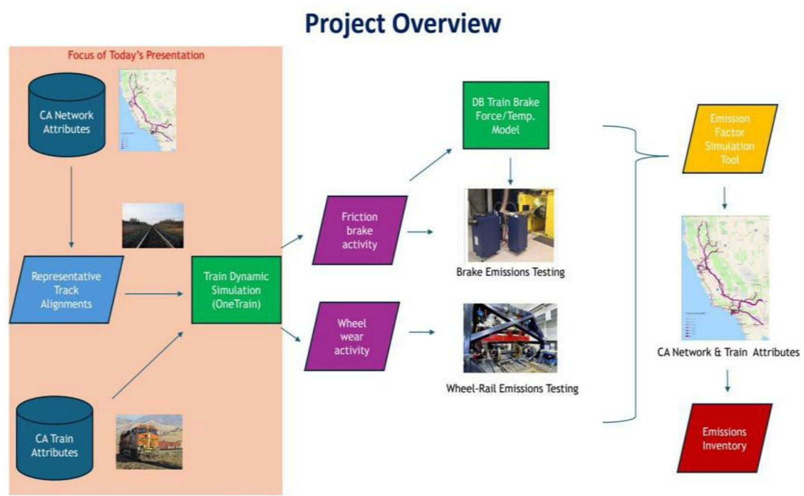

Figure 77 Project overview: California train and network attributes feed train dynamic simulation (OneTrain), brake force/temperature modeling, and wheel-rail and brake emissions testing to build an emissions inventory.

Figure 78 Example freight alignment (Cajon Pass): speed limit and elevation profiles along the route, illustrating how grade and speed shape disc-brake PM and dynamic-braking use.